The essential processes of FeS cluster assembly and mitochondrial protein import in parasitic protists

Ondřej Šmíd

Ph.D. Thesis

Thesis supervisor: Prof. RNDr. Jan Tachezy, Ph.D.

Prague 2008

Department of Parasitology
Faculty of Science, Charles University in Prague

Výsledky prezentované v doktorské práci Mgr. Ondřeje Šmída jsou společným dílem pracovníků Laboratoře biochemické a molekulární parazitologie PřF UK a spolupracujících týmů v České republice a v zahraničí. Prohlašuji, že autor se na jejich získání zasloužil významným dílem.

Data presented in this Ph.D. thesis are the results of collaboration within the team of Laboratory of Biochemical and Molecular Parasitology and with our Czech and foreign colleagues. I declare that the involvement of Mgr. Ondřej Šmíd in this work was substantial and contributed significantly to obtaining these results.

Prof. RNDr. Jan Tachezy, Ph.D.
Thesis supervisor

Děkuji Honzovi Tachezymu za inspirativní odborné vedení a Ivanovi Hrdému a panu prof. Kuldovi za cenné rady a pomoc nejen při řešení záhad kultivace parazitických protist a jejich biochemie. Rád bych také poděkoval Aničce Matuškové z Mikrobiologického ústavu AV ČR a Julovi Lukešovi z Parazitologického ústavu AV ČR za podnětnou spolupráci. Dík patří též všem pracovníkům katedry parazitologie PřF UK, zejména Heleně Kulíkové, Míše Marcinčikové a členům laboratoře molekulární a biochemické parazitologie.

CONTENTS

REVIEW

REVIEW

1. INTRODUCTION

Mitochondria of most eukaryotic organisms are organelles whose most prominent function in a cell is ATP production by oxidative phosphorylation. In this process, electrons from citric acid cycle pass through the respiratory chain to their final acceptor oxygen. The proton gradient generated by respiratory chain complexes on mitochondrial membrane is then used for ATP synthesis. Parasitic protists possess organelles that are often deviated structurally and functionally from the canonical mitochondrion. Protists that encounter aerobic enviroment during their lifecycle have mitochondria that are able to produce ATP by oxidative phosphorylation. Many protists however, like *Trichomonas vaginalis*, live in an oxygen-poor enviroment. Their mitochondria lost citric acid cycle and respiratory chain and employ anaerobic metabolic pathways for production of ATP by substrate-level phosphorylation. These mitochondria were named hydrogenosomes after the hallmark metabolic end product, the molecular hydrogen (Hrdy et al., 2008). Mitochondria of other protists, like those of *Giardia intestinalis*, *Entamoeba histolytica, Cryptosporidium parvum* or microsporidia, underwent more radical reductive evolution. They lost ability to produce ATP altogether, being downsized to remnant organelles called mitosomes (Tachezy and Smid, 2008).

Even though mitochondria are sometimes highly reduced, they are present in all eukaryotic organisms studied to date (van der Giezen and Tovar, 2005). It indicates that the organelle harbours fundamental process(es) required for life of a eukaryotic cell. In *Saccharomyces cerevisiae*, the model eukaryotic organism, the mitochondrion is a compartment where the crucial part of the essential iron-sulfur (FeS) cluster biosynthetic pathway is localized (Lill et al., 2006). FeS clusters are cofactors of a number of proteins, including those essential for DNA metabolism (Rad3, Pri2) and protein translation initiation (Rli1) (Lill and Muhlenhoff, 2008). The components of the FeS cluster biosynthesis are encoded in the nucleus and translated in the cytosol. Thus, machineries involved in mitochondrial protein import and maturation are also indispensable for *S. cerevisiae* (Lill et al., 2006).

Parasitic protists cause diseases that are major health burden worldwide. Understanding their biology is crucial for identification of novel chemotherapeutical targets. As the processes and pathways essential for cell survival and propagation are of particular interest, the focus of this review is to summarize current knowledge of the

vital processes of FeS cluster assembly and mitochondrial protein import in parasitic protists.

2. MITOCHONDRIA OF PARASITIC PROTISTS

Mitochondria *sensu lato* are various organelles of common evolutionary origin that form a continuum of metabolic and morphological manifestations. As the biochemical and morphological features are more apparent than evolutionary relationships, the different manifestations of mitochondria were given names that are still commonly used. In general, mitochondria *sensu stricto* define the textbook organelles with a genome that are able to produce ATP by oxidative phosphorylation. The molecular hydrogen-producing mitochondria were named eponymously. Hydrogenosomes are devoid of DNA and lost functional respiratory chain, producing ATP by substrate-level phosphorylation. The mitochondria that do not have DNA and produce neither ATP nor hydrogen were named mitosomes. Only little is known about the functions of mitosomes so far apart from the biogenesis of FeS clusters identified in some of them.

2.1. Mitochondrion of *Trypanosoma brucei*

Unlike most eukaryotes whose cells contain numerous mitochondria, *T. brucei* possesses a single, branched mitochondrion per cell. Instead of a single circular chromosome found in mitochondria of *S. cerevisiae*, the genome of *T. brucei* mitochondrion is organized into a kinetoplast, an elaborate structure of concatenated circular DNA molecules of two types, the longer maxicircles and shorter minicircles. Such an organized structure requires a highly complex machinery for its replication (Liu et al., 2005; Lukes et al., 2005). Gene expression in *T. brucei* mitochondria is dependent on extensive RNA editing (Lukes et al., 2005) and import of all tRNAs from cytosol (Bouzaidi-Tiali et al., 2007).

During the life cycle, *T. brucei* encounters very diverse enviroments of the mammalian blood and the digestive tract of the insect vector, the tse-tse fly. In reaction to different cellular needs with regards to its function, the mitochondrion of *T. brucei* undergoes dramatic metabolic changes upon transmission between the two hosts. An excess of glucose in the mammalian host permits the early bloodstream stage to employ glycolysis for energy generation (Michels et al., 2005), producing pyruvate as a major end product. Its mitochondrion lacks the cytochrome-dependent, proton gradient-generating electron transport chain and the activities of the citric acid cycle enzymes

and is thus impaired in its ability to produce ATP by oxidative phosphorylation (Clayton and Michels, 1996). In classical mitochondria, the proton gradient on inner mitochondrial membrane is used by F_0F_1 ATP synthase for production of ATP. In mitochondria of bloodstream form of *T. brucei*, despite the absence of respiratory chain, F_0F_1 ATP synthase is present and was demonstrated to be essential for the parasite. But instead of ATP synthesis, it catalyses the reverse reaction of ATP hydrolysis and exports protons from mitochondrial matrix, generating membrane potential required for mitochondrial function and biogenesis (Schnaufer et al., 2005; Brown et al., 2006). Through its functions as a sink for reducing equivalents from glycolysis, the mitochondrion still plays an indispensable role in the metabolism of bloodstages (Chaudhuri et al., 1998).

In the insect vector, trypanosomes live in a nutrient-poor environment, where they can only survive through an overall switch in their energy metabolism, primarily by activating the mitochondrion. In the active mitochondria of the insect (procyclic) stage, pyruvate is degraded with the benefit of additional ATP synthesis, mainly to acetate (van Hellemond et al., 1998). However, the main energy source of *T. brucei* in the tse-tse fly is the amino acid proline that is finally catabolized to succinate by the ATP-producing citric acid cycle enzyme succinyl-CoA synthetase. Even though all other citric acid cycle enzymes are active in procyclics, they do not function as a cycle for production of reducing equivalents (van Weelden et al., 2003). While the function of the part of the cycle leading to succinate is catabolic, the citric acid cycle intermediates citrate and malate are used for fatty acid synthesis and gluconeogenesis, respectively (van Weelden et al., 2005). The respiratory chain of the procyclic *T. brucei* mitochondrion is branched, comprising four NADH oxidases (complex I and II, rotenone-insensitive NADH:ubiquinone oxidoreductase and glycerol 3-phosphate dehydrogenase) and two ubiquinol oxidases (complex III and alternative oxidase). Of these, only complexes I and III translocate protons to be used for ATP production by ATP synthase. Thus, majority of mitochondrial ATP is produced by substrate-level phosphorylation. The essential function of the flexible respiratory chain is not ATP synthesis but re-oxidation of NADH generated by the pathways of substrate-level phosphorylation (Bochud-Allemann and Schneider, 2002).

2.2. Mitochondrion of *Plasmodium falciparum*

Asexual stages of *P. falciparum* have one mitochondrion per cell without cristae that is tightly connected with the apicoplast, the remnant plastid of apicomplexan protists. (For the excellent review please see van Dooren et al., 2006).Gametocytes harbour multiple mitochondria which develop tubular cristae. The mitochondrial genome of *P. falciparum* is extremely reduced and codes only for three respiratory chain components and rRNA. Energy metabolism of *P. falciparum* relies on glycolysis, the major end product of the parasite being lactate. Pyruvate cannot be further metabolized in the mitochondrion as *P. falciparum* lacks mitochondrial pyruvate dehydrogenase. Moreover, *P. falciparum* does not codes for any enzyme of fatty acid β-oxidation, an alternative source of acetyl-CoA. Consequently, even though all the enzymes involved are present, citric acid cycle does not function as a cycle generating reducing equivalents to be oxidized by respiratory chain with concomitant production of ATP. It has been hypothesized that parts of citric acid cycle may generate substrates for biosynthetic pathways or utilize amino acid as substrates (van Dooren et al., 2006).

Five donors feed electrons to respiratory chain via coenzyme Q instead of respiratory chain complex I that is missing in *P. falciparum*: (i) dihydroorotate dehydrogenase (DHOD), an enzyme of pyrimidine biosynthesis utilizing respiratory chain as an electron sink; (ii) succinate dehydrogenase (complex II); (iii) malate:quinone oxidoreductase; (iv) alternative NAD(P)H dehydrogenase; and (v) glycerol 3-phosphate dehydrogenase (van Dooren et al., 2006).

Respiratory complexes III and IV are the only electron acceptors downstream of coenzyme Q, generating proton gradient on the mitochondrial membrane. As homologues of the membrane part of F_0F_1 ATP synthase have not been detected in the *P. falciparum* genome and the main energy source glucose is catabolized to lactate in the cytosol of the asexual stages of the parasite, production of ATP by oxidative phosphorylation is most likely not the main function of respiratory chain. However, in other life stages of *P. falciparum*, especially those that encounter nutrient-poor environment of the insect vector, mitochondria may be involved in energy metabolism. Nevertheless, no direct evidence for the activity of ATP synthase has been presented in any stage of *P. falciparum* so far (van Dooren et al., 2006). The mitochondrial electron transport chain of erythrocytic stages of *P. falciparum* seems to be indispensable only for its function of an electron sink for DHOD, an essential enzyme for the parasite that cannot salvage pyrimidine nucleotides from its host. The electrochemical potential on

inner mitochondrial membrane, in most eukaryotes the result of the proton-exporting activity of respiratory chain complexes, can be generated by an alternative mechanism in the mitochondrion of *P. falciparum*. It has been hypothesized that ADP/ATP transporter together with the remnant ATP synthase may establish electrochemical potential of different concentrations of ADP^{3-} and ATP^{4-} accross the membrane, resulting in net negative charge in the mitochondrial matrix. Mitochondrial membrane potential was demonstrated to be essential for erythrocytic stages of *P. falciparum*, most likely for its role in mitochondrial protein import (Painter et al., 2007).

2.3. Hydrogenosome of *Trichomonas vaginalis*

The hydrogenosomes of *T. vaginalis* are separate vesicles without a genome limited by two tightly associated membranes. They harbour catabolic pathways that are important part of energy metabolism of *T. vaginalis*. Hydrogenosomes produce ATP by substrate-level phosphorylation in the pathway that begins with oxidative decarboxylation of pyruvate by pyruvate:ferredoxin oxidoreductase (PFOR), an FeS enzyme typically found in anaerobic bacteria and in few anaerobic eukaryotes. The electron acceptor in the PFOR reaction is a hydrogenosomal 2Fe2S ferredoxin. The reduced 2Fe2S ferredoxin is subsequently reoxidized by the hydrogenase, a molecular hydrogen-producing enzyme (Hrdy et al., 2008).

Acetyl-CoA produced by PFOR is catabolized to acetate, similarly as in *T. brucei*, by acetate:succinate CoA transferase. The formed succinyl-CoA is used by succinyl-CoA synthetase, the only citric acid cycle enzyme present in hydrogenosomes, for production of ATP or GTP. Another substrate of hydrogenosomal energy metabolism, malate, is degraded by malate dehydrogenase (decarboxylating) to pyruvate with concomitant production of NADH. Reoxidation of NADH was recently ascribed to the activity of two catalytic subunits of respiratory complex I that transfer the electrons to 2Fe2S ferredoxin. Apart from this remnant complex I, no other respiratory chain complexes nor cytochromes are present in hydrogenosomes of *T. vaginalis* (Hrdy et al., 2008).

2.4. Mitosome of *Cryptosporidium parvum*

The single mitosome of *C. parvum* is associated with nuclear membrane and is enveloped by rough endoplasmic reticulum. The inner mitosomal membrane does not form cristae, but it is highly folded, or it forms independent vesicles (Keithly et al.,

2005). No genome has been detected in the *C. parvum* mitosomes. Substrate-level phosphorylation and glycolysis in the parasite cytosol is the major source of ATP for *C. parvum*. However, participation of mitosomes on energy metabolism of *C. parvum* cannot be excluded (Henriquez et al., 2005; Keithly, 2008). Like in *P. falciparum*, components of the soluble part of F_0F_1 ATP synthase were identified in the genome of *C. parvum* that possess N-terminal extensions resembling mitochondrial targeting presequences, but membrane part of the F_0F_1 ATP synthase was not found. Moreover, a phosphate carrier protein, which in other eukaryotes transports phosphate to mitochondria for ATP generation, was detected in the genomic data with a similar N-terminal presequence (Henriquez et al., 2005). Experimental evidence suggests that membrane potential is generated by *C. parvum* mitosomes (Ctrnacta et al., 2006). But, unlike *P. falciparum*, no respiratory chain complexes were identified in the *C. parvum* genome. It was therefore hypothesized that a pyridine nucleotide transhydrogenase (PNT), for which a mitochondrial presequence was predicted, catalyzes the conversion of NAD+NADPH to NADH+NADP with coupled proton translocation from matrix to intermembrane space of the *C. parvum* mitosome. Similar reaction was demonstrated to be mediated by PNT under anaerobic conditions in the helminth *Hymenolepis diminuta* (Henriquez et al., 2005). In addition, an alternative oxidase possessing an N-terminal presequence was predicted to be targeted to the *C. parvum* mitosome (Roberts et al., 2004).

2.5. Mitosome of *Giardia intestinalis*

Mitosomes of *G. intestinalis* are vesicles bound by tightly packed double membrane without a genome (Tovar et al., 2003). The number of *G. intestinalis* mitosomes per cell ranges from 25 to 100 (Dolezal et al., 2005). The majority of *G. intestinalis* mitosomes are randomly distributed throughout the cytoplasm. Interestingly, some mitosomes form a rod-like structure between the two nuclei of *G. intestinalis* in close proximity to the flagellar basal bodies. This structure, which is invariably present in all cells, consists of several attached mitosomes organized between the axonemes of caudal flagella (Tovar et al., 2003; Dolezal et al., 2005; Regoes et al., 2005). No other metabolic function has been localized as yet to these organelles apart from biogenesis of FeS clusters (Tachezy and Dolezal, 2007).

2.6. Mitosome of *Entamoeba histolytica*

E. histolytica mitosomes are vesicles limited by two closely opposed membranes. A single mitosome was observed in most cells, but some cells contained two, and rarely three, organelles (Tovar et al., 1999). However, a later study revealed that mitosomes are rather abundant organelles of over 150 mitosomes per cell (Leon-Avila and Tovar, 2004). So far, no function in cellular metabolism has been ascribed to the *E. histolytica* mitosomes. The only proteins localized to these organelles are the chaperones Cpn60 (Tovar et al., 1999), Cpn10 (van der Giezen et al., 2005), and the ADP/ATP transporter supplying ATP for the funcion of chaperones (Chan et al., 2005).

2.7. Mitosomes of microsporidia

The microsporidian *Trachiplestophora hominis* contains between 7 and 47 mitosomes per cell throughout the cytoplasm (Williams et al., 2002). Unlike in *T. hominis*, only a few mitosome-like organelles are freely scattered in the cytoplasm of other microsporidia. Typically, they form a group of organelles which are associated with a spindle plaque, situated in a depression of the nuclear membrane (Vavra, 2005).
The only known function of the microsporidial remnant mitochondria is the assembly of FeS clusters (Goldberg et al., 2008).

3. BIOGENESIS OF FeS CLUSTERS

FeS clusters are protein cofactors coordinated on a polypeptide chain by cysteine residues. FeS cluster-containing proteins (FeS proteins) include enzymes (e.g. aconitase, ferrochelatase, pyruvate:ferredoxin oxidoreductase, endonuclease III), proteins involved in electron transport (e.g. ferredoxins, proteins of respiratory chain complexes) and regulators of biological processes (e.g. the oxygen sensor FNR of bacteria, the iron sensor IRP1 of mammals) (Johnson et al., 2005; Lill and Muhlenhoff, 2008). Because FeS clusters are composed of iron (Fe^{2+} and/or Fe^{3+}) and sulfide (S^{2-}), ions that are toxic in free form for the cell, FeS cluster assembly is a strictly controlled process mediated by a specific biosynthetic machinery (Johnson et al., 2005; Lill and Muhlenhoff, 2008).

3.1. FeS cluster assembly machineries

Three independent systems responsible for FeS cluster assembly have been described in bacteria. The ISC (**i**ron–**s**ulfur **c**luster) assembly machinery provides FeS clusters for

the maturation of various "housekeeping" FeS proteins (Zheng et al., 1998). The NIF (**ni**trogen **f**ixation) system is primarily responsible for the formation of the nitrogenase FeS clusters in the nitrogen-fixing bacteria (Kennedy and Dean, 1992). The SUF (**su**l**f**ur mobilization) system was demonstrated to repair FeS clusters under oxidative stress and iron-restricted conditions (Takahashi and Tokumoto, 2002). In eukaryotes, the machinery mediating FeS cluster assembly was shown to be of an ISC type. Phylogenetic analyses indicate that the mitochondrial ISC machinery was inherited from the proteobacterial endosymbiont (Tachezy et al., 2001). Components of the SUF system were found in the chloroplast and in the remnant plastid, apicoplast, of apicomplexan protists (Wilson et al., 2003). The SUF machinery was most likely inherited from cyanobacteria, the ancestors of plastids (Tachezy et al., 2001). Entamoebids and related protists are the only eukaryotes that possess components of the NIF system (Ali et al., 2004; van der Giezen et al., 2004; Gill et al., 2007).

3.2. The model eukaryotic FeS cluster assembly machinery

In all non-plant eukaryotes studied to date, FeS cluster assembly is performed by highly conserved components with similar or identical function (Fig. 1). (For the excellent review please see Lill and Muhlenhoff, 2008)

Fig. 1. Eukaryotic FeS cluster assembly machinery.

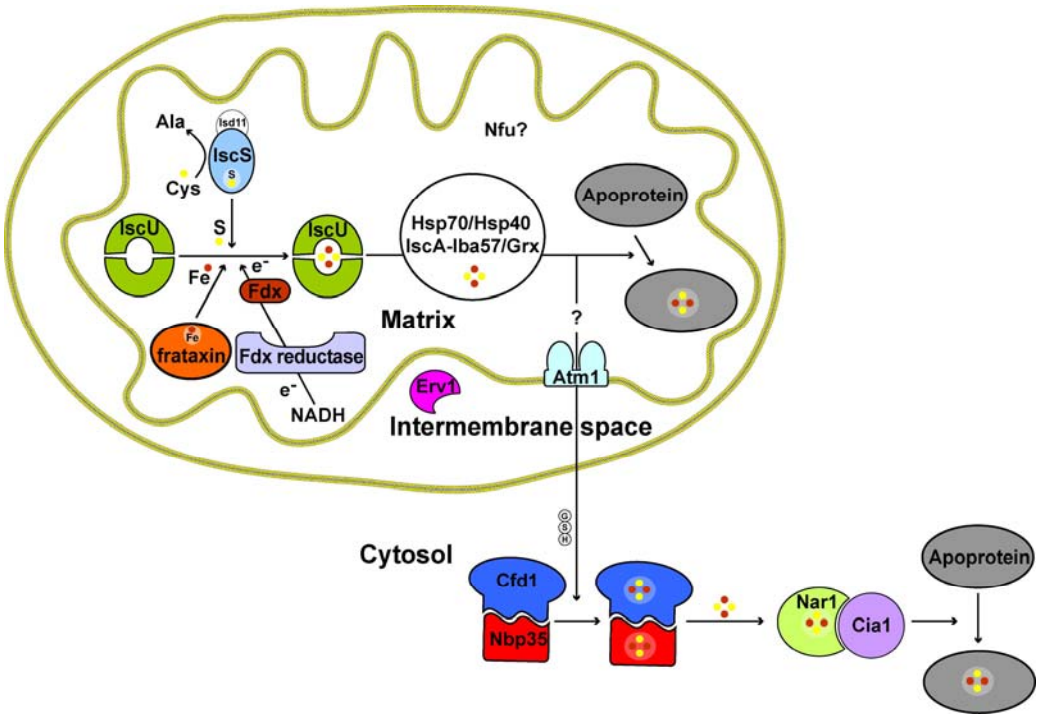

The crucial part of this biosynthetic pathway, occuring exclusively in the mitochondrion, is centered around IscU, a metallochaperone that serves as a scaffold for a new FeS cluster. The cysteine desulphurase IscS in complex with the protein Isd11 catalyzes mobilization of sulphur for the assembled FeS cluster from a cysteine molecule and delivers it to IscU. Iron is delivered to IscS/IscU complex most likely by the protein frataxin. At some point during the process of FeS cluster biogenesis, electrons are required. The mitochondrial [2Fe2S] ferredoxin and its NADH-dependent reductase form a short electron-transport chain that ends on the FeS cluster being assembled. No clear function has been ascribed to another component of FeS cluster assembly machinery, the protein Nfu. In *S. cerevisiae*, it plays an auxiliary role only, whereas in cyanobacteria and plastids it seems to function as an alternative scaffold for FeS assembly.

After the assembly on IscU, the new FeS cluster is transferred to apoproteins by the action of mitochondrial chaperones Hsp70 (Ssq1 in *S. cerevisiae*) and Hsp40 (Jac1 in *S. cerevisiae*). A nucleotide exchange factor Mge1 is required for function of Hsp70. In addition, proteins mitochondrial monothiol glutaredoxin (Grx5 of *S. cerevisiae*), IscA and Iba57 are also involved in the FeS cluster delivery to apoproteins. The monothiol glutaredoxin forms dimers with an FeS cluster bound by one cysteine residue per polypeptide chain and by two glutathione molecules per dimer (Picciocchi et al., 2007). The precise role of the mitochondrial monothiol glutaredoxin is not known. However, FeS cluster accumulation on IscU in glutaredoxin knock-out cells indicates the involvement of glutaredoxin in FeS cluster transfer from IscU to FeS apoproteins. In *S.cerevisiae*, IscA associated with Iba57 have been implicated in biogenesis of the mitochondrial 4Fe4S cluster-containing aconitase-like FeS proteins. In addition, IscA/Iba57 proteins were demonstrated to be essential for the activity, but not maturation, of the mitochondrial S-adenosylmethionine (SAM)-dependent FeS enzymes, namely biotin synthase and lipoic acid synthase.

Mitochondrial FeS cluster assembly machinery is required also for maturation of extramitochondrial FeS proteins. Even though it is still not known what kind of compound is exported from mitochondria, it is transported through the inner mitochondrial membrane by an ABC transporter Atm1. The export depends on the presence of the tripeptide glutathione and the intermembrane sulfhydryl oxidase Erv1 participates in the process. In the cytosol, extramitochondrial FeS proteins are assembled by the action of a machinery comprising two homologous NTPases Cfd1 and

Nbp35, the iron-only hydrogenase-like protein Nar1 and the WD40 repeat domains-containing protein Cia1. Cfd1 and Nbp35 form a complex serving as a scaffold for the assembly of an FeS cluster that is subsequently transferred to apoproteins by Nar1 and Cia1 (Lill et al., 2006; Lill and Muhlenhoff, 2008).

In *S. cerevisiae*, IscS, Isd11, IscU1/2, Hsp40 (Jac1), Mge1, [2Fe2S] ferredoxin Yah1, ferredoxin reductase Arh1, Erv1, GSH, Cfd1, Nbp35, Nar1 and Cia1 are the essential components of the FeS cluster assembly process (Lill and Muhlenhoff, 2005). As yet three FeS proteins not involved in FeS cluster generation were identified to be vital for cell survival, rendering FeS cluster assembly an indispensable biosynthetic pathway: Rli1, Rad3 and Pri2. Rli1, a protein conserved throughout Eukarya and Archaea, was shown to be involved in the fundamental process of protein translation initiation, most likely by mediating the assembly of RNA-protein complexes. Rad3 and Pri2 are involved in DNA metabolism. Rad3 plays a role in DNA repair while Pri2 is a primase required for DNA replication (Lill and Muhlenhoff, 2008).

3.3. FeS cluster assembly in *Trypanosoma brucei*

In the genome of *T. brucei*, genes coding for all components of FeS cluster assembly are present (Table 1). Essential function of IscS and IscU (Smid et al., 2006) and frataxin (Long et al., 2008) for procyclic *T. brucei* has been demonstrated by RNA interference (RNAi) knock-down experiments. All the studied proteins were localized exclusively in the mitochondrion, indicating that, like in *S. cerevisiae*, the FeS biosynthetic pathway is confined to this organelle. Down-regulation of IscS, IscU and frataxin expression by RNAi resulted in decreased activity of FeS-containing enzymes due to the lack of FeS centers in both the mitochondrion and cytosol, demonstrating that the mitochondrial FeS cluster assembly is required for cytosolic FeS protein maturation. Complexes I, II and III of respiratory chain, and aconitase are FeS proteins involved in critical steps of mitochondrial metabolism of *T. brucei*, which is substantially down-regulated in the bloodstream stages. Thus, the shortage of FeS clusters caused by knock-down of IscS, IscU and frataxin in procyclic *T. brucei* resulted in metabolic changes of the mitochondrion that mimicked interstagial transformation, as indicated most notably by the increase of excreted pyruvate as an end product of glucose metabolism (Smid et al., 2006; Long et al., 2008).

The monothiol glutaredoxin 1-C-Grx1 is most likely involved in FeS cluster assembly in the mitochondrion of *T. brucei*, being able to partially restore the growth phenotype

and aconitase activity of the Grx5-deficient mutant (Filser et al., 2008). The tripeptide glutathione is synthesized by the parasite, even though most of it is conjugated to spermidine to form bis(glutathionyl)spermidine. The molecule named trypanothione is used by the parasite instead of glutathione for protection from oxidant damage and toxic heavy metals (Muller et al., 2003).

3.4. FeS cluster assembly in *Plasmodium falciparum*

Apicomplexan parasites possess two organelles of endosymbiotic origin; the mitochondrion and the apicoplast, the remnant of an algal endosymbiont. Different machineries of FeS cluster synthesis are functional in the two organelles. In the mitochondrion, a system homologous to the *S. cerevisiae* FeS cluster assembly machinery ISC is most likely functional (Sato et al., 2003), while in the apicoplast a SUF machinery identical to the one of plant plastids is present . Of the former, most components were identified in the *P. falciparum* genome with the exception of the iron donor frataxin (Table 1) (Seeber, 2002; van Dooren et al., 2006). Interestingly, the highly reduced apicoplast genome of *P. falciparum* codes for SufB, a component of the SUF machinery (Seeber, 2002).

3.5. FeS cluster assembly in *Trichomonas vaginalis*

In the genome of *T. vaginalis*, genes coding for homologues of most components of FeS cluster assembly are present (Table 1) and the ability of hydrogenosomes to form FeS clusters on hydrogenosomal ferredoxin was experimentally demonstrated (Sutak et al., 2004). IscS, the key component of FeS assembly, is coded by two genes in *T. vaginalis* (TviscS1 and 2) (Tachezy et al., 2001), but only one (TviscS2) was demonstrated to be transcribed and localized to hydrogenosomes (Sutak et al., 2004).

Two genes coding for frataxin homologues were found in the genome of *T. vaginalis*. Hydrogenosomal localization was demonstrated for Tv-frataxin-2 that also partially restored defect in FeS assembly in mutant *S. cerevisiae* (Dolezal et al., 2007). Both Tv-frataxins were shown to be functional in the *T. brucei* mitochondrion. When overexpressed in mutant *T. brucei* cells in which endogenous frataxin was depleted by RNA interference, they rescued FeS cluster-defective fenotype (Long et al., 2008). Tv-frataxin-2 gene expression is upregulated under conditions of iron deficiency (Dolezal et al., 2007), unlike *S. cerevisiae* frataxin whose expression is stimulated by iron (Santos et al., 2004). Thus, it seems unlikely that the *T. vaginalis* proteins function as an

iron storage in *T. vaginalis*, a role suggested for the *S. cerevisiae* frataxin (Gakh et al., 2002a). *T. vaginalis* is as yet the only organism known to possess two functional frataxin homologues.

Four genes coding for homologues of IscA with a putative hydrogenosomal targeting sequence are present in *T. vaginalis* genome. As no aconitase-like proteins were identified in *T. vaginalis*, trichonomad IscA proteins may be required for the activity of S-adenosylmethionine (SAM)-dependent FeS enzymes in hydrogenosomes, such as HydE, a homologue of biotin synthase, and HydG. The two hydrogenosomal SAM-dependent enzymes together with the GTPase HydF were suggested to be involved in the maturation of the catalytic, hydrogen-activating (H) FeS cluster of the *T. vaginalis* hydrogenase (Putz et al., 2006).

The ABC transporter Atm1 and the sulfhydryl oxidase Erv1, components of the machinery that exports a compound needed for FeS protein maturation in the cytosol, are not present in trichomonad hydrogenosomes. Nevertheless, homologues of the cytosolic FeS protein maturation machinery comprising Nar1, Cfd1, Nbp35, and Cia1 are present in *T. vaginalis* (Tachezy and Smid, 2008).

3.6. FeS cluster assembly in *Cryptosporidium parvum*

Homologues of FeS cluster assembly proteins Isd11, IscA, Nfu were not detected in the genome of *C. parvum* while proteins with only limited similarity to glutaredoxin, Jac1, the ABC transporter Atm1 and sulfhydryl oxidase Erv1 were identified (Table 1) (Abrahamsen et al., 2004; Richards and van der Giezen, 2006). Mitosomal localization was verified for Hsp70. *C. parvum* IscU and IscS homologues possess N-terminal extensions that both targeted GFP to *S. cerevisiae* mitochondria (LaGier et al., 2003), suggesting that these components of FeS cluster assembly are localized in the remnant mitochondia of *C. parvum*. Expression of additional FeS assembly proteins frataxin, 2Fe2S ferredoxin (LaGier et al., 2003), and Nar1 (Stejskal et al., 2003) was demonstrated.

3.7. FeS cluster assembly in *Giardia intestinalis*

Mitosomal localization of homologues of IscU, IscS (Tovar et al., 2003), 2Fe2S ferredoxin (Dolezal et al., 2005), glutaredoxin (Smid et al., manuscript), and Hsp70 (Regoes et al., 2005) was demonstrated. Even though mitosome-rich fraction reconstituted FeS clusters on apoproteins (Tovar et al., 2003), a number of homologues

of FeS cluster assembly components that were shown to be essential in yeast were not identified in the genome of *G. intestinalis*, namely Isd11, ferredoxin reductase, the sulfhydryl oxidase Erv, and the non-essential frataxin and ABC transporter Atm (Table 1). These components are either highly divergent or non-homologous in *G. intestinalis* that they could not be identified, or are absent. Isd11 is a conserved protein in eukaryotes, essential for proper function of the eukaryotic IscS, but it is not present in bacterial systems. However, Isd11 seems to be absent also from the genome of *C. parvum* (Richards and van der Giezen, 2006). As for the protein components of the export machinery, the product of mitosomal FeS cluster assembly machinery may be transported to the cytosol by a similar, so far unknown transporter(s) and accesory proteins like from hydrogenosomes of *T. vaginalis*. The tripeptide glutathione has not been detected in *G. intestinalis* (Brown et al., 1993). However, the enzymes responsible for its synthesis, glutamate-cysteine ligase and glutathione synthase, are present in the *G. intestinalis* genome together with putative glutathione reductase and glutathione S-transferase. This finding together with the mitosomal localization of the monothiol glutaredoxin that was shown to coordinate FeS cluster by glutathione (Picciocchi et al., 2007; Smid et al., 2008b) indicate that the tripeptide may be present in *G. intestinalis*, albeit in concentration below the detection limit of the techniques used (Brown et al., 1993; Smid et al., 2008b).

3.8. FeS cluster assembly in *Entamoeba histolytica*

Unlike other eukaryotes, *E. histolytica* does not possess mitochondrial or plastid type of FeS assembly (Table 1). Instead, NifS and NifU, proteins of the homologous NIF system, were identified in the *E. histolytica* genome and suggested to be functional in the cytosol (Ali et al., 2004; van der Giezen et al., 2004). Phylogenetic reconstruction indicated lateral gene transfer to be the origin of NifS and NifU proteins in *E. histolytica*, with the ε-proteobacterium of the *Campylobacter* or *Helicobacter* species as most probable donor organism (van der Giezen et al., 2004). It was hypothesized that the same niche, the human gut, enabled the gene transfer from the bacterium to *E. histolytica* (van der Giezen et al., 2004). However, NIF homologues were also found in *Mastigamoeba balamuthi*, a related but free-living anaerobic protist (Gill et al., 2007). Moreover, same as in *E. histolytica*, localization of the respective protein products seems to be cytosolic (J. Tachezy, personal communication). Thus, the lateral gene transfer of NifS and NifU to *E. histolytica* probably occured before the protist adapted

to the parasitic lifestyle (Gill et al., 2007).

Table 1. FeS cluster assembly machinery of parasitic protists. Asterisk denotes essential components in *S. cerevisiae*. + high sequence similarity; ? limited sequence similarity; - no sequence similarity.

Saccharomyces cerevisiae	*Trypanosoma brucei*	*Plasmodium falciparum*	*Trichomonas vaginalis*	*Cryptosporidium parvum*	*Giardia intestinalis*	*Entamoeba histolytica*	*Encephalitozoon cuniculi*
IscS*	+	+	+	+	+	NIFS	+
Isd11*	+	+	+	-	-	-	?
IscU*	+	+	+	+	+	NIFU	+
IscA	+	+	+	-	+	-	-
ferredoxin*	+	+	+	+	+	+	+
ferredoxin reductase*	+	+	-	+	-	-	+
frataxin	+	-	+	+	-	-	+
Nfu	+	+	+	-	-	-	-
glutaredoxin	+	+	-	?	+	-	?
glutathione*	+	+	-	-	?	-	?
mtHsp70	+	+	+	+	+	+	+
Jac1*	?	+	+	?	+	?	+
Mge1*	+	+	?	+	+	?	-
Atm1	+	+	-	?	-	-	?
Erv1*	+	+	-	?	-	-	+
Nar1*	+	?	+	+	?	+	+
Cfd1*	+	?	+	+	+	+	+
Nbp35*	+	+	+	+	+	+	+
Cia1*	+	+	+	+	?	+	+

3.9. FeS cluster assembly in microsporidia

Homologues of most components of the mitochondrial FeS cluster assembly machinery were identified in the *Encephalitozoon cuniculi* genome with the exception of accessory proteins IscA, Nfu, and Mge1 (Table 1) (Katinka et al., 2001). IscU, IscS, frataxin and Hsp70 homologues were shown to localize to *E. cuniculi* mitosomes and funcionality of frataxin and glutaredoxin of *E. cuniculi* was demonstrated by the complementation of FeS cluster assembly deficiency in the respective *S. cerevisiae* mutants (Goldberg et al., 2008). The same approach was used for demonstration of the functional homology of *T. hominis* IscU. Co-expression of *T. hominis* IscS and Isd11 in *E. coli* resulted in a complex with cysteine desulphurase activity while expression of IscS alone led to the production of insoluble and inactive protein (Goldberg et al., 2008). Interestingly, unlike in *E. cuniculi* where all examined components of FeS cluster assembly machinery were localized to mitosomes, in *T. hominis* IscS and Hsp70 homologues were found in mitosomes while IscU and frataxin were detected in the cytosol

(Goldberg et al., 2008). ATP for the function of Hsp70 in FeS cluster biosynthesis is most likely imported from the parasite cytosol by the action of an unusual ADP/ATP translocase with homology to the nucleotide trasporter of plastids and bacterial intracellular parasites *Rickettsia* and *Chlamydia* (Tsaousis et al., 2008). Enzymes of glutathione synthesis are absent from the *E. cuniculi* genome. However, the presence of a gene for glutathione peroxidase in the genome of *E. cuniculi* indicates that the parasite may use glutathione synthesized by the host cell.

4. MITOCHONDRIAL PROTEIN IMPORT AND MATURATION

4.1. The eukaryotic model

4.1.1 Mitochondrial protein import

Although mitochondria harbour DNA, most mitochondrial proteins are nuclear encoded and must be specifically targeted to the organelle where they function. The information for import of mitochondrial proteins is either coded by their cleavable N-terminal extension or it is internal, being embedded within the polypeptide chain, or both. Alternatively, C-terminal targeting sequences resembling the N-terminal presequence might direct precursors to mitochondria (Lee et al., 1999; Gerber et al., 2004; Neupert and Herrmann, 2007).

N-terminal targeting presequences are typically 10 to 80 amino acid residues long and share a low degree of sequence homology. Typically, they are rich in positively-charged amino acid residues (arginine, lysine), hydroxylated residues (serine, threonine) and hydrophobic residues but devoid of negatively-charged amino acid residues (aspartate, glutamate)(Habib et al., 2007). In most presequences, an arginine residue at the position -2 from the cleavage site is present (Gakh et al., 2002b). Mitochondrial targeting presequences are also distinguished by the ability to form a positively-charged amphipathic α-helix whose opposite sides contain mainly hydrophilic and hydrophobic amino acids, respectively (Habib et al., 2007). In the absence of additional sorting information, proteins with N-terminal presequences are targeted to mitochondrial matrix. Internal targeting signals are mainly composed of hydrophobic amino acids and lack defined patterns. They are present in proteins that are destined to all mitochondrial subcompartments (Habib et al., 2007). Mitochondrial import signals are specifically recognised by receptors on the mitochondrial surface,

and the proteins are subsequently imported by translocases of the outer and inner mitochondrial membranes (for excellent recent reviews see Baker et al., 2007; Neupert and Herrman, 2007).

TRANSLOCASE OF OUTER MITOCHONDRIAL MEMBRANE

N-terminal presequences interact with the mitochondrial receptor protein Tom20 while internal signals are recognized by Tom70 (Abe et al., 2000; van Wilpe et al., 1999; Wu and Sha, 2006; Neupert and Herrmann, 2007). These receptors are integral outer mitochondrial membrane proteins exposed to the cytosol. They are clustered together with a general import pore formed by the β-barrel Tom40 and associated proteins Tom22, Tom5, Tom6 and Tom7 to the TOM complex (**t**ranslocase of the **o**uter mitochondrial **m**embrane; Fig. 2) (Neupert and Herrmann, 2007; Baker et al., 2007).

Fig. 2. The TOM complex.

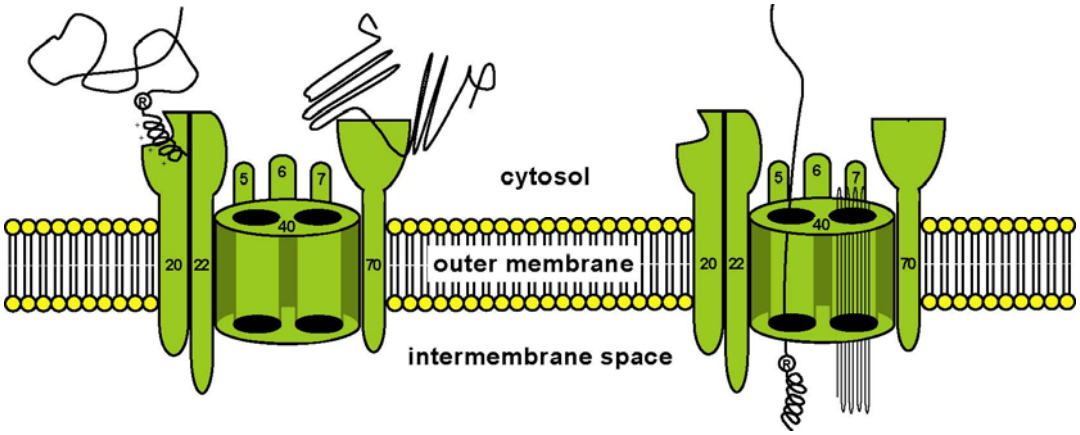

Once proteins are translocated through the outer membrane by the TOM complex, they follow one of five import pathways: **(1)** Most intermembrane proteins are released to intermembrane space after passing through the TOM complex. They are trapped in the intermembrane space by their folding that is stabilized by cofactors (metal ions or heme)(Diekert et al., 2001) or disulfide bridges (Bihlmaier et al., 2007). The latter are introduced into imported proteins by Mia40, a protein of the intermembrane space anchored in the inner mitochondrial membrane, whose activity relies on the function of another intermembrane space protein, Erv1, the conserved essential sulfhydryl oxidase (Bihlmaier et al., 2007) (Fig. 3). **(2)** All presequence-carrying proteins of mitochondrial matrix, most proteins of inner membrane and some of those targeted to intermembrane space are directed to the translocase of the inner membrane complex 23. **(3)** Most proteins of inner mitochondrial membrane are guided by small chaperones (Tim9,

Tim10) through the intermembrane space to translocase of the inner membrane complex 22. **(4)** Some proteins are inserted into the inner membrane by Oxa1 complex from the mitochondrial matrix. **(5)** Outer membrane proteins are integrated into the membrane by the sorting and assembly machinery complex.

Fig. 3. Trapping of imported proteins in the mitochondrial intermembrane space.

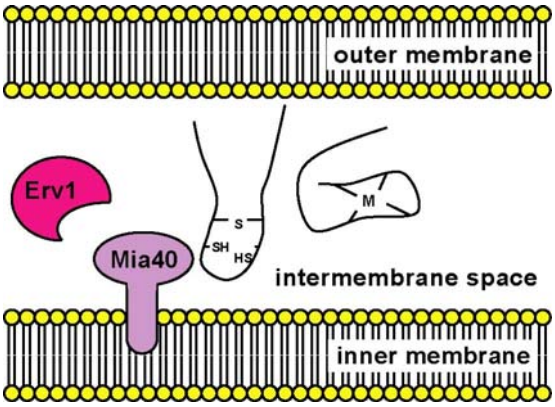

TRANSLOCASE OF INNER MITOCHONDRIAL MEMBRANE COMPLEX 23

The **t**ranslocase of the **i**nner mitochondrial **m**embrane complex **23** (TIM23) is composed of a protein-translocating channel and a protein import motor (Fig. 4). The membrane pore is assembled from integral membrane proteins Tim17, Tim21, Tim23 and Tim50. Tim17 and Tim23 form a core of the translocase (Martinez-Caballero et al., 2007) while Tim50 is a receptor of imported proteins (Mokranjac et al., 2003). The translocation of the presequence through the TIM23 pore requires membrane potential (Martin et al., 1991; Truscott et al., 2001). Once on the matrix side of TIM23, the presequence is bound by the mitochondrial chaperone Hsp70 recruited by a matrix protein Tim44 (D'Silva et al., 2004).

Hsp70 is an ATPase whose affinity to protein substrates and Tim44 depends on the nucleotide state. Hsp70 with bound ATP has a higher affinity to Tim44 than the ADP form. The ATP-binding Hsp70 associates with imported preproteins. After hydrolysis of ATP, the substrate binding pocket of Hsp70 closes, resulting in tight binding of substrates. The exchange of ADP by ATP on Hsp70 occurs through the nucleotide free state, a step that requires the action of the nucleotide exchange protein Mge1 (Liu et al., 2003). The activity of Hsp70 is regulated by import motor proteins Pam18 and Pam16 that are brought to the vicinity of Hsp70 by Tim44. Pam18 stimulates ATP-hydrolysing activity of Hsp70 while Pam16 is a negative regulator of Pam18 (D'Silva et al., 2008). Binding of Hsp70 prevents backward sliding of imported

preproteins and leads to their stepwise transport to the mitochondrial matrix (Neupert and Herrmann, 2007). The molecular motor is powered by ATP needed in the reaction cycle for binding of the polypeptide chain to Hsp70 and for release of Hsp70 from Tim44.

Fig. 4. Import of matrix proteins by the TIM23 complex.

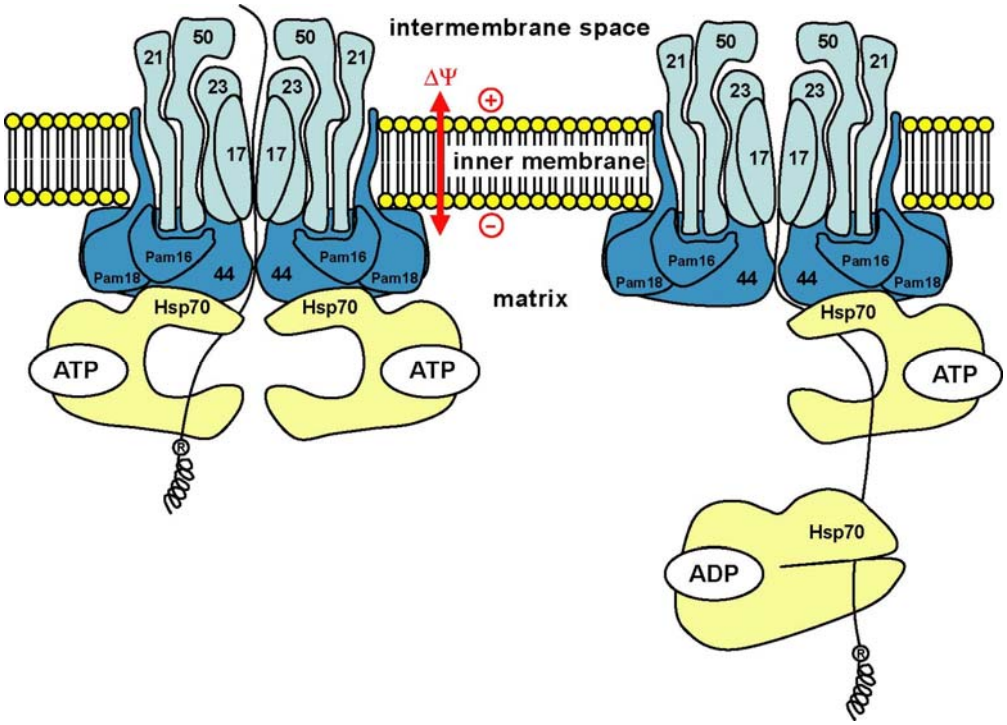

Inner membrane proteins imported by TIM23 possess, in addition to N-terminal targeting sequence, a stop-transfer signal that arrests the precursor during the import reaction at the level of the inner membrane and promotes the lateral insertion into the lipid bilayer (Fig.5) (Meier et al., 2005).

Fig. 5. Import of proteins of the inner membrane and intermembrane space by the TIM23 complex. Intermembrane proteins are processed by IMP.

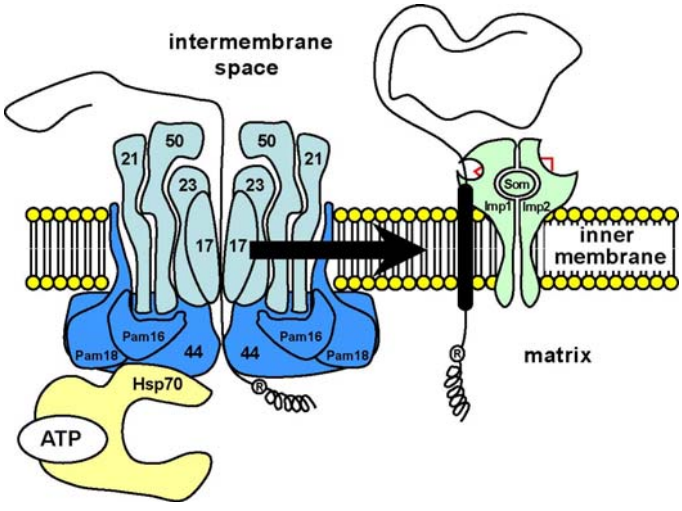

The stop-transfer signal is characteristic by the presence of highly hydrophobic amino acid residues that are followed by charged residues. Proline is absent from these signal sequences (Meier et al., 2005). Some proteins localized in the intermembrane space are arrested in the inner membrane by the stop-transfer signal and subsequently released by the protease of inner mitochondrial membrane (IMP, see below) (Langer, 2000; Herlan et al., 2004; Burri et al., 2005).

TRANSLOCASE OF INNER MITOCHONDRIAL MEMBRANE COMPLEX 22

Mitochondrial carrier proteins and Tim17, Tim22 and Tim23 subunits are recognized by chaperones that are capable of guiding hydrophobic proteins through intermembrane space to the translocase of the inner mitochondrial membrane complex 22 (TIM22) that inserts them to the inner membrane (Fig. 6). Tim9 and Tim10 form hexamers that, most likely, bind hydrophobic regions of imported inner membrane proteins (Webb et al., 2006). A homologous complex of Tim8 and Tim 13 recognizes the same set of substrates as the Tim9/10 chaperone (Gentle et al., 2007). The core of the TIM22 complex is the integral membrane protein Tim22 to which the membrane proteins Tim54 and Tim18 are accessory components (Kerscher et al., 2000; Hwang et al., 2007). Tim9, Tim10 and Tim12 are associated with the intermembrane side of the TIM22 as a protein complex that may play a vital role for substrate recognition by the TIM22 (Gebert et al., 2008). Integration of imported proteins into the inner membrane by TIM22 is fuelled by electrochemical potential on the inner mitochondrial membrane (Peixoto et al., 2007).

Fig. 6. Import of inner membrane proteins by the TIM22 complex.

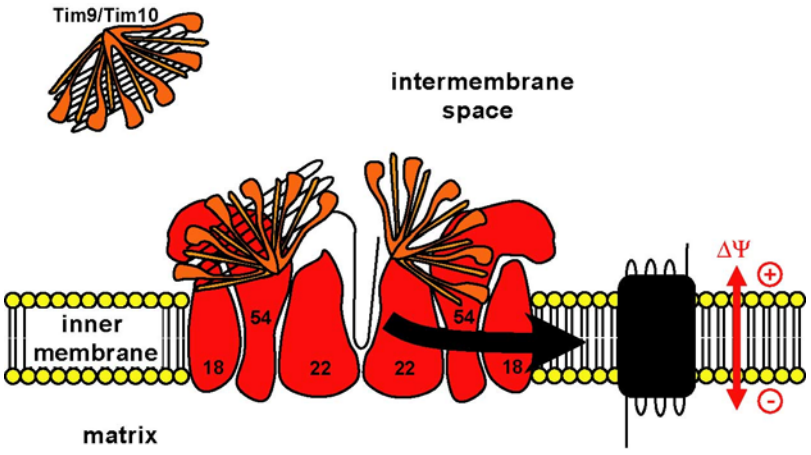

OXA1

Some inner membrane proteins follow the so called conservative sorting pathway that resembles the export of membrane proteins in bacteria and reflects that of the prokaryotic ancestors of mitochondria. These proteins are first imported into the mitochondrial matrix by the action of TOM and TIM23 complexes. After cleavage of the N-terminal presequence (see below), they are recognized by the Oxa1 that inserts them into the inner mitochondrial membrane (Fig. 7)(Jia et al., 2007). The sorting signal sequence is rich in negatively charged residues. Membrane insertion by Oxa1 depends on the membrane potential, most likely because the transfer of the negatively charged regions to the positively charged intermembrane space drives the insertion reaction (Herrmann et al., 1997).

Fig. 7. Sorting of inner membrane proteins by Oxa1.

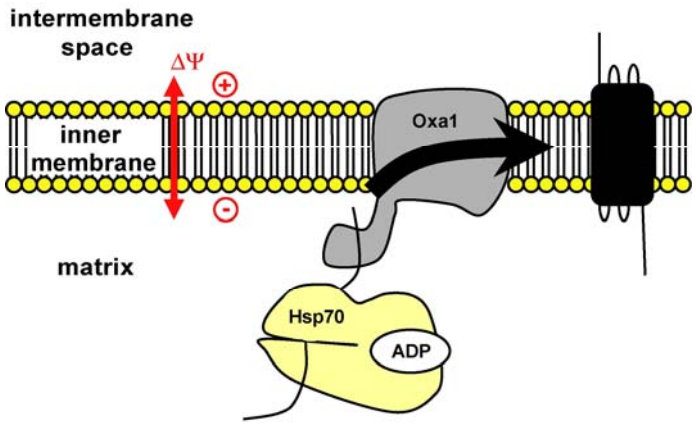

SORTING AND ASSEMBLY MACHINERY COMPLEX

In the intermembrane space, β-barrel proteins of outer mitochondrial membrane are guided by the hexameric Tim9/Tim10 and Tim8/13 complexes to the **s**orting and **a**ssembly **m**achinery complex (SAM) that inserts them to the outer membrane (Fig. 8)(Wiedemann et al., 2003). SAM is composed of a β-barrel protein Sam50 associated on the cytosolic face with two essential proteins, Sam35 and Sam37. Sam35 seems to function in substrate binding while Sam37 is required for release of substrates from the SAM complex (Chan and Lithgow, 2008). Membrane proteins Mdm12 and Mmm1 associated with the SAM complex assist β-barrel protein insertion into the outer membrane (Meisinger et al., 2007). The β-barrel protein Mdm10 is specifically involved in Tom40 membrane insertion (Meisinger et al., 2004). The outer mitochondrial

membrane protein Mim1 that also associates with the SAM complex is required for efficient membrane insertion and assembly of Tom20 and Tom70 (Becker et al., 2008).

Fig. 8. Sorting of outer membrane proteins by the SAM complex.

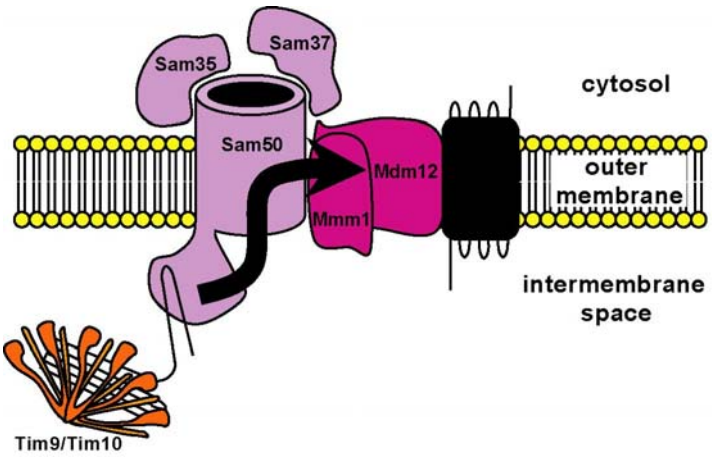

4.1.2 Mitochondrial protein maturation

N-terminal mitochondrial targeting presequences present on most proteins imported to mitochondrial matrix interfere with protein function and/or its stability (Mukhopadhyay et al., 2007). Therefore, they are cleaved off after import by a mitochondrial processing peptidase (MPP). In all mitochondria studied so far, MPP functions as a heterodimer. The catalytic beta subunit (βMPP) binds a zinc cation by amino acid residues of the conserved motif $HXXEHX_{76}E$ that is a hallmark for the metallopeptidases of the M16 family. The regulatory alpha subunit (αMPP) is characterized by the presence of a stretch of glycine residues in a flexible loop that is essential for interaction with a substrate (Nagao et al., 2000; Nishino et al., 2007). The two subunits form a large central cavity for accommodation of the substrate during processing. Due to a number of glutamate residues interspersed on both alpha and beta subunits, the cavity is hydrophilic and negatively charged (Fig. 9)(Taylor et al., 2001).

The positively charged residues of N-terminal targeting presequences bind to the glutamates of MPP by means of electrostatic interaction (Kitada and Ito, 2001). In most presequences, the arginine of the presequence proximal to the cleavage site at position P_2 or P_3 is present. Mutational analyses indicated that the P_2 (P_3) arginine is important for processing site recognition by MPP and interacts with the glutamate of the active site of MPP (Kitada et al., 2003). Positively-charged residues distal from the processing site of short presequences bind to acidic residues on βMPP while those of longer

presequences at positions from P_7 might reach to glutamates of αMPP (Kojima et al., 1998; Shimokata et al., 1998; Kojima et al., 2001; Taylor et al., 2001; Kitada et al., 2003). This interaction helps stabilize the MPP-presequence complex (Kitada et al., 2003). When distal positively-charged residues are mutated, the processing activity of MPP with such presequences is less efficient (Niidome et al., 1994; Kojima et al., 1998).

Fig. 9. The structure and charge distribution of *S. cerevisiae* MPP (Taylor et al., 2001). **A**, α and β subunits of the MPP are shown in grey and yellow, respectively. Zinc binding residues of the β subunit are highlighted in green while the glycine-rich loop of the α subunit is red. **B** and **C**, Charge distribution within the cavities of α and β MPP subunits, respectively. Red and blue colours denote negative and positive charge (±5 kT/e where kT is thermal energy and e is unit charge), respectively, whereas white denote relatively non-polar regions.

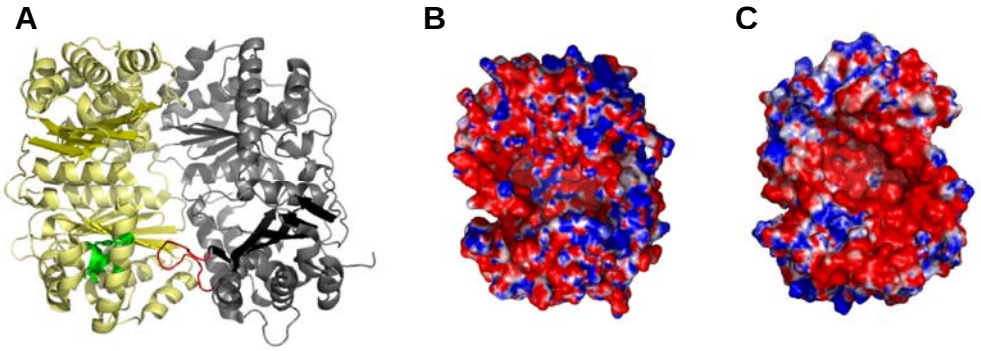

It is unclear whether the secondary structure of the presequence plays any role in interaction with MPP since the presequence is in extended conformation inside the MPP cavity (Taylor et al., 2001). Helix-breaking residues such as glycine and proline as well as hydroxylated residues serine and threonine are often present among basic residues of presequences (Habib et al., 2007). Proline and glycine residues are required for bending of longer presequences inside the MPP central cavity towards the alpha subunit (Kojima et al., 2001). Amino acid sequence C-terminal from the cleavage site is important for efficient processing, too. P_1' residue is recognized by a S_1' phenylalanine residue of the beta subunit (Taylor et al., 2001) while P_2' and P_3' interact with the glycine-rich loop (Nishino et al., 2007).

Gene duplication of the single-subunit ancestral peptidase of the mitochondrial endosymbiont (Kitada et al., 2007), protein dimerization and subunit specialization enabled the processing peptidase to recognize and accommodate such heterogeneous substrates. Originally, the hydrophillic peptidase was localized in the organellar matrix. For efficient cleavage of targeting presequences during or immediatelly after the import

into the matrix (Glaser and Dessi, 1999), a portion of the processing peptidase associated with the endosymbiont bc_1 complex of respiratory chain (Braun and Schmitz, 1995; Murcha et al., 2004), eventually becoming essential for mitochondrial bc_1 complex assembly and stability as Core 1 and 2 proteins (Xia et al., 1997; Glaser and Dessi, 1999).

In higher plants, Core 1 and 2 are identical with βMPP and αMPP subunits, respectively, that same as the matrix-localized α/βMPP cleave mitochondrial targeting presequences (Glaser and Dessi, 1999). In other organisms studied to date, including green algae (Nurani et al., 1997; Brumme et al., 1998), one or both Core proteins diverged from MPP subunits, losing the conserved zinc binding motif or glycine rich loop essential for MPP activity (Xia et al., 1997; Glaser and Dessi, 1999; Deng et al., 2001). The divergence of Core proteins as structural parts of bc_1 complex from the active MPP localized in mitochondrial matrix allowed for separate regulation of mitochondrial respiration and protein import (Howell et al., 2007).

After cleavage by MPP, a number of imported mitochondrial proteins reveals a characteristic octapeptide motif (F/L/I)(S/X)(S/T/X)(T/S/G)XXXX. The motif is recognized and processed by mitochondrial intermediate peptidase (MIP), a soluble monomeric metallopeptidase localized in mitochondrial matrix (Gakh et al., 2002b).

Many proteins targeted to intermembrane space possess bipartite presequence costisting of an MPP-cleavable targeting signal that is followed by an intermembrane-space sorting signal. The latter is processed by inner membrane peptidase, IMP (Fig. 5). The *S. cerevisiae* Imp is a membrane-associated serine endopeptidase comprising catalytic Imp1 and Imp2 subunits and a regulatory subunit Som1. Interestingly, the two Imp subunits cleave different sets of substrates. Imp2 recognizes and processes substrates with an alanine residue at the position P_1 and a serine at P_3. By contrast, Imp1 cleaves substrates with an asparagine at P_3. Imp1 and Imp2 are homologous proteins, related to the type I bacterial leader peptidases that process N-terminal signal of precursors traversing the bacterial membrane. Same as MPP, the two homologous Imp subunits evolved from the bacterial peptidase by gene duplication. Divergence of substrate specificity of the two active subunits allowed for a higher number of substrates to be recognized and processed. As the regulatory Som1 subunit is not homologous to any bacterial protein, it has been added to the IMP most likely by the host during the evolution of the mitochondrion (Gakh et al., 2002b).

Fig. 10. Overview of the mitochondrial protein import machinery.

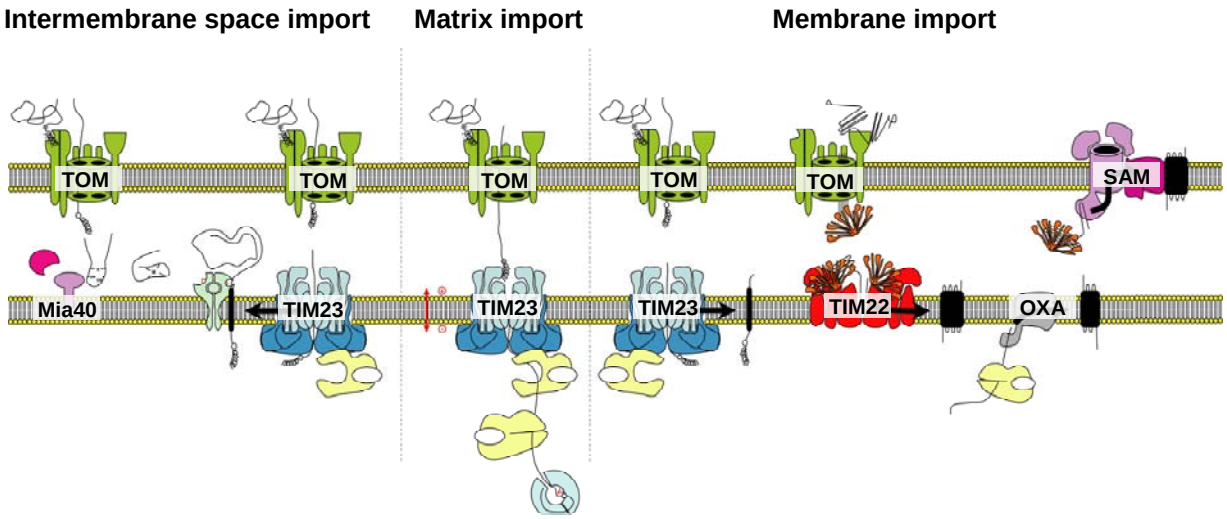

4.2. Mitochondrial protein import and maturation in *Trypanosoma brucei*

Proteins imported to the *T. brucei* mitochondrion utilize either the N-terminal extension or an internal signal for targeting to the organelle (Schneider et al., 2008). In general, N-terminal mitochondrial presequences of *T. brucei* are similar in composition to those of *S. cerevisiae* but shorter, ranging from 9 to 44 amino acid residues. Nevertheless, even the short (9 amino acid residues) presequence of lipoamide dehydrogenase targeted the precursor protein to yeast mitochondria *in vivo* and *in vitro* (Hausler et al., 1997). The *T. brucei* presequences often contain $MX_{1\text{-}2}$(K/R)(K/R) motif where *X* is usually a hydrophobic amino acid residue (Hausler et al., 1997; Priest and Hajduk, 2003).

Interestingly, no components of the TOM complex were identified in the *T. brucei* genome so far and only a single homologue of the evolutionarily related translocases Tim17, Tim22 and Tim23 has been found in *T. brucei* (TbTim17) that functions most likely as both TIM23 and TIM22 complex (Gentle et al., 2007; Singha et al., 2008; Schneider et al., 2008). The presequence import motor consisting of Pam18, Tim44, and mtHsp70 homologues identified in the genome may associate with TbTim17 to import presequence-containing precursors while the homologues of Tim9, Tim10 and Tim8/13 may guide carrier proteins to the TbTim17 and outer membrane proteins to the SAM complex (Gentle et al., 2007). Oxa homologues were suggested to be responsible for insertion of inner membrane proteins from mitochondrial matrix (Schneider et al., 2008) (Fig. 11).

T. brucei aconitase, the enzyme of citric acid cycle, is localized in both the mitochondrion and the cytosol. It has been hypothesized that the dual localization of the enzyme is caused either by inefficient targeting information of the uncleaved N-terminal sequence or by aborted translocation into the mitochondrion as reported for the *S. cerevisiae* fumarase that is released back to cytosol after cleavage by MPP (Saas et al., 2000). Import of several proteins into isolated *T. brucei* mitochondria was examined, including (i) the Rieske protein that is translocated into the matrix and then exported to intermembrane space; (ii) the chaperone Hsp70 of mitochondrial matrix; (iii) the NADH dehydrogenase subunit K (NdhK), a matrix protein associated with transmembrane subunits of NADH dehydrogenase; (iv) the transmembrane terminal alternative oxidase (TAO); (v) cytochrome oxidase subunit IV (COXIV), a matrix protein associated with cytochrome oxidase complex; and (vi) intermembrace space protein cytochrome c_1. Import into the procyclic mitochondria of the precursors of the Rieske iron-sulfur protein, Hsp70 (Priest and Hajduk, 1996), NdhK (Bertrand and Hajduk, 2000), TAO, and COXIV (Williams et al., 2008) depends on membrane potential as well as on cytosolic and mitochondrial matrix ATP. By contrast, the import of the intermembrace space protein cytochrome c_1 into the mitochondrion of procyclics does not require membrane potential and matrix ATP, however, it is dependent on cytosolic pool of ATP (Priest and Hajduk, 2003). Interestingly, cytochrome c_1 possesses on its C-terminus a sequence that is reminiscent of mitochondrial targeting presequence that may be inserted into the inner membrane after the protein translocation from mitochondrial matrix to the intermembrane space, as was suggested for the *S. cerevisiae* homologue (Priest and Hajduk, 2003). The requirements for efficient import of the precursor NdhK into the mitochondrion of bloodstream *T. brucei* were identical as those for import into procyclics mitochondria (Bertrand and Hajduk, 2000). Unexpectedly, import of TAO and COXIV into the mitochondrion of bloodstream stage of *T. brucei* was not abolished after dissipation of membrane potential (Williams et al., 2008).

Rieske protein, Hsp70, TAO, COXIV, and NhdK were demonstrated to be processed in mitochondrial matrix by a metallopeptidase, most likely by MPP (Priest and Hajduk, 1996; Bertrand and Hajduk, 2000; Williams et al., 2008). Indeed, genes coding for homologues of α and βMPP subunits proteins were identified in the *T. brucei* genome (Berriman et al., 2005). The Rieske protein possesses bipartite presequence. After initial cleavage in mitochondrial matrix, the Rieske protein is translocated into the intermembrane space where the protein is processed by another metallopeptidase. The

characteristic octapeptide cleavage motif and metal ion requirements suggest that the peptidase responsible for the Rieske protein cleavage might be the mitochondrial intermediate peptidase relocated from mitochondrial matrix to intermembrane space (Priest and Hajduk, 1996). In addition to MPP and MIP, a gene for a single Imp subunit homologue is present in the *T. brucei* genome, however, the regulatory subunit Som1 seems to be missing (Berriman et al., 2005) (Fig. 11).

Fig. 11. Mitochondrial protein import machinery of *T. brucei*.

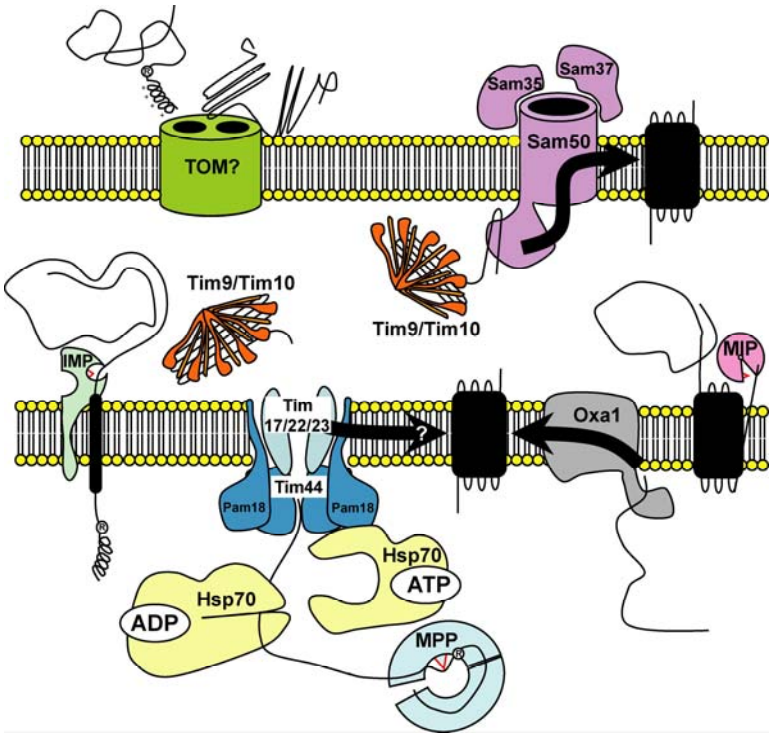

4.3. Mitochondrial protein import and maturation in *Plasmodium falciparum*

N-terminal presequences targeting mitochondrial proteins to the *P. falciparum* mitochondria differ in relative amino acid frequencies from mitochondrial presequences of other eukaryotes. Alanine, glycine, proline and arginine are under-represented while phenylalanine, isoleucine, lysine, asparagine and tyrosine occur more than two times as often in *P. falciparum* mitochondrial presequences (Bender et al., 2003). Despite these differences that reflect overall amino acid composition of *P. falciparum* proteome, most likely caused by low G + C content, other characteristics of mitochondrial targeting sequences are conserved, including positive net charge (Bender et al., 2003). N-terminal part of Cpn60 and IscS homologues (Sato et al., 2003) as well as the presequence of citrate synthase (Tonkin et al., 2004) were sufficient to guide GFP passenger protein to

mitochondria. Besides the N-terminal extension, inner targeting signal is present in membrane proteins of *P. falciparum* mitochondria (van Dooren et al., 2006).

In the genome of *P. falciparum*, genes coding for homologues of the core components of TOM complex, Tom40 and Tom22, were identified. The protein product of Tom22 was shown to be localized to mitochondria (van Dooren et al., 2006). Of the TIM23 complex, Tim23, Tim17, Tim50 homologues were found in the genome whereas a clear homologue of Tim21 is missing as in other protists (van Dooren et al., 2006; Dyall and Dolezal, 2008). Protein import motor components Hsp70, Tim44, Mge1, and Pam18 seem to be present based on genomic data (Dolezal et al., 2005; van Dooren et al., 2006). Genes coding for all small Tim proteins, Tim9, Tim10, Tim8 and Tim13 were identified (Gentle et al., 2007). The inner membrane protein Tim22 was found in the *P. falciparum* genome, however, Tim18 and Tim54, additional components of the TIM22 complex, were not (van Dooren et al., 2006). Conservative sorting of the inner membrane proteins seems to be functional in *P. falciparum* as gene coding for Oxa1 was detected. Sam50 of the outer membrane was identified in the *P. falciparum* genome (Dolezal et al., 2006) (Fig. 12).

Fig. 12. Mitochondrial protein import machinery of *P. falciparum.*.

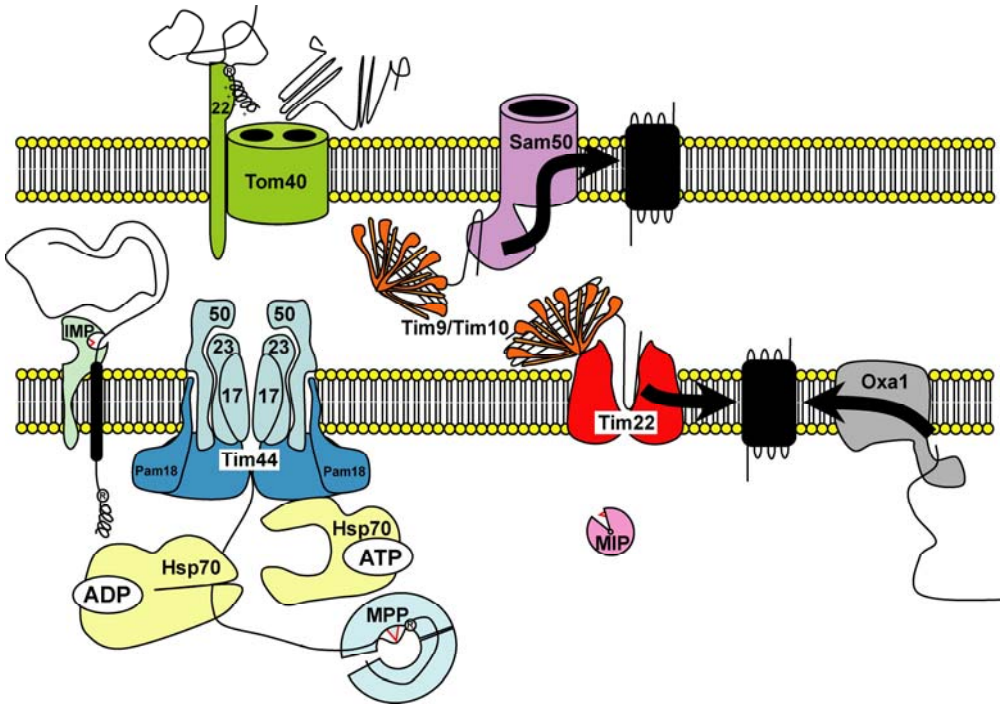

Based on genomic data, the αMPP and βMPP subunits are most likely identical with Core 2 and 1 proteins of the respiratory chain complex III, respectively, resembling a

situation in the plant mitochondrion. Interestingly, all apicomplexan protists whose genome sequences are available possess only the two MPP subunits and no Core proteins (our unpublished observation). The ability of the αMPP and βMPP proteins to form an active processing peptidase within the complex III was noted to correlate with the presence of a chloroplast in a cell. Complex III of plants with the chloroplast exhibited peptidase activity while complex III purified from *Polytomella*, a non-green alga, did not (Brumme et al., 1998). The absence of core proteins in plastid-harbouring protists Apicomplexa suggests that the active αMPP and βMPP subunits may be part of respiratory chain complex III. So far, the reason for the requirement of a proteolytically active complex III is not known.

In the genome of *P. falciparum*, a putative Imp homologue is present as well as a homologue of MIP (Fig. 12). The IMP regulatory subunit Som1 was not identified (Gardner et al., 2002).

4.4. Hydrogenosomal protein import and maturation in *Trichomonas vaginalis*

Proteins imported to *T. vaginalis* hydrogenosomes possess the targeting information either as a N-terminal extension or internal signal, or both (Dyall and Dolezal, 2008). The length of the 22 N-terminal presequences that have been experimentally verified range from 4 to 19 amino acid resides (Smid et al., 2008a). The primary structure of hydrogenosomal presequences is rather conserved when compared to mitochondrial presequences, most prominent is the presence and functional requirement of leucine after the initial methionine (Bradley et al., 1997; Dyall and Dolezal, 2008). Hydrogenosomal presequences can be classified into two groups based on the presence or absence of distal positively-charged residues (Smid et al., 2008a).

The presequences of hydrogenosomal proteins ferredoxin, β-subunit of succinyl CoA synthetase and pyruvate:ferredoxin oxidoreductase were reported to guide a passenger protein to *T. brucei* and *S. cerevisiae* mitochondria, albeit with low efficiency (Hausler et al., 1997). However, presequence of Tv-frataxin, eight amino acid residues long and containing proximal arginine only, directed the preprotein to *T. brucei* mitochondrion (Long et al., 2008) but not to *S. cerevisiae* mitochondria (Dolezal et al., 2007). The membrane ADP/ATP carrier protein Hmp31 was demonstrated to possess an unusual, negatively charged cleavable N-terminal presequence together with an internal signal. The presequence was found to be dispensable for targeting and integration of Hmp31 in the membrane, but was necessary and sufficient for directing a passenger

protein to soluble hydrogenosomal fraction (Dyall et al., 2000). By contrast, the β-barrel protein Hmp35 of hydrogenosomal membranes carries an internal signal only (Dyall et al., 2003).

A homologue of the core component of the SAM complex, Sam50, was detected together with components of the TIM23 complex, namely Tim17 and Tim23 (Dolezal et al., 2006). Protein import motor seems to be present in the hydrogenosomes of *T. vaginalis* as homologues of Hsp70 (Bui et al., 1996), Tim44 (Dolezal et al., 2006), and Mge1 (Dyall and Dolezal, 2008) are present in the *T. vaginalis* genome and Pam18 was localized to hydrogenosomes (Dolezal et al., 2005) (Fig. 14). However, no homologues of components of the TOM, TIM22 or small Tims were identified in the genome of *T. vaginalis* (Dolezal et al., 2006; Dyall and Dolezal, 2008). Thus, protein import machinery into *T. vaginalis* hydrogenosomes is either simplified when compared to the mitochondrial one and/or highly divergent or, alternatively, functionally similar but evolutionarily unrelated.

Hydrogenosomal processing peptidase (HPP) functions as a heterodimer comprising divergent homologues of αMPP and βMPP subunits, αHPP and βHPP, respectively. Unlike mitochondrial processing peptidase, a homodimer of βHPP subunits cleaves a fluorescent substrate with low efficiency *in vitro* (Arretz et al., 1994; Brown et al., 2007; Smid et al., 2008a). Neither Imp nor Som1 of IMP were detected and only a putative candidate for a homologue of MIP without targeting sequence is present in the *T. vaginalis* genome (Carlton et al., 2007) (Fig. 14).

Fig. 14. Hydrogenosomal protein import machinery of *T. vaginalis*.

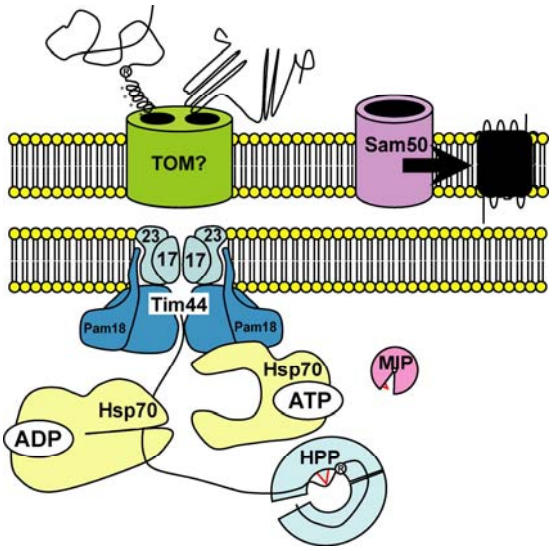

4.5. Mitosomal protein import and maturation in *Cryptosporidium parvum*

Unlike *P. falciparum* mitochondrial presequences, the amino acid composition of *C. parvum* Hsp70 N-terminal mitosomal presequence is similar to presequences of other eukaryotes. Moreover, it was sufficient for targeting of passenger GFP protein to *S. cerevisiae* and *Toxoplasma gondii* mitochondria (Slapeta and Keithly, 2004). N-terminal portion of *C. parvum* Cpn60 targeted passenger GFP protein to *S. cerevisiae* mitochondria as did predicted mitosomal leaders of *C. parvum* IscS and IscU (LaGier et al., 2003).

A reduced set of protein import machinery components was identified in the *C. parvum* genome: Tom40 and Sam50 of the outer membrane (Dolezal et al., 2006), a hybrid chaperone protein Tim8-13 (Gentle et al., 2007), inner membrane TIM23 translocase proteins Tim17 and Tim23 (Dolezal et al., 2006), and protein import motor components Hsp70 (Slapeta and Keithly, 2004), Pam18 and Tim44 (Henriquez et al., 2005). Genes coding for both αMPP and βMPP homologues are present in the *C. parvum* genome. Clear homologues of MIP and the regulatory Som1 subunit of IMP are missing, but a gene coding for the catalytic Imp subunit homologue can be detected (Abrahamsen et al., 2004) (Fig. 13).

Fig. 13. Mitosomal protein import machinery of *C. parvum*.

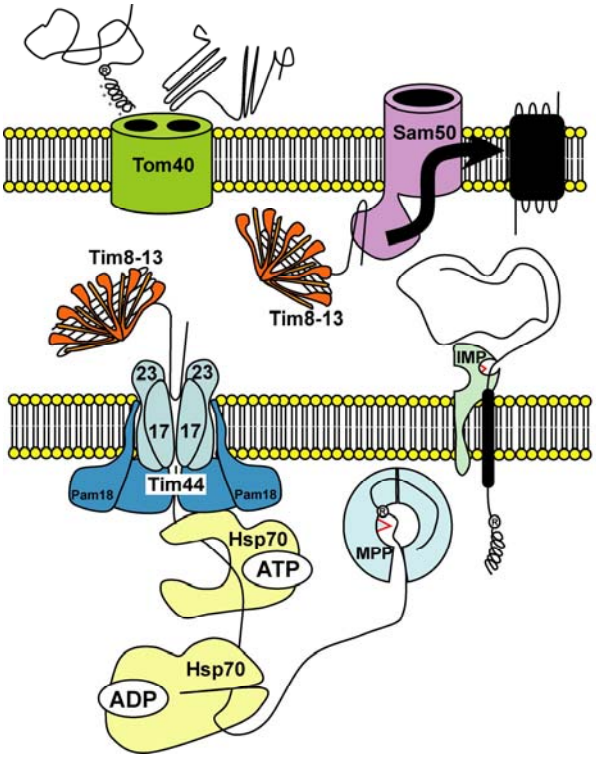

4.6. Mitosomal protein import and maturation in *Giardia intestinalis*

The targeting information for import of mitosomal proteins was shown to be either on an N-terminal extension or present as an internal signal (Dolezal et al., 2005). Three proteins of *G. intestinalis* were demonstrated to possess cleavable N-terminal extensions: IscU, ferredoxin, and IscA (Dolezal et al., 2005; Smid et al., 2008a). Mitosomal presequences resemble mitochondrial presequences in that they are rich in hydrophobic and hydroxylated amino acid residues, but they lack distal positively-charged amino acid residues (Smid et al., 2008a). The IscU and ferredoxin targeting sequences were able to direct proteins into hydrogenosomes of *T. vaginalis* (Dolezal et al., 2005). N-terminal part of mitosomal ferredoxin comprising a cleavable presequence and seven amino acid residues of the mature protein guided the passenger GFP protein to mitochondria of human kidney cells (Regoes et al., 2005). In addition to the cleavable presequence, IscU contains a signal localized within the mature part of the protein that is sufficient to guide IscU without the N-terminal presequence to mitosomes, although with lower efficiency (Dolezal et al., 2005). Most likely, the mitosomal import of mature IscU depends on the N-terminal part of the protein as the IscU without first eight amino acid residues did not target the passenger GFP protein to mitosomes (Regoes et al., 2005). In contrast to ferredoxin, IscA and IscU, mitosomal matrix proteins IscS, Cpn60 and mtHsp70 lack N-terminal targeting sequences and import into the mitosome is driven only by an internal signal (Dolezal et al., 2005; Regoes et al., 2005).

Of the protein import machinery, only homologues of Pam18 and mitochondrial Hsp70 were identified in the genome of *G. intestinalis* and their mitosomal localization was demonstrated (Dolezal et al., 2005; Dyall and Dolezal, 2008). The question whether the mitosomal protein import machinery is extremely reduced, or composed of components that are either too divergent or unrelated is currently under investigation.

N-terminal extensions of mitosomal preproteins are cleaved by mitosomal processing peptidase (GPP). As yet uniquely among eukaryotes, GPP of *G. intestinalis* is functional as a monomer homologous to the βMPP subunit. Even though the quaternary structure of GPP is markedly different from MPP, biochemical properties of the two metallopeptidases are comparable. Sophisticated phylogenetic analyses indicated that GPP most probably evolved by reduction of a formerly heterodimeric enzyme and not directly from the monomeric bacterial protease presumably present in mitochondrial endosymbiont (Smid et al., 2008a; Kitada et al., 2007). Comparison of tertiary structures and substrate specifities of GPP, HPP, and MPP suggested that the

co-evolution with presequences was the major selective force shaping the three processing peptidases and provided a possible explanation of GPP reduction. In mitochondria, αMPP is involved in (i) initial recognition of hundreds of substrates of varying sequence and length and (ii) immobilization of longer substrates by interaction with their distal positively charged residues during processing. Mitosomes of *G. intestinalis* are highly simplified organelles. The reduction of overall protein content was accompanied by shortening of mitosomal targeting presequences, a trend that can be seen in other organisms (Hausler et al., 1997; Bradley et al., 1997; Burri et al., 2006). The low number of short presequences that, in addition, do not contain distal positively charged residues, most likely allowed for the loss of α subunit of the mitosomal processing peptidase, leading to reduction of a formerly heterodimeric enzyme to a functional βGPP monomer (Smid et al., 2008a). Apart from GPP, no other mitochondrial processing peptidase homologue was found in the *G. intestinalis* genome (Morrison et al., 2007).

4.7. Mitosomal protein import and maturation in *Entamoeba histolytica*

Similarly to *T. vaginalis* hydrogenosomal presequences, N-terminal extension of Cpn60 required for the protein mitosomal localization possesses leucine as the amino acid residue after the first methionine and is enriched in serine residues (Tovar et al., 1999). In addition to Cpn60, such presequences were found to be present on Hsp70 and pyridine nucleotide transhydrogenase (Bakatselou et al., 2003), but the localization of these proteins has not been verified yet. Mitosomal localization of Cpn10, a co-chaperone of Cpn60, was demonstrated (van der Giezen et al., 2005). Like all known mitochondrial Cpn10 of other eukaryotes, Cpn10 of *E. histolytica* does not possess an N-terminal presequence. The targeting information is carried within the mature part of the protein, same as the information for mitosomal localization of the identified ADP/ATP transporter (Chan et al., 2005). Of the mitosomal protein import machinery, only a mitochondrial Hsp70 (Arisue et al., 2002), a single βMPP homologue and a putative MIP gene were identified in the genome of *E. histolytica* thus far (Loftus et al., 2005).

4.8. Mitosomal protein import and maturation in microsporidia

N-terminal portions of the predicted mitosomal proteins of the two microsporidia whose genome was or is being sequenced, *E. cuniculi* and *Antonospora locustae*, respectively,

lack defined characteristics. Full length *A. locustae* ferredoxin, frataxin, glyceraldehyde 3-phosphate dehydrogenase (G3PDH), Imp subunit 2, ferredoxin reductase (FNR), and *E. cuniculi* IscU guided passenger GFP to *S. cerevisiae* mitochondria. Of these proteins, only *A. locustae* G3PDH N-terminal extension alone was able to target passenger GFP to the yeast mitochondria. Nevertheless, N-terminally truncated version of the *A. locustae* G3PDH-GFP fusion protein was targeted to the yeast mitochondria, too, indicating that the protein employs an additional internal targeting signal. Besides *A. locustae* G3PDH-GFP, internal targeting information has been shown to be responsible for mitochondrial localization of *A. locustae* FNR-GFP; other examined fusion proteins possessed the targeting information on their N-termini (Burri et al., 2006).

A reduced mitochondrial protein import machinery is present in the mitosomes of microsporidia. Based on genomic data of *E. cuniculi*, a putative Tom70 receptor together with the core component of the translocation pore Tom40 seem to form the TOM40 complex of the outer membrane (Katinka et al., 2001). Genes coding for Sam50 of the SAM (Dolezal et al., 2006), Tim22 of the TIM22 and Tim17 of the TIM23 complexes (Burri et al., 2006) were detected in the *E. cuniculi* genome. A homologue of mitochondrial Hsp70 (Peyretaillade et al., 1998) is the only identified component of the import motor. Proteins are processed only in the mitosomes of *A. locustae* by Imp2, the only homologue of a mitochondrial protease identified so far (Burri et al., 2006) (Fig. 15).

Fig. 15. Mitosomal protein import machinery of microsporidia.

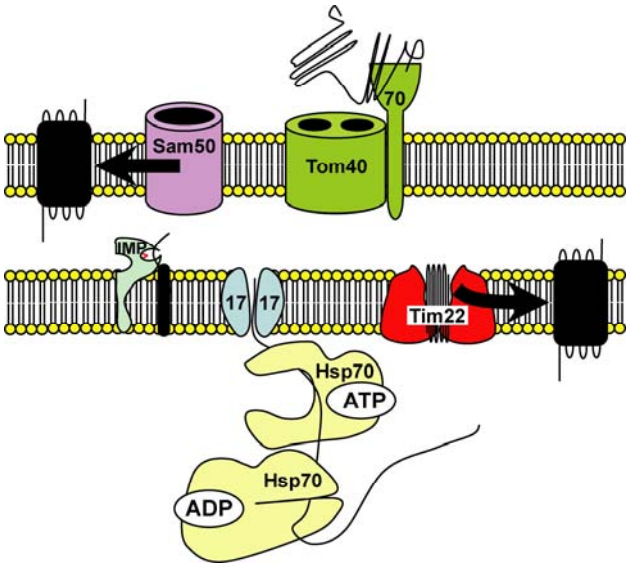

5. REFERENCES

1. Abe, Y., Shodai, T., Muto, T., Mihara, K., Torii, H., Nishikawa, S., Endo, T., Kohda, D. (2000). Structural basis of presequence recognition by the mitochondrial protein import receptor Tom20. *Cell* 100:551-560.

2. Abrahamsen, M.S., Templeton, T.J., Enomoto, S., Abrahante, J.E., Zhu, G., Lancto, C.A., Deng, M., Liu, C., Widmer, G., Tzipori, S. ***et al.*** (2004). Complete genome sequence of the apicomplexan, Cryptosporidium parvum. *Science* 304:441-445.

3. Ali, V., Shigeta, Y., Tokumoto, U., Takahashi, Y., Nozaki, T. (2004). An intestinal parasitic protist, Entamoeba histolytica, possesses a non-redundant nitrogen fixation-like system for iron-sulfur cluster assembly under anaerobic conditions. *J Biol Chem* 279:16863-16874.

4. Arisue, N., Sanchez, L.B., Weiss, L.M., Muller, M., Hashimoto, T. (2002). Mitochondrial-type hsp70 genes of the amitochondriate protists, Giardia intestinalis, Entamoeba histolytica and two microsporidians. *Parasitol Int* 51:9-16.

5. Arretz, M., Schneider, H., Guiard, B., Brunner, M., Neupert, W. (1994). Characterization of the mitochondrial processing peptidase of Neurospora crassa. *J Biol Chem* 269:4959-4967.

6. Bakatselou, C., Beste, D., Kadri, A.O., Somanath, S., Clark, C.G. (2003). Analysis of genes of mitochondrial origin in the genus Entamoeba. *J Eukaryot Microbiol* 50:210-214.

7. Baker, M.J., Frazier, A.E., Gulbis, J.M., Ryan, M.T. (2007). Mitochondrial protein-import machinery: correlating structure with function. *Trends Cell Biol* 17:456-464.

8. Becker, T., Pfannschmidt, S., Guiard, B., Stojanovski, D., Milenkovic, D., Kutik, S., Pfanner, N., Meisinger, C., Wiedemann, N. (2008). Biogenesis of the mitochondrial TOM complex: Mim1 promotes insertion and assembly of signal-anchored receptors. *J Biol Chem* 283:120-127.

9. Bender, A., van Dooren, G.G., Ralph, S.A., McFadden, G.I., Schneider, G. (2003). Properties and prediction of mitochondrial transit peptides from Plasmodium falciparum. *Mol Biochem Parasitol* 132:59-66.

10. Berriman, M., Ghedin, E., Hertz-Fowler, C., Blandin, G., Renauld, H., Bartholomeu, D.C., Lennard, N.J., Caler, E., Hamlin, N.E., Haas, B. ***et al.*** (2005). The genome of the African trypanosome Trypanosoma brucei. *Science* 309:416-422.

11. Bertrand, K.I. , Hajduk, S.L. (2000). Import of a constitutively expressed protein into mitochondria from procyclic and bloodstream forms of Trypanosoma brucei. *Mol Biochem Parasitol* 106:249-260.

12. Bihlmaier, K., Mesecke, N., Terziyska, N., Bien, M., Hell, K., Herrmann, J.M. (2007). The disulfide relay system of mitochondria is connected to the respiratory chain. *J Cell Biol* 179:389-395.

13. Bochud-Allemann, N. , Schneider, A. (2002). Mitochondrial substrate level phosphorylation is essential for growth of procyclic Trypanosoma brucei. *J Biol Chem* 277:32849-32854.

14. Bouzaidi-Tiali, N., Aeby, E., Charriere, F., Pusnik, M., Schneider, A. (2007). Elongation factor 1a mediates the specificity of mitochondrial tRNA import in T. brucei. *EMBO J* 26:4302-4312.

15. Bradley, P.J., Lahti, C.J., Plumper, E., Johnson, P.J. (1997). Targeting and translocation of proteins into the hydrogenosome of the protist Trichomonas: similarities with mitochondrial protein import. *EMBO J* 16:3484-3493.

16. Braun, H.P. , Schmitz, U.K. (1995). Are the 'core' proteins of the mitochondrial bc1 complex evolutionary relics of a processing protease? *Trends Biochem Sci* 20:171-175.

17. Brown, D.M., Upcroft, J.A., Upcroft, P. (1993). Cysteine is the major low-molecular weight thiol in Giardia duodenalis. *Mol Biochem Parasitol* 61:155-158.

18. Brown, M.T., Goldstone, H.M., Bastida-Corcuera, F., gadillo-Correa, M.G., McArthur, A.G., Johnson, P.J. (2007). A functionally divergent hydrogenosomal peptidase with protomitochondrial ancestry. *Mol Microbiol* 64:1154-1163.

19. Brown, S.V., Hosking, P., Li, J., Williams, N. (2006). ATP synthase is responsible for maintaining mitochondrial membrane potential in bloodstream form Trypanosoma brucei. *Eukaryot Cell* 5:45-53.

20. Brumme, S., Kruft, V., Schmitz, U.K., Braun, H.P. (1998). New insights into the co-evolution of cytochrome c reductase and the mitochondrial processing peptidase. *J Biol Chem* 273:13143-13149.

21. Bui, E.T.N., Bradley, P.J., Johnson, P.J. (1996). A common evolutionary origin for mitochondria and hydrogenosomes. *Proc Natl Acad Sci U S A* 93:9651-9656.

22. Burri, L., Strahm, Y., Hawkins, C.J., Gentle, I.E., Puryer, M.A., Verhagen, A., Callus, B., Vaux, D., Lithgow, T. (2005). Mature DIABLO/Smac is produced by the IMP protease complex on the mitochondrial inner membrane. *Mol Biol Cell* 16:2926-2933.

23. Burri, L., Williams, B.A., Bursac, D., Lithgow, T., Keeling, P.J. (2006). Microsporidian mitosomes retain elements of the general mitochondrial targeting system. *Proc Natl Acad Sci U S A* 103:15916-15920.

24. Carlton, J.M., Hirt, R.P., Silva, J.C., Delcher, A.L., Schatz, M., Zhao, Q., Wortman, J.R., Bidwell, S.L., Alsmark, U.C., Besteiro, S. *et al.* (2007). Draft genome sequence of the sexually transmitted pathogen Trichomonas vaginalis. *Science* 315:207-212.

25. Chan, K.W., Slotboom, D.J., Cox, S., Embley, T.M., Fabre, O., van der Giezen, M., Harding, M., Horner, D.S., Kunji, E.R.S., Leon-Avila, G. *et al.* (2005). A novel ADP/ATP transporter in the mitosome of the microaerophilic human parasite Entamoeba histolytica. *Current Biology* 15:737-742.

26. Chan, N.C. , Lithgow, T. (2008). The Peripheral Membrane Subunits of the SAM Complex Function Codependently in Mitochondrial Outer Membrane Biogenesis. *Mol Biol Cell* 19:126-136.

27. Chaudhuri, M., Ajayi, W., Hill, G.C. (1998). Biochemical and molecular properties of the Trypanosoma brucei alternative oxidase. *Molecular and Biochemical Parasitology* 95:53-68.

28. Clayton, C.E. , Michels, P. (1996). Metabolic compartmentation in African trypanosomes. *Parasitology Today* 12:465-471.

29. Ctrnacta, V., Ault, J.G., Stejskal, F., Keithly, J.S. (2006). Localization of pyruvate:NADP+ oxidoreductase in sporozoites of Cryptosporidium parvum. *J Eukaryot Microbiol* 53:225-231.

30. D'Silva, P., Liu, Q., Walter, W., Craig, E.A. (2004). Regulated interactions of mtHsp70 with Tim44 at the translocon in the mitochondrial inner membrane. *Nat Struct Mol Biol* 11:1084-1091.

31. D'Silva, P.R., Schilke, B., Hayashi, M., Craig, E.A. (2008). Interaction of the j-protein heterodimer pam18/pam16 of the mitochondrial import motor with the translocon of the inner membrane. *Mol Biol Cell* 19:424-432.

32. Deng, K., Shenoy, S.K., Tso, S.C., Yu, L., Yu, C.A. (2001). Reconstitution of mitochondrial processing peptidase from the core proteins (subunits I and II) of bovine heart mitochondrial cytochrome bc(1) complex. *J Biol Chem* 276:6499-6505.

33. Diekert, K., de Kroon, A.I., Ahting, U., Niggemeyer, B., Neupert, W., de, K.B., Lill, R. (2001). Apocytochrome c requires the TOM complex for translocation across the mitochondrial outer membrane. *EMBO J* 20:5626-5635.

34. Dolezal, P., Dancis, A., Lesuisse, E., Sutak, R., Hrdy, I., Embley, T.M., Tachezy, J. (2007). Frataxin, a conserved mitochondrial protein, in the hydrogenosome of Trichomonas vaginalis. *Eukaryot Cell* 6:1431-1438.

35. Dolezal, P., Likic, V., Tachezy, J., Lithgow, T. (2006). Evolution of the molecular machines for protein import into mitochondria. *Science* 313:314-318.

36. Dolezal, P., Smid, O., Rada, P., Zubacova, Z., Bursac, D., Sutak, R., Nebesarova, J., Lithgow, T., Tachezy, J. (2005). Giardia mitosomes and trichomonad hydrogenosomes share a common mode of protein targeting. *Proc Natl Acad Sci U S A* 102:10924-10929.

37. Dyall, S.D., Dolezal, P. in *Hydrogenosomes and Mitosomes: Mitochondria of Anaerobic Eukaryotes*, eds Tachezy, J. (Springer Berlin / Heidelberg), pp 21-73.

38. Dyall, S.D., Koehler, C.M., gadillo-Correa, M.G., Bradley, P.J., Plumper, E., Leuenberger, D., Turck, C.W., Johnson, P.J. (2000). Presence of a member of the mitochondrial carrier family in hydrogenosomes: conservation of membrane-targeting pathways between hydrogenosomes and mitochondria. *Mol Cell Biol* 20:2488-2497.

39. Dyall, S.D., Lester, D.C., Schneider, R.E., gadillo-Correa, M.G., Plumper, E., Martinez, A., Koehler, C.M., Johnson, P.J. (2003). Trichomonas vaginalis Hmp35, a putative pore-forming hydrogenosomal membrane protein, can form a complex in yeast mitochondria. *J Biol Chem* 278:30548-30561.

40. Filser, M., Comini, M.A., Molina-Navarro, M.M., Dirdjaja, N., Herrero, E., Krauth-Siegel, R.L. (2008). Cloning, functional analysis, and mitochondrial localization of Trypanosoma brucei monothiol glutaredoxin-1. *Biol Chem* 389:21-32.

41. Gakh, O., Adamec, J., Gacy, A.M., Twesten, R.D., Owen, W.G., Isaya, G. (2002a). Physical evidence that yeast frataxin is an iron storage protein. *Biochemistry* 41:6798-6804.

42. Gakh, O., Cavadini, P., Isaya, G. (2002b). Mitochondrial processing peptidases. *Biochim Biophys Acta* 1592:63-77.

43. Gardner, M.J., Hall, N., Fung, E., White, O., Berriman, M., Hyman, R.W., Carlton, J.M., Pain, A., Nelson, K.E., Bowman, S. *et al.* (2002). Genome sequence of the human malaria parasite Plasmodium falciparum. *Nature* 419:498-511.

44. Gebert, N., Chacinska, A., Wagner, K., Guiard, B., Koehler, C.M., Rehling, P., Pfanner, N., Wiedemann, N. (2008). Assembly of the three small Tim proteins precedes docking to the mitochondrial carrier translocase. *EMBO Rep* 9:548-554.

45. Gentle, I.E., Perry, A.J., Alcock, F.H., Likic, V.A., Dolezal, P., Ng, E.T., Purcell, A.W., McConnville, M., Naderer, T., Chanez, A.L. *et al.* (2007). Conserved motifs reveal details of ancestry and structure in the small TIM chaperones of the mitochondrial intermembrane space. *Mol Biol Evol* 24:1149-1160.

46. Gerber, J., Neumann, K., Prohl, C., Muhlenhoff, U., Lill, R. (2004). The yeast scaffold proteins Isu1p and Isu2p are required inside mitochondria for maturation of cytosolic Fe/S proteins. *Mol Cell Biol* 24:4848-4857.

47. Gill, E.E., az-Trivino, S., Barbera, M.J., Silberman, J.D., Stechmann, A., Gaston, D., Tamas, I., Roger, A.J. (2007). Novel mitochondrion-related organelles in the anaerobic amoeba Mastigamoeba balamuthi. *Mol Microbiol* 66:1306-1320.

48. Glaser, E. , Dessi, P. (1999). Integration of the mitochondrial-processing peptidase into the cytochrome bc1 complex in plants. *J Bioenerg Biomembr* 31:259-274.

49. Goldberg, A.V., Molik, S., Tsaousis, A.D., Neumann, K., Kuhnke, G., Delbac, F., Vivares, C.P., Hirt, R.P., Lill, R., Embley, T.M. (2008). Localization and functionality of microsporidian iron-sulphur cluster assembly proteins. *Nature* 452:624-628.

50. Habib, S.J., Neupert, W., Rapaport, D. (2007). Analysis and prediction of mitochondrial targeting signals. *Methods Cell Biol* 80:761-781.

51. Hausler, T., Stierhof, Y.D., Blattner, J., Clayton, C. (1997). Conservation of mitochondrial targeting sequence function in mitochondrial and hydrogenosomal proteins from the early-branching eukaryotes Crithidia, Trypanosoma and Trichomonas. *Eur J Cell Biol* 73:240-251.

52. Henriquez, F.L., Richards, T.A., Roberts, F., McLeod, R., Roberts, C.W. (2005). The unusual mitochondrial compartment of Cryptosporidium parvum. *Trends Parasitol* 21:68-74.

53. Herlan, M., Bornhovd, C., Hell, K., Neupert, W., Reichert, A.S. (2004). Alternative topogenesis of Mgm1 and mitochondrial morphology depend on ATP and a functional import motor. *J Cell Biol* 165:167-173.

54. Herrmann, J.M., Neupert, W., Stuart, R.A. (1997). Insertion into the mitochondrial inner membrane of a polytopic protein, the nuclear-encoded Oxa1p. *EMBO J* 16:2217-2226.

55. Howell, K.A., Cheng, K., Murcha, M.W., Jenkin, L.E., Millar, A.H., Whelan, J. (2007). Oxygen initiation of respiration and mitochondrial biogenesis in rice. *J Biol Chem* 282:15619-15631.

56. Hrdy, I., Tachezy, J., Muller, M. in *Hydrogenosomes and Mitosomes: Mitochondria of Anaerobic Eukaryotes*, eds Tachezy, J. (Springer Berlin / Heidelberg), pp 113-145.

57. Hwang, D.K., Claypool, S.M., Leuenberger, D., Tienson, H.L., Koehler, C.M. (2007). Tim54p connects inner membrane assembly and proteolytic pathways in the mitochondrion. *J Cell Biol* 178:1161-1175.

58. Jia, L., Dienhart, M.K., Stuart, R.A. (2007). Oxa1 directly interacts with Atp9 and mediates its assembly into the mitochondrial F1Fo-ATP synthase complex. *Mol Biol Cell* 18:1897-1908.

59. Johnson, D.C., Dean, D.R., Smith, A.D., Johnson, M.K. (2005). Structure, function, and formation of biological iron-sulfur clusters. *Annu Rev Biochem* 74:247-281.

60. Katinka, M.D., Duprat, S., Cornillot, E., Metenier, G., Thomarat, F., Prensier, G., Barbe, V., Peyretaillade, E., Brottier, P., Wincker, P. *et al.* (2001). Genome sequence and gene compaction of the eukaryote parasite Encephalitozoon cuniculi. *Nature* 414:450-453.

61. Keithly, J.S. in *Hydrogenosomes and Mitosomes: Mitochondria of Anaerobic Eukaryotes*, eds Tachezy, J. (Springer Berlin / Heidelberg), pp 231-253.

62. Keithly, J.S., Langreth, S.G., Buttle, K.F., Mannella, C.A. (2005). Electron tomographic and ultrastructural analysis of the Cryptosporidium parvum relict mitochondrion, its associated membranes, and organelles. *J Eukaryot Microbiol* 52:132-140.

63. Kennedy, C. , Dean, D. (1992). The nifU, nifS and nifV gene products are required for activity of all three nitrogenases of Azotobacter vinelandii. *Mol Gen Genet* 231:494-498.

64. Kerscher, O., Sepuri, N.B., Jensen, R.E. (2000). Tim18p is a new component of the Tim54p-Tim22p translocon in the mitochondrial inner membrane. *Mol Biol Cell* 11:103-116.

65. Kitada, S. , Ito, A. (2001). Electrostatic recognition of matrix targeting signal by mitochondrial processing peptidase. *J Biochem* 129:155-161.

66. Kitada, S., Uchiyama, T., Funatsu, T., Kitada, Y., Ogishima, T., Ito, A. (2007). A protein from a parasitic microorganism, Rickettsia prowazekii, can cleave the signal sequences of proteins targeting mitochondria. *J Bacteriol* 189:844-850.

67. Kitada, S., Yamasaki, E., Kojima, K., Ito, A. (2003). Determination of the cleavage site of the presequence by mitochondrial processing peptidase on the substrate binding scaffold and the multiple subsites inside a molecular cavity. *J Biol Chem* 278:1879-1885.

68. Kojima, K., Kitada, S., Ogishima, T., Ito, A. (2001). A proposed common structure of substrates bound to mitochondrial processing peptidase. *J Biol Chem* 276:2115-2121.

69. Kojima, K., Kitada, S., Shimokata, K., Ogishima, T., Ito, A. (1998). Cooperative formation of a substrate binding pocket by alpha- and beta-subunits of mitochondrial processing peptidase. *J Biol Chem* 273:32542-32546.

70. LaGier, M.J., Tachezy, J., Stejskal, F., Kutisova, K., Keithly, J.S. (2003). Mitochondrial-type iron-sulfur cluster biosynthesis genes (IscS and IscU) in the apicomplexan Cryptosporidium parvum. *Microbiology* 149:3519-3530.

71. Langer, T. (2000). AAA proteases: cellular machines for degrading membrane proteins. *Trends Biochem Sci* 25:247-251.

72. Lee, C.M., Sedman, J., Neupert, W., Stuart, R.A. (1999). The DNA helicase, Hmi1p, is transported into mitochondria by a C-terminal cleavable targeting signal. *J Biol Chem* 274:20937-20942.

73. Leon-Avila, G. , Tovar, J. (2004). Mitosomes of Entamoeba histolytica are abundant mitochondrion-related remnant organelles that lack a detectable organellar genome. *Microbiology* 150:1245-1250.

74. Lill, R., Dutkiewicz, R., Elsasser, H.P., Hausmann, A., Netz, D.J., Pierik, A.J., Stehling, O., Urzica, E., Muhlenhoff, U. (2006). Mechanisms of iron-sulfur protein maturation in mitochondria, cytosol and nucleus of eukaryotes. *Biochim Biophys Acta* 1763:652-667.

75. Lill, R. , Muhlenhoff, U. (2005). Iron-sulfur-protein biogenesis in eukaryotes. *Trends Biochem Sci* 30:133-141.

76. Lill, R. , Muhlenhoff, U. (2008). Maturation of iron-sulfur proteins in eukaryotes: mechanisms, connected processes, and diseases. *Annu Rev Biochem* 77:669-700.

77. Liu, B., Liu, Y., Motyka, S.A., Agbo, E.E., Englund, P.T. (2005). Fellowship of the rings: the replication of kinetoplast DNA. *Trends Parasitol* 21:363-369.

78. Liu, Q., D'Silva, P., Walter, W., Marszalek, J., Craig, E.A. (2003). Regulated cycling of mitochondrial Hsp70 at the protein import channel. *Science* 300:139-141.

79. Loftus, B., Anderson, I., Davies, R., Alsmark, U.C., Samuelson, J., Amedeo, P., Roncaglia, P., Berriman, M., Hirt, R.P., Mann, B.J. *et al.* (2005). The genome of the protist parasite Entamoeba histolytica. *Nature* 433:865-868.

80. Long, S., Jirku, M., Mach, J., Ginger, M.L., Sutak, R., Richardson, D., Tachezy, J., Lukes, J. (2008). Ancestral roles of eukaryotic frataxin: mitochondrial frataxin function and heterologous expression of hydrogenosomal Trichomonas homologues in trypanosomes. *Mol Microbiol*.

81. Lukes, J., Hashimi, H., Zikova, A. (2005). Unexplained complexity of the mitochondrial genome and transcriptome in kinetoplastid flagellates. *Curr Genet* 48:277-299.

82. Martin, J., Mahlke, K., Pfanner, N. (1991). Role of An Energized Inner Membrane in Mitochondrial Protein Import - Delta-Psi Drives the Movement of Presequences. *J Biol Chem* 266:18051-18057.

83. Martinez-Caballero, S., Grigoriev, S.M., Herrmann, J.M., Campo, M.L., Kinnally, K.W. (2007). Tim17p regulates the twin pore structure and voltage gating of the mitochondrial protein import complex TIM23. *J Biol Chem* 282:3584-3593.

84. Meier, S., Neupert, W., Herrmann, J.M. (2005). Proline residues of transmembrane domains determine the sorting of inner membrane proteins in mitochondria. *J Cell Biol* 170:881-888.

85. Meisinger, C., Pfannschmidt, S., Rissler, M., Milenkovic, D., Becker, T., Stojanovski, D., Youngman, M.J., Jensen, R.E., Chacinska, A., Guiard, B. *et al.* (2007). The morphology proteins Mdm12/Mmm1 function in the major beta-barrel assembly pathway of mitochondria. *EMBO J* 26:2229-2239.

86. Meisinger, C., Rissler, M., Chacinska, A., Szklarz, L.K., Milenkovic, D., Kozjak, V., Schonfisch, B., Lohaus, C., Meyer, H.E., Yaffe, M.P. *et al.* (2004). The mitochondrial morphology protein Mdm10 functions in assembly of the preprotein translocase of the outer membrane. *Dev Cell* 7:61-71.

87. Michels, P.A., Moyersoen, J., Krazy, H., Galland, N., Herman, M., Hannaert, V. (2005). Peroxisomes, glyoxysomes and glycosomes (review). *Mol Membr Biol* 22:133-145.

88. Mokranjac, D., Paschen, S.A., Kozany, C., Prokisch, H., Hoppins, S.C., Nargang, F.E., Neupert, W., Hell, K. (2003). Tim50, a novel component of the TIM23 preprotein translocase of mitochondria. *EMBO J* 22:816-825.

89. Morrison, H.G., McArthur, A.G., Gillin, F.D., Aley, S.B., Adam, R.D., Olsen, G.J., Best, A.A., Cande, W.Z., Chen, F., Cipriano, M.J. *et al.* (2007). Genomic minimalism in the early diverging intestinal parasite Giardia lamblia. *Science* 317:1921-1926.

90. Mukhopadhyay, A., Yang, C.S., Wei, B., Weiner, H. (2007). Precursor Protein Is Readily Degraded in Mitochondrial Matrix Space if the Leader Is Not Processed by Mitochondrial Processing Peptidase. *J Biol Chem* 282:37266-37275.

91. Muller, S., Liebau, E., Walter, R.D., Krauth-Siegel, R.L. (2003). Thiol-based redox metabolism of protozoan parasites. *Trends Parasitol* 19:320-328.

92. Murcha, M.W., Elhafez, D., Millar, A.H., Whelan, J. (2004). The N-terminal extension of plant mitochondrial carrier proteins is removed by two-step processing: the first cleavage is by the mitochondrial processing peptidase. *J Mol Biol* 344:443-454.

93. Nagao, Y., Kitada, S., Kojima, K., Toh, H., Kuhara, S., Ogishima, T., Ito, A. (2000). Glycine-rich region of mitochondrial processing peptidase alpha-subunit is essential for binding and cleavage of the precursor proteins. *J Biol Chem* 275:34552-34556.

94. Neupert, W. , Herrmann, J.M. (2007). Translocation of proteins into mitochondria. *Annu Rev Biochem* 76:723-749.

95. Niidome, T., Kitada, S., Shimokata, K., Ogishima, T., Ito, A. (1994). Arginine Residues in the Extension Peptide Are Required for Cleavage of A Precursor by Mitochondrial Processing Peptidase - Demonstration Using Synthetic Peptide As A Substrate. *J Biol Chem* 269:24719-24722.

96. Nishino, T.G., Kitano, K., Kojima, K., Ogishima, T., Ito, A., Kitada, S. (2007). Spatial orientation of mitochondrial processing peptidase and a preprotein revealed by fluorescence resonance energy transfer. *J Biochem* 141:889-895.

97. Nurani, G., Eriksson, M., Knorpp, C., Glaser, E., Franzen, L.G. (1997). Homologous and heterologous protein import into mitochondria isolated from the green alga Chlamydomonas reinhardtii. *Plant Mol Biol* 35:973-980.

98. Painter, H.J., Morrisey, J.M., Mather, M.W., Vaidya, A.B. (2007). Specific role of mitochondrial electron transport in blood-stage Plasmodium falciparum. *Nature* 446:88-91.

99. Peixoto, P.M., Grana, F., Roy, T.J., Dunn, C.D., Flores, M., Jensen, R.E., Campo, M.L. (2007). Awaking TIM22, a dynamic ligand-gated channel for protein insertion in the mitochondrial inner membrane. *J Biol Chem* 282:18694-18701.

100. Peyretaillade, E., Broussolle, V., Peyret, P., Metenier, G., Gouy, M., Vivares, C.P. (1998). Microsporidia, amitochondrial protists, possess a 70-kDa heat shock protein gene of mitochondrial evolutionary origin. *Mol Biol Evol* 15:683-689.

101. Picciocchi, A., Saguez, C., Boussac, A., Cassier-Chauvat, C., Chauvat, F. (2007). CGFS-type monothiol glutaredoxins from the cyanobacterium Synechocystis PCC6803 and other evolutionary distant model organisms possess a glutathione-ligated [2Fe-2S] cluster. *Biochemistry* 46:15018-15026.

102. Priest, J.W. , Hajduk, S.L. (1996). In vitro import of the Rieske iron-sulfur protein by trypanosome mitochondria. *J Biol Chem* 271:20060-20069.

103. Priest, J.W. , Hajduk, S.L. (2003). Trypanosoma brucei cytochrome c1 is imported into mitochondria along an unusual pathway. *J Biol Chem* 278:15084-15094.

104. Putz, S., Dolezal, P., Gelius-Dietrich, G., Bohacova, L., Tachezy, J., Henze, K. (2006). Fe-hydrogenase maturases in the hydrogenosomes of Trichomonas vaginalis. *Eukaryot Cell* 5:579-586.

105. Regoes, A., Zourmpanou, D., Leon-Avila, G., van der, G.M., Tovar, J., Hehl, A.B. (2005). Protein import, replication, and inheritance of a vestigial mitochondrion. *J Biol Chem* 280:30557-30563.

106. Richards, T.A. , van der Giezen, M. (2006). Evolution of the Isd11-IscS complex reveals a single alpha-proteobacterial endosymbiosis for all eukaryotes. *Mol Biol Evol* 23:1341-1344.

107. Roberts, C.W., Roberts, F., Henriquez, F.L., Akiyoshi, D., Samuel, B.U., Richards, T.A., Milhous, W., Kyle, D., McIntosh, L., Hill, G.C. ***et al.*** (2004). Evidence for mitochondrial-derived alternative oxidase in the apicomplexan parasite Cryptosporidium parvum: a potential anti-microbial agent target. *Int J Parasitol* 34:297-308.

108. Saas, J., Ziegelbauer, K., von, H.A., Fast, B., Boshart, M. (2000). A developmentally regulated aconitase related to iron-regulatory protein-1 is localized in the cytoplasm and in the mitochondrion of Trypanosoma brucei. *J Biol Chem* 275:2745-2755.

109. Santos, R., Buisson, N., Knight, S.A., Dancis, A., Camadro, J.M., Lesuisse, E. (2004). Candida albicans lacking the frataxin homologue: a relevant yeast model for studying the role of frataxin. *Mol Microbiol* 54:507-519.

110. Sato, S., Rangachari, K., Wilson, R.J. (2003). Targeting GFP to the malarial mitochondrion. *Mol Biochem Parasitol* 130:155-158.

111. Schnaufer, A., Clark-Walker, G.D., Steinberg, A.G., Stuart, K. (2005). The F1-ATP synthase complex in bloodstream stage trypanosomes has an unusual and essential function. *EMBO J* 24:4029-4040.

112. Schneider, A., Bursac, D., Lithgow, T. (2008). The direct route: a simplified pathway for protein import into the mitochondrion of trypanosomes. *Trends Cell Biol* 18:12-18.

113. Seeber, F. (2002). Biogenesis of iron-sulphur clusters in amitochondriate and apicomplexan protists. *Int J Parasitol* 32:1207-1217.

114. Shimokata, K., Kitada, S., Ogishima, T., Ito, A. (1998). Role of alpha-subunit of mitochondrial processing peptidase in substrate recognition. *J Biol Chem* 273:25158-25163.

115. Singha, U.K., Peprah, E., Williams, S., Walker, R., Saha, L., Chaudhuri, M. (2008). Characterization of the mitochondrial inner membrane protein translocator Tim17 from Trypanosoma brucei. *Mol Biochem Parasitol* 159:30-43.

116. Slapeta, J. , Keithly, J.S. (2004). Cryptosporidium parvum mitochondrial-type HSP70 targets homologous and heterologous mitochondria. *Eukaryot Cell* 3:483-494.

117. Smid, O., Horakova, E., Vilimova, V., Hrdy, I., Cammack, R., Horvath, A., Lukes, J., Tachezy, J. (2006). Knock-downs of iron-sulfur cluster assembly proteins IscS and IscU down-regulate the active mitochondrion of procyclic Trypanosoma brucei. *J Biol Chem* 281:28679-28686.

118. Smid, O., Matuskova, A., Harris, S., Kucera, T., Novotny, M., Horvathova, L., Hrdy, I., Kutejova, E., Hirt, R.P., Embley, T.M. ***et al.*** (2008a). Reductive evolution of the mitochondrial processing peptidases of unicellular parasites ***(under review).***

119. Smid, O., Sutak, R., Tachezy, J. (2008b). Monothiol glutaredoxin in the mitosomes of Giardia intestinalis ***(manuscript in preparation).***

120. Stejskal, F., Slapeta, J., Ctrnacta, V., Keithly, J.S. (2003). A Narf-like gene from Cryptosporidium parvum resembles homologues observed in aerobic protists and higher eukaryotes. *FEMS Microbiol Lett* 229:91-96.

121. Sutak, R., Dolezal, P., Fiumera, H.L., Hrdy, I., Dancis, A., Delgadillo-Correa, M., Johnson, P.J., Muller, M., Tachezy, J. (2004). Mitochondrial-type assembly of FeS centers in the hydrogenosomes of the amitochondriate eukaryote Trichomonas vaginalis. *Proc Natl Acad Sci U S A* 101:10368-10373.

122. Tachezy, J., Dolezal, P. in *Origin of Mitochondria and Hydrogenosomes*, eds Martin, W., Muller, M. (Springer Berlin / Heidelberg), pp 105-133.

123. Tachezy, J., Sanchez, L.B., Muller, M. (2001). Mitochondrial type iron-sulfur cluster assembly in the amitochondriate eukaryotes Trichomonas vaginalis and

Giardia intestinalis, as indicated by the phylogeny of IscS. *Mol Biol Evol* 18:1919-1928.

124. Tachezy, J., Smid, O. in *Hydrogenosomes and Mitosomes: Mitochondria of Anaerobic Eukaryotes*, eds Tachezy, J. (Springer Berlin / Heidelberg), pp 201-230.

125. Takahashi, Y. , Tokumoto, U. (2002). A third bacterial system for the assembly of iron-sulfur clusters with homologs in archaea and plastids. *J Biol Chem* 277:28380-28383.

126. Taylor, A.B., Smith, B.S., Kitada, S., Kojima, K., Miyaura, H., Otwinowski, Z., Ito, A., Deisenhofer, J. (2001). Crystal structures of mitochondrial processing peptidase reveal the mode for specific cleavage of import signal sequences. *Structure* 9:615-625.

127. Tonkin, C.J., van Dooren, G.G., Spurck, T.P., Struck, N.S., Good, R.T., Handman, E., Cowman, A.F., McFadden, G.I. (2004). Localization of organellar proteins in Plasmodium falciparum using a novel set of transfection vectors and a new immunofluorescence fixation method. *Mol Biochem Parasitol* 137:13-21.

128. Tovar, J., Fischer, A., Clark, C.G. (1999). The mitosome, a novel organelle related to mitochondria in the amitochondrial parasite Entamoeba histolytica. *Mol Microbiol* 32:1013-1021.

129. Tovar, J., Leon-Avila, G., Sanchez, L.B., Sutak, R., Tachezy, J., van der, G.M., Hernandez, M., Muller, M., Lucocq, J.M. (2003). Mitochondrial remnant organelles of Giardia function in iron-sulphur protein maturation. *Nature* 426:172-176.

130. Truscott, K.N., Kovermann, P., Geissler, A., Merlin, A., Meijer, M., Driessen, A.J., Rassow, J., Pfanner, N., Wagner, R. (2001). A presequence- and voltage-sensitive channel of the mitochondrial preprotein translocase formed by Tim23. *Nat Struct Biol* 8:1074-1082.

131. Tsaousis, A.D., Kunji, E.R., Goldberg, A.V., Lucocq, J.M., Hirt, R.P., Embley, T.M. (2008). A novel route for ATP acquisition by the remnant mitochondria of Encephalitozoon cuniculi. *Nature* 453:553-556.

132. van der Giezen, M., Cox, S., Tovar, J. (2004). The iron-sulfur cluster assembly genes iscS and iscU of Entamoeba histolytica were acquired by horizontal gene transfer. *BMC Evol Biol* 4:7.

133. van der Giezen, M., Leon-Avila, G., Tovar, J. (2005). Characterization of chaperonin 10 (Cpn10) from the intestinal human pathogen Entamoeba histolytica. *Microbiology* 151:3107-3115.

134. van der Giezen, M. , Tovar, J. (2005). Degenerate mitochondria. *EMBO Rep* 6:525-530.

135. van Dooren, G.G., Stimmler, L.M., McFadden, G.I. (2006). Metabolic maps and functions of the Plasmodium mitochondrion. *FEMS Microbiol Rev* 30:596-630.

136. van Hellemond, J.J., Opperdoes, F.R., Tielens, A.G.M. (1998). Trypanosomatidae produce acetate via a mitochondrial acetate : succinate CoA transferase. *Proc Natl Acad Sci USA* 95:3036-3041.

137. van Weelden, S.W., Fast, B., Vogt, A., van der, M.P., Saas, J., van Hellemond, J.J., Tielens, A.G., Boshart, M. (2003). Procyclic Trypanosoma brucei do not use Krebs cycle activity for energy generation. *J Biol Chem* 278:12854-12863.

138. van Weelden, S.W., van Hellemond, J.J., Opperdoes, F.R., Tielens, A.G. (2005). New functions for parts of the Krebs cycle in procyclic Trypanosoma brucei, a cycle not operating as a cycle. *J Biol Chem* 280:12451-12460.

139. van Wilpe, S., Ryan, M.T., Hill, K., Maarse, A.C., Meisinger, C., Brix, J., Dekker, P.J., Moczko, M., Wagner, R., Meijer, M. *et al.* (1999). Tom22 is a multifunctional organizer of the mitochondrial preprotein translocase. *Nature* 401:485-489.

140. Vavra, J. (2005). "Polar vesicles" of microsporidia are mitochondrial remnants ("mitosomes")? *Folia Parasitol (Praha)* 52:193-195.

141. Webb, C.T., Gorman, M.A., Lazarou, M., Ryan, M.T., Gulbis, J.M. (2006). Crystal structure of the mitochondrial chaperone TIM9.10 reveals a six-bladed alpha-propeller. *Mol Cell* 21:123-133.

142. Wiedemann, N., Kozjak, V., Chacinska, A., Schonfisch, B., Rospert, S., Ryan, M.T., Pfanner, N., Meisinger, C. (2003). Machinery for protein sorting and assembly in the mitochondrial outer membrane. *Nature* 424:565-571.

143. Williams, B.A., Hirt, R.P., Lucocq, J.M., Embley, T.M. (2002). A mitochondrial remnant in the microsporidian Trachipleistophora hominis. *Nature* 418:865-869.

144. Williams, S., Saha, L., Singha, U.K., Chaudhuri, M. (2008). Trypanosoma brucei: differential requirement of membrane potential for import of proteins into mitochondria in two developmental stages. *Exp Parasitol* 118:420-433.

145. Wilson, R.J., Rangachari, K., Saldanha, J.W., Rickman, L., Buxton, R.S., Eccleston, J.F. (2003). Parasite plastids: maintenance and functions. *Philos Trans R Soc Lond B Biol Sci* 358:155-162.

146. Wu, Y. , Sha, B. (2006). Crystal structure of yeast mitochondrial outer membrane translocon member Tom70p. *Nat Struct Mol Biol* 13:589-593.

147. Xia, D., Yu, C.A., Kim, H., Xia, J.Z., Kachurin, A.M., Zhang, L., Yu, L., Deisenhofer, J. (1997). Crystal structure of the cytochrome bc1 complex from bovine heart mitochondria. *Science* 277:60-66.

148. Zheng, L., Cash, V.L., Flint, D.H., Dean, D.R. (1998). Assembly of iron-sulfur clusters. Identification of an iscSUA-hscBA-fdx gene cluster from Azotobacter vinelandii. *J Biol Chem* 273:13264-13272.

Giardia mitosomes and trichomonad hydrogenosomes share a common mode of protein targeting

Pavel Dolezal*, Ondrej Smíd*, Petr Rada*, Zuzana Zubácová*, Dejan Bursać†, Robert Suták*, Jana Nebesárová‡, Trevor Lithgow†, and Jan Tachezy*§

*Department of Parasitology, Charles University, Vinicna 7, 128 44 Prague 2, Czech Republic; ‡Laboratory of Electron Microscopy, Institute of Parasitology of the Academy of Science of the Czech Republic, Branisovska 31, 37005 Ceske Budejovice, Czech Republic; and †Department of Biochemistry and Molecular Biology and Bio21 Molecular Science and Biotechnology Institute, University of Melbourne, Parkville 3010, Australia

Edited by Jeffrey D. Palmer, Indiana University, Bloomington, IN, and approved June 13, 2005 (received for review January 14, 2005)

Mitochondria are archetypal organelles of endosymbiotic origin in eukaryotic cells. Some unicellular eukaryotes (protists) were considered to be primarily amitochondrial organisms that diverged from the eukaryotic lineage before the acquisition of the premitochondrial endosymbiont, but their amitochondrial status was recently challenged by the discovery of mitochondria-like double membrane-bound organelles called mitosomes. Here, we report that proteins targeted into mitosomes of *Giardia intestinalis* have targeting signals necessary and sufficient to be recognized by the mitosomal protein import machinery. Expression of these mitosomal proteins in *Trichomonas vaginalis* results in targeting to hydrogenosomes, a hydrogen-producing form of mitochondria. We identify, in *Giardia* and *Trichomonas*, proteins related to the component of the translocase in the inner membrane from mitochondria and the processing peptidase. A shared mode of protein targeting supports the hypothesis that mitosomes, hydrogenosomes, and mitochondria represent different forms of the same fundamental organelle having evolved under distinct selection pressures.

biogenesis | FeS cluster assembly | Pam18 | matrix-located processing peptidase | ferredoxin

Mitosomes are double-membrane bound organelles found in some unicellular eukaryotes, including *Entamoeba histolytica* (1, 2) and microsporidians such as *Trachipleistophora hominis* (3). The name "mitosome" (synonym: crypton) was proposed to indicate that the organelles are highly reduced (cryptic) mitochondria (1). More recently, mitosomes were identified in the human intestinal parasite *Giardia intestinalis* (4), which has often been considered to be among the earliest branching eukaryotes (5, 6). The apparent lack of mitochondria in *Giardia* had led to the hypothesis that *Giardia* separated from other eukaryotes before the acquisition of mitochondria (7). The presence of mitosomes in *Giardia* provides evidence that even if *Giardia* really is an early branching eukaryote, it nevertheless split from other eukaryotes after the mitochondrial endosymbiosis event (4). This view is further supported by identification of several genes of putative mitochondrial origin on the *Giardia* genome (8, 9).

A key piece of evidence for identifying the mitosomes in *Giardia* was the discovery that they contain components of the protein machinery responsible for iron sulfur cluster assembly (10). Cysteine desulfurase (IscS) and a scaffold protein (IscU) carry out the crucial steps in biosynthesis of Fe-S centers. In eukaryotes, this process takes place exclusively in double membrane-bound organelles including mitochondria (11), hydrogenosomes (12), and chloroplasts (13). Phylogenetic analyses placed the *Giardia* IscS (GiiscS) within the mitochondrion/hydrogenosome clade (10, 14). In addition, GiiscS and *Giardia* scaffold protein (GiiscU) colocalized inside vesicles surrounded by a double membrane and high-speed cellular fractions of *Giardia* catalyzed reconstitution of FeS clusters in an apoprotein lacking FeS moieties (4). Based on these data, it has been proposed that the GiiscS- and GiiscU-containing vesicles are highly reduced mitochondrial homologues or mitosomes.

The presence of a common type of FeS assembly machinery in *Giardia* mitosomes, trichomonad hydrogenosomes, and mitochondria argues for a common evolutionary history of these organelles (4); however, it does not refute contentions that these organelles each arose independently from related species of bacterial endosymbionts (15). One problem is the absence of knowledge concerning the biogenesis of the mitosomes, the evidence that provided strong arguments for a common progenitor of hydrogenosomes and mitochondria (16, 17). Proteins targeted into the mitochondria are synthesized in cytosol with an N-terminal extension for protein targeting; however, many have internal targeting signals. Both sorts of targeting information are recognized by the outer (TOM) and inner (TIM) membrane translocases (18, 19). The mitochondrial matrix proteins are further translocated through the TIM23 complex, with energy supplied by a PAM complex. The PAM complex includes an integral membrane protein with a J domain referred to either as Pam18 (20) or Tim14 (21). After translocation, N-terminal presequences are then cleaved by a matrix-located processing peptidase (MPP) (22). Proteins targeted to hydrogenosomes have N-terminal extensions that carry targeting information (23). Interestingly, initial work on the proteins assembling Fe-S centers in *Giardia* showed that two mitosomal proteins, GiiscU (4) and [2Fe2S] ferredoxin (24), have also predicted N-terminal extensions, whereas such an extension was absent in GiiscS (4).

To provide insight into the biogenesis of *Giardia* mitosomes, we investigated and compared targeting of GiiscS, GiiscU, and [2Fe2S] ferredoxin to *Giardia* mitosomes and to hydrogenosomes in *Trichomonas vaginalis*. We show that mitosomes and hydrogenosomes share a common mode of protein targeting that, like protein import into mitochondria, can make use of N-terminal or internal targeting signals. Initial sequence analysis and cell localization studies suggests that *Giardia* and *Trichomonas* have protein import machinery that shares common components with the protein import machinery of mitochondria and mitochondria-like processing peptidases.

Materials and Methods

Cell Cultivation. *G. intestinalis* strain WB (American Type Culture Collection) was grown in TYI-S-33 medium supplemented with antibiotics (25). *T. vaginalis* strain T1 (kindly provided by P. J. Johnson, University of California, Los Angeles) was maintained in TYM medium (26). *Saccharomyces cerevisiae* strain YPH499 was grown in a rich medium as described in ref. 12.

This paper was submitted directly (Track II) to the PNAS office.

Abbreviations: GiiscS, *Giardia* cysteine desulfurase; GiiscU, *Giardia* scaffold protein; MPP, matrix-located processing peptidase.

§To whom correspondence should be addressed. E-mail: tachezy@natur.cuni.cz.

Selectable Transformation of *G. intestinalis* and *T. vaginalis*. The plasmid pONDRA-HA was constructed by modifying pRANneoGDHluc (27). The luc gene was replaced with the HA tag cassette from TagVag vector (28), and the 5′ UTR of GDH was modified for further cloning. The *giiscu*, *gifdx*, Δ*giiscu*, Δ*gifdx*, and *giα-tub* genes were amplified by PCR from genomic DNA and introduced into plasmids for transformation as described in ref. 27. All primers used in this study are described in supporting information, which is published as supporting information on the PNAS web site. For *T. vaginalis* transformation, *Giardia* genes were subcloned into the plasmid TagVag (28). Cells were transformed and selected as described in ref. 12. Iterative BLAST searches were used to identify the Pam18 orthologous sequences from *G. intestinalis* (protein accession no. EAA37663) and *T. vaginalis* (orf 95394.m00357) (29). BLAST searches of GIARDIADB for members of the M16 protease family revealed Giβ MPP (EAA39560). The *tvpam18*, *gipam18*, and *tvβmpp* genes were amplified, cloned, and expressed in *Giardia* and *Trichomonas* as above.

Immunofluorescent Microscopy. Mitosomal proteins were stained in fixed *G. intestinalis* and *T. vaginalis* cells with mouse α-HA mAb (12). In double-labeling experiments, *G. intestinalis* clathrin heavy chain, disulfide isomerase, and GiiscU were detected with rabbit polyclonal Abs (A. Hehl, University of Zürich, Zürich; ref. 4). Hydrogenosomal malic enzyme was detected by rabbit polyclonal Ab (30). Details are given in supporting information.

Preparation of Subcellular Fractions. *Giardia* subcellular fractions were obtained by differential and sucrose gradient centrifugation of the cell homogenate as detailed in supporting information. Percoll-purified hydrogenosomes and cytosol of *T. vaginalis* were prepared as described in ref. 12. Mitochondria were isolated from the *S. cerevisiae* strain YPH499 as described in ref. 31. To remove proteins not imported into the organelles, hydrogenosomes were incubated 60 min with 200 μg/ml trypsin in ST buffer (250 mM sucrose/0.5 mM KCl/10 mM Tris·HCl, pH 7.2) at 37°C and washed twice with 5 mg/ml soybean trypsin inhibitor in ST buffer.

Mitosome-rich fractions were processed for electron microscopy with a modified method of Tokuyasu (32). Ultrathin frozen sections were labeled with mouse α-HA mAb and 10 nm gold-labeled goat α-mouse Ab and observed in a Jeol 1010 electron microscope, as detailed in supporting information.

Protein Processing Assay. GiiscU and ΔGiiscU were cloned into pSP64T (Promega). The constructs were incubated with TNT Quick Coupled Transcription/Translation System (Promega) according to the manufacturer's protocol. Synthesized proteins were precipitated by 60% ammonium sulfate (wt/vol in water), and the resulting precipitate dissolved in buffer (20 mM Tris/1 mM KCl/10 mM $MgCl_2$/0.5% Triton). Organelles (100 μg of protein) were mixed with ^{35}S-labeled protein in the same buffer. Mitochondrial and hydrogenosomal samples were incubated for various times at 30°C and 37°C, and samples were analyzed by SDS/PAGE and autoradiography.

GiiscU Expression and Determination of Processing Site. GiiscU was expressed in *E. coli* by using pQE30 vector (Qiagen) and was affinity purified under native conditions (Qiagen). Protein (≈150 μg) was incubated for 60 min in 10 mM Hepes (pH 7.5)/0.1 mM $MnCl_2$/0.5 mM DTT with 4 μg of recombinant rat MPP (kindly provided by J. Adamec, Academy of Sciences, Prague, Czech Republic) (33). The reaction was inhibited by addition of 10 mM EDTA, and samples were separated on SDS/PAGE gels, blotted to poly(vinylidene difluoride) membrane and stained with Coomassie brilliant blue. Selected protein bands were subjected to N-terminal protein sequencing by Edman degradation.

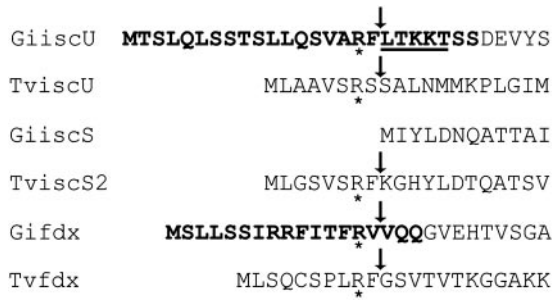

Fig. 1. N-terminal regions of *Giardia* and *Trichomonas* IscU, IscS, and [2Fe-2S] ferredoxins. MITOPROT (http://ihg.gsf.de/ihg/mitoprot.html) predicted targeting sequences are highlighted in bold. PSORT II (http://psort.nibb.ac.jp) cleavage sites (arrows) are shown, and arginines (at position −2 relative to the cleavage site) highlighted by asterisks. N-terminal amino acid sequences determined in GiiscU, retrieved from *Giardia*, or processed *in vitro* by recombinant rat MPP are underlined.

The HA-tagged GiiscU was immunoprecipitated from *G. intestinalis* transformants by using proteinA Sepharose (Sigma), coupled with α-HA mAb adopting the method from ref. 34. Details are given in supporting information.

Results

Targeting of GiiscU, GiiscS, and Gifdx into Mitosomes. *GiiscU*, *Gifdx*, *GiiscS*, and the truncated forms (Δ*giiscU* and Δ*gifdx*) lacking 26 and 18 aa of predicted N-terminal extensions (Fig. 1), respectively, were overexpressed in *Giardia* and *Trichomonas* with a C-terminal HA tag (27, 28). The products of *giiscS*, *giiscU*, and *gifdx* were found in a number of vesicles (30 ± 6 per cell) with a distribution characteristic of mitosomes (4): between the two *Giardia* nuclei in close proximity to the basal bodies and in the lateral and posterior parts of the cell (Fig. 2*A*). Tagged GiiscS colocalized with native GiiscU in double-labeling experiments (data not shown). These vesicles were clearly distinct from the endoplasmic reticulum and peripheral vesicles beneath the plasma membrane (Fig. 2*B*). Subsequently, the mitosome containing fraction from *giiscU* transformants were purified from the homogenate by differential and gradient centrifugation. Immunoelectron microscopy revealed the presence of tagged GiiscU within organelles of ≈184 × 140 nm in diameter, and surrounded by two membranes (Fig. 2*D*). These features indicate that all three proteins were translocated into *Giardia* mitosomes (4).

The N-terminal extensions predicted for Gifdx and GiiscU are necessary for targeting the proteins to mitosomes: weak labeling of mitosomes was observed in cells expressing Δ*giiscU* that lacks the 26-residue N-terminal sequence, and no organellar labeling was observed in the cells expressing Δ*Gifdx* lacking its 18-residue extension (Fig. 2*A*). The targeting function of these N-terminal leader sequences was confirmed by Western blot analysis of the cellular fractions (Fig. 2*C*), with GiiscU and Gifdx present exclusively in the mitosome-rich fraction. By contrast, the majority of ΔGiiscU was found in the cytosol, and no organellar signal was detected for ΔGifdx, although it did not accumulate within the cytosol either. To be certain that ΔGiFdx was expressed, we compared mRNA levels of *gifdx* and Δ*gifdx* in corresponding transformants. No difference in *gifdx* and Δ*gifdx* transcription was found (supporting information). Thus, failure of ΔGifdx to be targeted to mitosomes likely results in degradation of the apoprotein by proteolysis, as previously reported for the apoform of Leu1p in yeast (35).

N-Terminal Targeting Sequence-Independent Import of GiiscS. No N-terminal targeting sequence was predicted for GiiscS. To

EVOLUTION

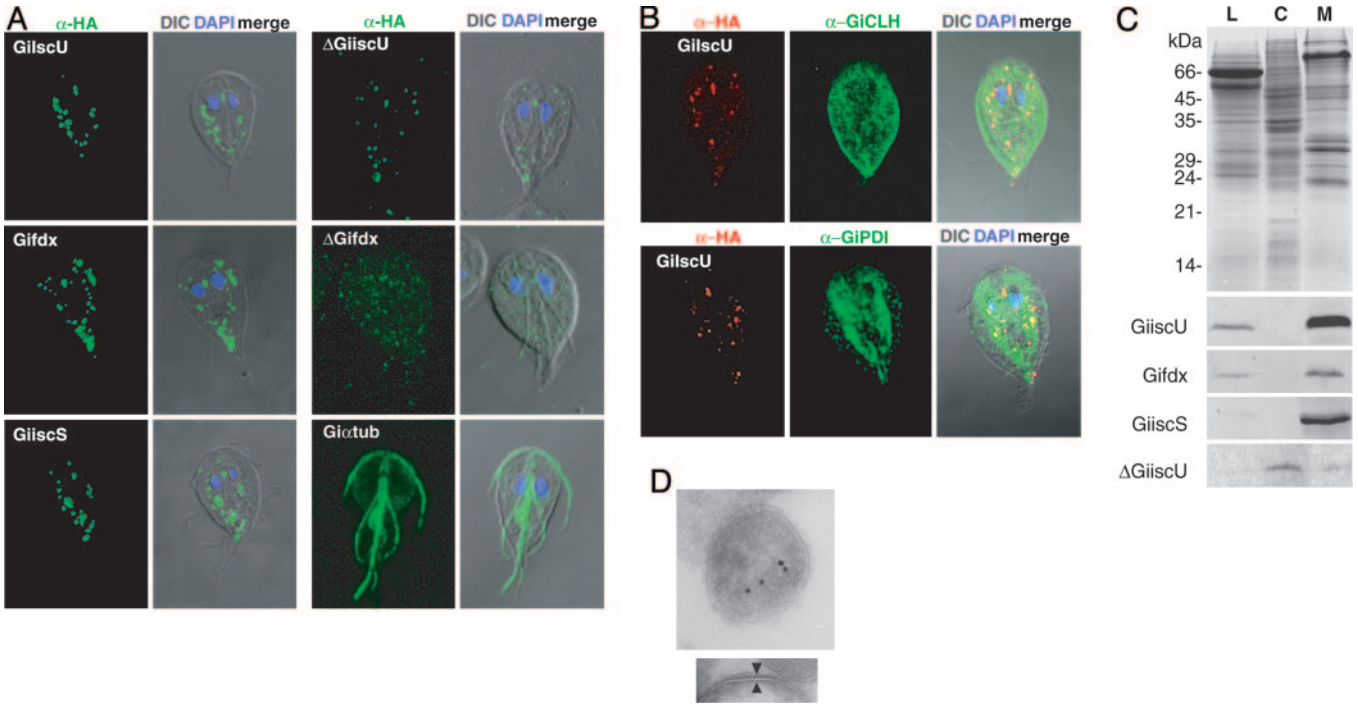

Fig. 2. Cellular localization of tagged GiiscU, GiiscS, and Gifdx in *G. intestinalis* transformants. (*A*) Transformed *Giardia* cell lines were stained for immunofluorescence microscopy with mouse α-HA tag Ab (green). GiiscU and Gifdx, the complete preproteins possessing N-terminal presequences; ΔGiiscU and ΔGifdx, truncated forms lacking the N-terminal presequences. GiiscS does not possess recognizable N-terminal presequence. *Giardia* α-tubulin (Giαtub) was used as a control. Merged images are given for immunofluorescent staining, the nuclei (blue) stained with DAPI, and differential interference contrast (DIC). (*B*) Mitosomes stained for GiiscU (red); peripheral vesicles and structures of endoplasmic reticulum stained for clathrin light chain (α-GiCLH Ab) and protein disulfide isomerase (α-GiPDI Ab), respectively, (green). (*C*) Total cell lysate (L), cytosolic (C), and mitosomal (M) fractions were prepared from transformed cells and analyzed by SDS/PAGE (*Top*) and Western blots (bottom four blots). (*D*) Immunoelectron microscopy of the mitosomes purified from *giiscU* transformants. Tagged GiiscU was detected in the organelles by the mouse α-HA Ab and 10 nm gold-labeled goat α-mouse Ab. Arrowheads indicate the double (outer and inner) membranes of the mitosome.

examine which part of the 434-aa protein is required for targeting to mitosomes, the protein was truncated and the N-terminal 202 residues (GiiscSN1/2) or C-terminal 232 residues (GiiscSC1/2) expressed in *T. vaginalis*. Both fragments of the protein were delivered into the hydrogenosomes (Fig. 3*C*). These results indicate that IscS contains multiple targeting signals within the protein.

Conservation of Protein Targeting in Mitosomes and Hydrogenosomes. To determine whether the mitosomal targeting sequences on GiiscU and Gifdx can function to target proteins to hydrogenosomes, the giardial genes were overexpressed in *T. vaginalis.* Immunofluorescence labeling of trichomonad cells expressing tagged GiiscU, Gifdx, and GiiscS localized these proteins to discrete structures surrounding trichomonad nuclei and cytoskeletal structures, the cell distribution typical for hydrogenosomes (Fig. 3*A*). The labeling of tagged proteins also colocalized with malic enzyme, a marker protein for hydrogenosomes. Stronger malic enzyme signal corresponds to its abundance in hydrogenosomes (30). In contrast, the absence of N-terminal leader sequences on ΔGiiscU and ΔGifdx abrogated the delivery of the proteins into the target organelle with the majority of each protein accumulating in the cytosol (Fig. 3*B*).

The N-terminal extension of GiiscU is not only necessary, but sufficient, for targeting of this protein into the hydrogenosomes. Attaching the extension of GiiscU to the N terminus of α-tubulin delivers a significant proportion of this passenger protein into the hydrogenosomes, whereas no giardial α-tubulin was found in the organelles when expressed without the GiiscU targeting sequence (Fig. 3*B*).

Processing of a Mitosomal Targeting Sequence. The detection of GiiscU expressed in *T. vaginalis* hydrogenosomes revealed the presence of two bands of 20 and 17 kDa corresponding to the predicted molecular mass of the GiiscU precursor and its mature form, respectively. In *Giardia*, the size of tagged GiiscU detected in mitosomes of the cells expressing the complete *giiscU* was identical to its truncated form expressed in Δ*giiscU* transformants. These observations indicated processing of N-terminal targeting sequence within the target organelles (Fig. 4*A*). To test whether specific metallopeptidases, which are known to mediate cleavage of targeting sequences in mitochondria (33) and possibly in hydrogenosomes (23), can process the giardial targeting sequences, we incubated *in vitro* translated GiiscU preprotein with lysates of yeast mitochondria or trichomonad hydrogenosomes. The mitochondrial lysate efficiently catalyzed the cleavage of GiiscU in a time-dependent manner (Fig. 4*B*), as did the hydrogenosomal extract (Fig. 4*C*). The cleavage was inhibited by the addition of EDTA, indicating that a metalloprotease is involved. Pretreatment of the hydrogenosomal lysate with hexokinase to remove ATP did not affect the cleavage, which excludes a possibility that the observed processing was catalyzed by ATP-dependent proteases. To determine the protein cleavage site, GiiscU preprotein was incubated with recombinant rat MPP (Fig. 4*D*). The N-terminal sequence of the major cleavage product (inhibitable by EDTA) revealed that the MPP cleaved the GiiscU precursor between Phe-18 and Leu-19 with arginine at −2 position (Fig. 1). Finally, overexpressed GiiscU was immunoprecipitated from a giardial high-speed pellet to verify whether native cleavage site in *Giardia* corresponds to that catalyzed by recombinant MPP (supporting information). Indeed, the N-terminal sequence of the GiiscU retrieved from

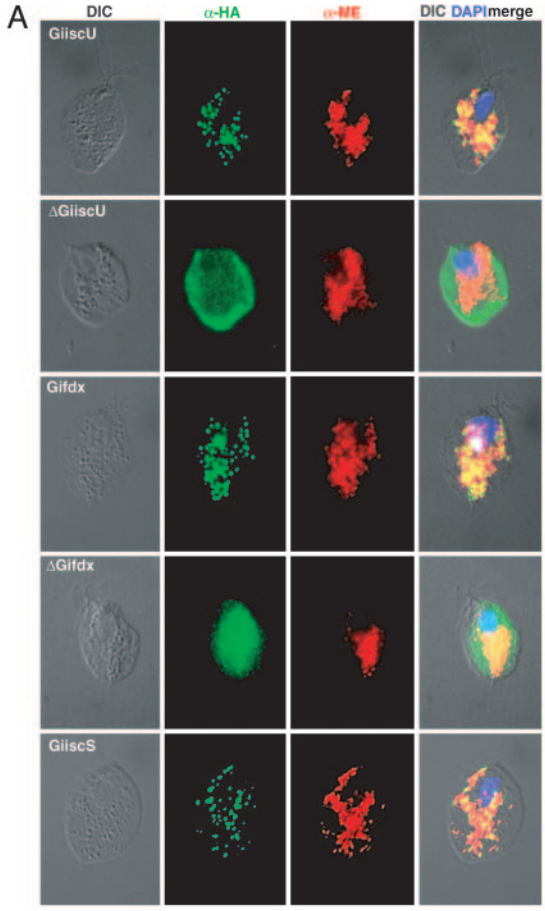

Fig. 3. Targeting of the mitosomal proteins GiiscU, Gifdx, and GiisS into *T. vaginalis* hydrogenosomes. (*A*) The *Giardia* proteins were each expressed in trichomonads with a C-terminal HA tag (green). A rabbit polyclonal Ab recognizing the hydrogenosomal malic enzyme (α-ME) was used as a marker for hydrogenosomes (red). The nuclei were stained with DAPI (blue). DIC, differential interference contrast. (*B*) Total cell lysate (L), cytosol (C), and hydrogenosomal (H) fractions were prepared from transformed *Trichomonas* cells and analyzed by SDS/PAGE and Western blots.

Giardia started with Leu-19 (Fig. 1). Although it is not yet clear how generally applicable PSORT (http://psort.nibb.ac.jp) will be for predicting cleavage sites in mitosomal proteins, in the case of GiiscU, the prediction was successful.

Homologs of the β-subunit of MPP are encoded in the genomes of *G. intestinalis* and *T. vaginalis*. Both of these β-MPP-like sequences possess characteristic His-X-X-Glu-His zinc-binding motifs and PSORT-predicted presequences (supporting information). Overexpression of β-MPP in *G. intestinalis* showed its colocalization with GiiscU in mitosomes (Fig. 5).

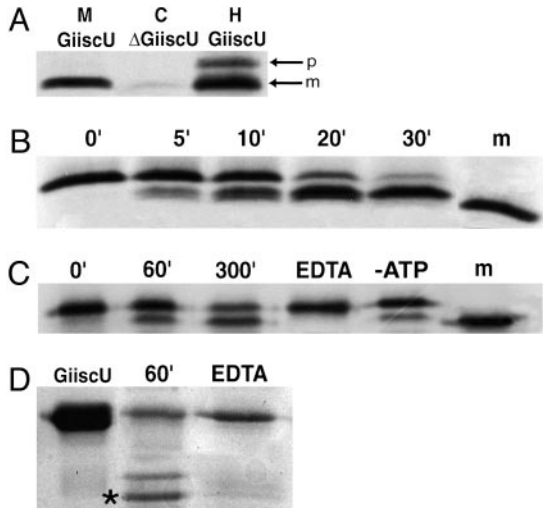

Fig. 4. Processing of GiiscU. (*A*) M, GiiscU detected in mitosomes of *Giardia*; C, N-terminal truncated form of GiiscU retained in the cytosol of Δ*giiscu* transformants; H, two forms of GiiscU in the hydrogenosomes represent the precursor (p) and the processed (m) protein. (*B*) Time-dependent processing of *in vitro* translated, ^{35}S-labeled GiiscU precursor in the presence of yeast mitochondrial lysate. The mature-sized form of GiiscU (m). (*C*) GiiscU precursor was ^{35}S-labeled and incubated with lysate prepared from *T. vaginalis* hydrogenosomes with or without 10 mM EDTA. ATP-depleted lysate (−ATP) by using hexokinase (34). (*D*) GiiscU precursor incubated for 60 min with rat MPP (33). The N terminus of major cleavage product (asterisk) was determined by microsequencing.

A Subunit of the Mitochondrial PAM Complex in Mitosomes and Hydrogenosomes. Although only partial information is available on the genome sequence from *G. intestinalis* and *T. vaginalis*, we have initiated iterative BLAST analyses (29) to search for homologs of the components of the mitochondrial protein import machinery. The Pam18-related sequences in Fig. 5*C* all predict to have a transmembrane segment, followed by a conserved charged region and a J domain characterized by the absence of a predicted "helix IV" (37). To determine their subcellular location, GiPam18 and TvPam18 were expressed as HA-tagged proteins in *G. intestinalis* and *T. vaginalis*. The proteins of both origins were delivered into both hydrogenosomes and mitosomes and colocalized with the marker proteins, GiiscU and malic enzyme, respectively (Fig. 5 *A* and *B*).

Discussion

Our study provides evidence that mitosomes of *G. intestinalis*, hydrogenosomes, and mitochondria share a similar mode of protein targeting and translocation. This finding supports the hypothesis that mitosomes, hydrogenosomes, and mitochondria represent different forms of the same fundamental organelle that have evolved under distinct selection pressures (38).

Three giardial proteins were selected to compare their targeting and translocation into mitosomes and hydrogenosomes: GiiscS, GiiscU, and [2Fe2S] ferredoxin (Gifdx). These proteins are homologues of the key components of the FeS cluster assembly machinery operating in mitochondria and hydrogenosomes (11, 12). Association of GiiscS and GiiscU with giardial mitosomes has been reported in ref. 4, whereas the intracellular localization of Gifdx has not been studied. When GiiscS, GiiscU, and Gifdx were overexpressed in *G. intestinalis* or *T. vaginalis*, all three proteins were specifically delivered into the mitosomes or into the hydrogenosomes, respectively. The delivery of the proteins was mediated by two different mechanisms requiring either N-terminal targeting sequences (Gifdx, GiiscU) or internal targeting sequences (GiiscS). The N-terminal extensions

EVOLUTION

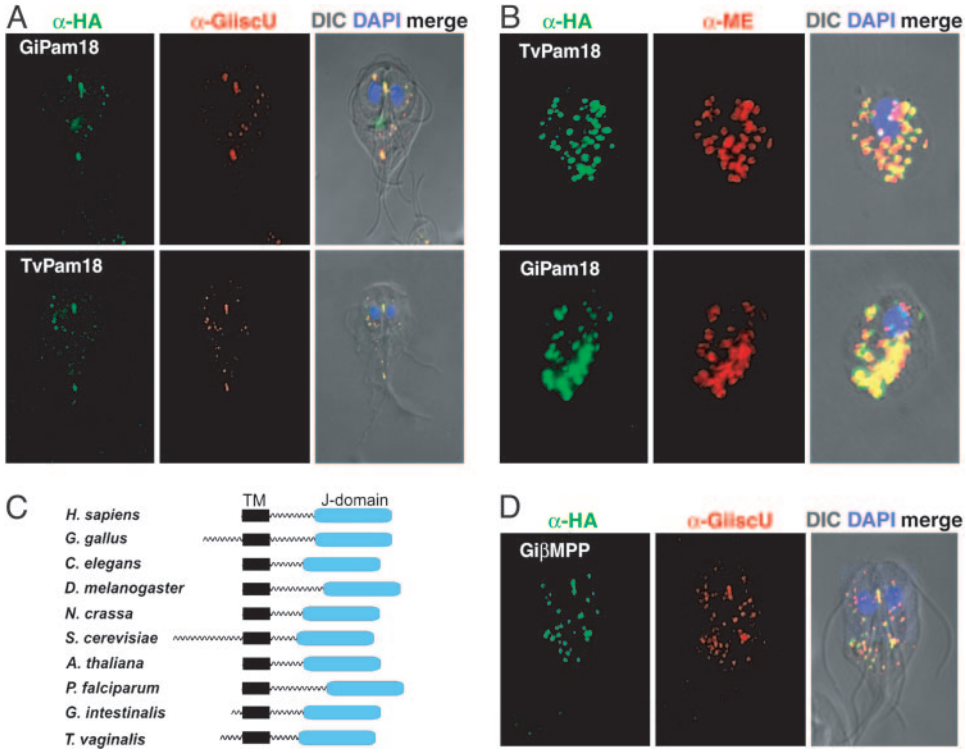

Fig. 5. Cellular localization of tagged GiPam18, TvPam18, and GiβMPP. Transformed cell lines of *G. intestinalis* (*A* and *D*) and *T. vaginalis* (*B*) were stained for immunofluorescence microscopy with mouse α-Ha Ab (green). GiiscU was detected by polyclonal rabbit α-GiiscU Ab (red). The merged images are given for immunofluorescent staining, the nuclei (blue) stained with DAPI. (*C*) Domain structure of GiPam18 and TvPam18 compared with other members of the Pam18/Tim14 family. Ten of the most diverse sequences were aligned with CLUSTALW (supporting information). The N-terminal extension segments were located in the intermembrane space (20), transmembrane segments (TM) were predicted with DAS (36), and the J domain (blue) was characterized as described in ref. 37.

predicted in GiiscU and Gifdx are both necessary and sufficient for targeting to mitosomes and resemble the targeting sequences found in mitochondrial and hydrogenosomal proteins in that they (*i*) are rich in serine and arginine residues, (*ii*) are predicted to form amphipathic helices, and (*iii*) possess cleavage site motifs recognized by mitochondrial-type processing peptidases.

In mitochondria, MPP is an EDTA-sensitive metalloprotease that consists of two subunits. Genes coding for α and β subunits of MPP can be found widely in eukaryotes, including animals, fungi, and plants (22). Although the hydrogenosomal processing peptidase has not been biochemically characterized, protein processing in hydrogenosomes was observed (23), and sequences for each subunit of MPP are annotated in the *T. vaginalis* genome. We found a putative β-MPP subunit in the *Giardia* genome and showed that the protein is delivered into mitosomes. EDTA-sensitive cleavage of the GiiscU N-terminal targeting sequence was observed with purified rat MPP and with hydrogenosomal extracts, and analysis of GiiscU isolated from *Giardia* indicated that protein processing also occurred *in situ*.

Protein targeting sequences and their processing peptidase are common in mitosomes, hydrogenosome and mitochondria. Are the fundamental components of the TOM and TIM complexes also to be found in *Trichomonas* and *Giardia*? It is clear now that although some components of the mitochondrial protein import machinery might have evolved after the radiation of the main eukaryotic lineages (39), several components of the TOM (29) and TIM (40) complexes were likely present at the earliest stage in the conversion of the endosymbiont that gave rise to mitochondria. Our data predicts that these primitive components of the TOM and TIM complexes will be present in hydrogenosomes and mitosomes. In at least one case, Tim14/Pam18, this prediction has been fulfilled. Although there are 26 different proteins containing J domains in yeast, only Pam18/Tim14 (and its paralog Mdj2) contain a transmembrane segment, a charged linker domain, and a J domain without the characteristic "helix IV" (37). The function of Tim14/Pam18 is to dock to the TIM23 complex, assist Tim44 to bind the mitochondrial Hsp70, and to directly stimulate ATP hydrolysis catalysed by Hsp70 to promote protein translocation across the mitochondrial membranes (20, 21). We do not currently have an assay system capable of dissecting the function of the Pam18-related proteins of *Giardia* and *Trichomonas*, but the presence of GiPam18 in mitosomes and TvPam18 in hydrogenosomes provides an indication that the protein translocation machinery of these organelles and mitochondria might be built around commonly derived components. More sensitive means of sequence analysis may be required to identify further subunits of the TOM and TIM complexes, and we have initiated studies to build hidden Markov models for this purpose.

The endosymbiotic event of an α-proteobacterium that gave rise to mitochondria and related organelles is of great interest because this event might represent the moment of the origin of the eukaryotic cell itself (41). Studying the fate of the ancestral endosymbiont in different eukaryotes promises to uncover the nature and primary role of the organelle for eukaryotes. The fact that hydrogenosomes and mitochondria recognize the targeting signals of mitosomal proteins indicates that these organelles possess a common protein import mechanism and suggests that all these organelles share, through common descent, what must have been among the earliest features of the first "mitochondriate" organisms.

We thank M. Marcincikova for the excellent technical support; M. Embley, M. Müller, and S. Ralph for the comments on the manuscript; and Z. Voburka from the Czech Academy of Science for protein

microsequencing. This work was supported by Grant Agency of the Czech Republic Grant 204/04/0435 (to J.T.), a Fogarty International Research Collaboration Award (to J.T. and Miklos Müller), and a grant from the Australian Research Council (to T.L.). The use of sequencing information from *G. lamblia* (www.mbl.edu/Giardia) and *T. vaginalis* (www.tigr.org/tdb/e2k1/tvg) genome databases is acknowledged.

1. Tovar, J., Fischer, A. & Clark, C. G. (1999) *Mol. Microbiol.* **32,** 1013–1021.
2. Mai, Z., Ghosh, S., Frisardi, M., Rosenthal, B., Rogers, R. & Samuelson, J. (1999) *Mol. Cell. Biol.* **19,** 2198–2205.
3. Williams, B. A., Hirt, R. P., Lucocq, J. M. & Embley, T. M. (2002) *Nature* **418,** 865–869.
4. Tovar, J., Leon-Avila, G., Sánchez, L. B., Sutak, R., Tachezy, J., van der Giezen, M., Hernandez, M., Müller, M. & Lucocq, J. M. (2003) *Nature* **426,** 172–176.
5. Adam, R. D. (2001) *Clin. Microbiol. Rev.* **14,** 447–475.
6. Best, A. A., Morrison, H. G., McArthur, A. G., Sogin, M. L. & Olsen, G. J. (2004) *Genome Res.* **14,** 1537–1547.
7. Cavalier-Smith, T. (1987) *Cold Spring Harbor Symp. Quant. Biol.* **52,** 805–824.
8. Hashimoto, T., Sanchez, L. B., Shirakura, T., Müller, M. & Hasegawa, M. (1998) *Proc. Natl. Acad. Sci. USA* **95,** 6860–6865.
9. Roger, A. J., Svard, S. G., Tovar, J., Clark, C. G., Smith, M. W., Gillin, F. D. & Sogin, M. L. (1998) *Proc. Natl. Acad. Sci. USA* **95,** 229–234.
10. Tachezy, J., Sanchez, L. B. & Müller, M. (2001) *Mol. Biol. Evol.* **18,** 1919–1928.
11. Lill, R. & Kispal, G. (2000) *Trends Biochem. Sci.* **25,** 352–356.
12. Sutak, R., Dolezal, P., Fiumera, H. L., Hrdy, I., Dancis, A., Delgadillo-Correa, M., Johnson, P. J., Müller, M. & Tachezy, J. (2004) *Proc. Natl. Acad. Sci. USA* **101,** 10368–10373.
13. Pilon-Smits, E. A., Garifullina, G. F., Abdel-Ghany, S., Kato, S., Mihara, H., Hale, K. L., Burkhead, J. L., Esaki, N., Kurihara, T. & Pilon, M. (2002) *Plant Physiol.* **130,** 1309–1318.
14. Emelyanov, V. V. (2003) *FEMS Microbiol. Lett.* **226,** 257–266.
15. Dyall, S. D., Brown, M. T. & Johnson, P. J. (2004) *Science* **304,** 253–257.
16. van der Giezen, M., Slotboom, D. J., Horner, D. S., Dyal, P. L., Harding, M., Xue, G. P., Embley, T. M. & Kunji, E. R. (2002) *EMBO J.* **21,** 572–579.
17. Emelyanov, V. V. (2001) *FEBS Lett.* **501,** 11–18.
18. Neupert, W. (1997) *Annu. Rev. Biochem.* **66,** 863–917.
19. Rehling, P., Wiedemann, N., Pfanner, N. & Truscott, K. N. (2001) *Crit. Rev. Biochem. Mol. Biol.* **36,** 291–336.
20. Truscott, K. N., Voos, W., Frazier, A. E., Lind, M., Li, Y., Geissler, A., Dudek, J., Muller, H., Sickmann, A., Meyer, H. E., *et al.* (2003) *J. Cell Biol.* **163,** 707–713.
21. Mokranjac, D., Sichting, M., Neupert, W. & Hell, K. (2003) *EMBO J.* **22,** 4945–4956.
22. Gakh, O., Cavadini, P. & Isaya, G. (2002) *Biochim. Biophys. Acta* **1592,** 63–77.
23. Bradley, P. J., Lahti, C. J., Plümper, E. & Johnson, P. J. (1997) *EMBO J.* **16,** 3484–3493.
24. Nixon, J. E., Wang, A., Field, J., Morrison, H. G., McArthur, A. G., Sogin, M. L., Loftus, B. J. & Samuelson, J. (2002) *Eukaryotic Cell* **1,** 181–190.
25. Keister, D. B. (1983) *Trans. R. Soc. Trop. Med. Hyg.* **77,** 487–488.
26. Diamond, L. S. (1957) *J. Parasitol.* **43,** 488–490.
27. Sun, C. H., Chou, C. F. & Tai, J. H. (1998) *Mol. Biochem. Parasitol.* **92,** 123–132.
28. Hrdy, I., Hirt, R. P., Dolezal, P., Bardonova, L., Foster, P. G., Tachezy, J. & Embley, T. M. (2004) *Nature* **432,** 618–622.
29. Macasev, D., Whelan, J., Newbigin, E., Silva-Filho, M. C., Mulhern, T. D. & Lithgow, T. (2004) *Mol. Biol. Evol.* **21,** 1557–1564.
30. Drmota, T., Proost, P., Van Ranst, M., Weyda, F., Kulda, J. & Tachezy, J. (1996) *Mol. Biochem. Parasitol.* **83,** 221–234.
31. Murakami, H., Pain, D. & Blobel, G. (1988) *J. Cell Biol.* **107,** 2051–2057.
32. Tokuyasu, K. T. (1981) *J. Electron Microsc.* **30,** 93–94.
33. Adamec, J., Gakh, O., Spizek, J. & Kalousek, F. (1999) *Arch. Biochem. Biophys.* **370,** 77–85.
34. Mühlenhoff, U., Richhardt, N., Gerber, J. & Lill, R. (2002) *J. Biol. Chem.* **277,** 29810–29816.
35. Mühlenhoff, U., Balk, J., Richhardt, N., Kaiser, J. T., Sipos, K., Kispal, G. & Lill, R. (2004) *J. Biol. Chem.* **279,** 36906–36915.
36. Cserzo, M., Wallin, E., Simon, I., von Heijne, G. & Elofsson, A. (1997) *Protein Eng.* **10,** 673–676.
37. Walsh, P., Bursac, D., Law, Y. C., Cyr, D. & Lithgow, T. (2004) *EMBO Rep.* **5,** 567–571.
38. Embley, T. M., van der Giezen, M., Horner, D. S., Dyal, P. L., Bell, S. & Foster, P. G. (2003) *IUBMB Life* **55,** 387–395.
39. Likic, V. A., Perry, A., Hulett, J., Derby, M., Traven, A., Waller, R. F., Keeling, P. J., Koehler, C. M., Curran, S. P., Gooley, P. R., *et al.* (2005) *J. Mol. Biol.* **347,** 81–93.
40. Herrmann, J. M. (2003) *Trends Microbiol.* **11,** 74–79.
41. Martin, W. & Russell, M. J. (2003) *Philos. Trans. R. Soc. Lond., B, Biol. Sci.* **358,** 59–83.

THE JOURNAL OF BIOLOGICAL CHEMISTRY VOL. 281, NO. 39, pp. 28679–28686, September 29, 2006

Knock-downs of Iron-Sulfur Cluster Assembly Proteins IscS and IscU Down-regulate the Active Mitochondrion of Procyclic *Trypanosoma brucei*[*][S]

Received for publication, December 27, 2005, and in revised form, June 26, 2006 Published, JBC Papers in Press, August 1, 2006, DOI 10.1074/jbc.M513781200

Ondrej Smíd[‡], Eva Horáková[§], Vanda Vilímová[‡], Ivan Hrdý[‡], Richard Cammack[¶], Anton Horváth[‖], Julius Lukeš[§], and Jan Tachezy[‡1]

From the [‡]Department of Parasitology, Faculty of Science, Charles University, 12844 Prague, Czech Republic, the [§]Institute of Parasitology, Academy of Sciences of the Czech Republic and Faculty of Biology, University of South Bohemia, 35007 České Budějovice, Czech Republic, the [¶]Department of Life Sciences, King's College, London, WC2R 2LS, United Kingdom, and the [‖]Faculty of Natural Sciences, Comenius University, 84215 Bratislava, Slovakia

Transformation of the metabolically down-regulated mitochondrion of the mammalian bloodstream stage of *Trypanosoma brucei* to the ATP-producing mitochondrion of the insect procyclic stage is accompanied by the *de novo* synthesis of citric acid cycle enzymes and components of the respiratory chain. Because these metabolic pathways contain multiple iron-sulfur (FeS) proteins, their synthesis, including the formation of FeS clusters, is required. However, nothing is known about FeS cluster biogenesis in trypanosomes, organisms that are evolutionarily distant from yeast and humans. Here we demonstrate that two mitochondrial proteins, the cysteine desulfurase TbiscS and the metallochaperone TbiscU, are functionally conserved in trypanosomes and essential for this parasite. Knock-downs of TbiscS and TbiscU in the procyclic stage by means of RNA interference resulted in reduced activity of the marker FeS enzyme aconitase in both the mitochondrion and cytosol because of the lack of FeS clusters. Moreover, down-regulation of TbiscS and TbiscU affected the metabolism of procyclic *T. brucei* so that their mitochondria resembled the organelle of the bloodstream stage; mitochondrial ATP production was impaired, the activity of the respiratory chain protein complex ubiquinol-cytochrome-*c* reductase was reduced, and the production of pyruvate as an end product of glucose metabolism was enhanced. These results indicate that mitochondrial FeS cluster assembly is indispensable for completion of the *T. brucei* life cycle.

Trypanosoma brucei is one of the most important protozoan pathogens, responsible for human sleeping sickness and nagana in livestock. Moreover, because the genome of *T. brucei* has recently been completely sequenced (1), and the cells are amenable to approaches of involving reverse genetics (2), *T. brucei* has become a new model organism, which is evolutionarily highly divergent from classical models such as *Saccharomyces cerevisiae*. While yeast and other fungi are more related to metazoa including humans (eukaryotic group Opisthokonta), trypanosomatids belong to the distant eukaryotic group called Excavata (3, 4). This group is formed exclusively of unicellular eukaryotes, many of them with highly modified mitochondria (5). The mitochondrion of *T. brucei* is of particular interest, because it undergoes dramatic metabolic and structural changes during the cell cycle between the blood of the mammalian host and the digestive tract of the tsetse fly. An excess of glucose in the mammalian host permits the bloodstream stage to employ glycolysis for energy generation, a significant part of which is localized to specialized peroxisomes called glycosomes (6), producing pyruvate as a major end product. Consequently, the mitochondrion lacks the cytochrome-dependent electron transport chain and the activities of the citric acid cycle enzymes and is thus impaired in its ability to produce ATP by oxidative phosphorylation (7). Through its functions as a sink for reducing equivalents from glycolysis, the mitochondrion still plays an indispensable role in the metabolism of blood stages (8). In the insect vector, trypanosomes encounter a nutrient-poor environment, where they can only survive through an overall switch in their energy metabolism, primarily by activating the mitochondrion. In the active mitochondria of procyclics, pyruvate is degraded with the benefit of additional ATP synthesis, mainly to acetate and succinate (9). However, most of the excreted succinate is produced in glycosomes (10). This transformation is accompanied by the *de novo* synthesis of iron-sulfur (FeS)[2] clusters and maturation of a number of FeS proteins including electron-transporting subunits of the mitochondrial respiratory chain (complexes I, II, and III) and aconitase, an enzyme with dual localization in the mitochondrion and cytosol (9).

The biogenesis of FeS clusters is a recently discovered process essential for both prokaryotic and eukaryotic cells (11, 12). In eukaryotes, the *de novo* formation of FeS clusters was first discovered in mitochondria (13) and later in other organelles of

* This work was supported by Grant Agency of the Czech Republic Grant 204/04/0435 (to J. T.), Grant Agency of the Czech Academy of Sciences Grants 5022302 and Z60220518, and Ministry of Education of the Czech Republic Grant 6007665801 (to J. L.). The costs of publication of this article were defrayed in part by the payment of page charges. This article must therefore be hereby marked "*advertisement*" in accordance with 18 U.S.C. Section 1734 solely to indicate this fact.

[S] The on-line version of this article (available at http://www.jbc.org) contains supplemental figures.

[1] To whom correspondence should be addressed: Dept. of Parasitology, Faculty of Science, Charles University in Prague, Viničná 7, 128 44 Prague 2, Czech Republic. Tel.: 420-221-951-811; Fax: 420-224-919-704; E-mail: tachezy@natur.cuni.cz.

[2] The abbreviations used are: FeS, iron-sulfur; RNAi, RNA interference; HPLC, high pressure liquid chromatography; MRP2, mitochondrial RNA-binding protein 2.

endosymbiotic origin including hydrogenosomes, mitosomes, and plastids (14–18). The machinery responsible for mitochondrial FeS cluster assembly consists of at least 10 different proteins, the key components being pyridoxal 5-phosphate-dependent cysteine desulfurase IscS, which generates sulfur (S^0) from cysteine, and the metallochaperone IscU, which provides the molecular scaffold for the formation of a transient FeS cluster (11). The transient FeS cluster is transferred from IscU to apoproteins during FeS protein maturation (19).

In *S. cerevisiae*, mitochondria were shown to play an essential role not only in the biosynthesis of mitochondrial FeS proteins but also in the maturation of FeS proteins localized in the cytosol and nucleus. For example, this essential requirement for the FeS cluster assembly machinery was demonstrated for Rli1, a cytosolic FeS protein that is indispensable to ribosomal functionality (19, 20). A different model was proposed for the biogenesis of FeS clusters in human cells. In addition to mitochondria, several components of the mitochondrial FeS cluster assembly machinery were detected in the cytosol and nucleus (21–23), and the ability of their cytosolic forms to promote *de novo* FeS cluster formation was demonstrated (24).

Because no information is available on FeS cluster assembly in trypanosomes, we investigated the function of mitochondria of *T. brucei* procyclics in this process. Initially, we identified the main components of its FeS cluster assembly machinery and constructed cell lines in which the expression of the IscS and IscU genes was down-regulated by means of RNA interference (RNAi). Analyses of the resulting phenotypes provide the first insight into FeS cluster biogenesis in the mitochondria of parasitic protists and support the hypothesis that the mitochondrion plays a fundamental and evolutionary conserved role in cellular FeS cluster assembly throughout the eukaryotes.

EXPERIMENTAL PROCEDURES

Construction of Vectors, Transfection, Cloning, RNAi Induction, and Growth—A 424-bp fragment of the TbiscS2 gene (supplemental material) was amplified by PCR from the *T. brucei* 427 genomic DNA using oligonucleotides IscS-F1 (5′-CACCATATGGTAGAGATGAAGCGTGATT) and IscS-R1 (5′-CACAAGCTTTTTCCTTCCATCAGCAAGT) (added NdeI and HindIII restriction sites are underlined), was cloned into pCR2.1 TOPO® (Invitrogen) and subcloned in pZJM (25). Similarly, a large portion of the TbiscU gene (nucleotides 44–528; see supplemental material) was amplified with the primers IscU-F1 (5′-CACCTCGAGCAGCCTCACTTCGGTCACT) and IscU-R1 (5′-TGCACGGATCCCCAACAGCCTCGGACTTAG) (added XhoI and BamHI restriction sites are underlined) and cloned into p2T7-177 (26). The procyclic *T. brucei* strain 29-13, transgenic for T7 RNA polymerase and the tetracycline repressor, was grown in SDM-79 medium in the presence of hygromycin and G418 (27). Transfection, selection and cloning were performed as described elsewhere (28). Synthesis of double-stranded RNA was induced by the addition of 2 μg/ml tetracycline. Growth curves of parental cells and clonal cell lines were obtained using the Z2 Cell Counter (Beckman Coulter Inc., Fullerton, CA) over a period of 8 days after the induction of RNAi. Following confirmation of successful RNAi (see below), one clone for each TbiscS2 and TbiscU was used for further experiments.

Reverse Transcription-PCR Analysis and Northern Blotting—DNA enriched for TbiscS2 mRNA was synthesized by reverse transcription of poly(A)$^+$ RNA with IscS-R2 (5′-CGAATTAAATCTGCCACTTGCGTC) and used as a template for amplification of the 5′ end region of this mRNA with IscS-R3 (5′-GGCAATATTGTTGGACTCCGTTGC) and the upstream spliced leader-specific primer SLTb1 (5′-AACTAACGCTATTATTAGAACAGT). Three sequenced clones were identical.

Total RNA was isolated from 5×10^7 exponentially growing noninduced and RNAi-induced cells by extraction with Tri Reagent (Sigma-Aldrich). TbiscS2 or TbiscU gene probes were labeled by random priming with [α-^{32}P]dATP (MP Biomedicals, Irvine, CA). Hybridization was carried out using standard procedure (28). The radioactive signal was detected using storage phosphorimaging.

Preparation of Antibodies and Immunoblot Analysis—The coding region of TbiscS2 and TbiscU was subcloned into a pQE30 vector (Qiagen) incorporating an N-terminal His_6 tag. Soluble protein was obtained from induced bacterial cells under denaturating conditions using affinity chromatography as described in the manufacturer's instructions. Polyclonal antibodies against recombinant TbiscS were prepared by immunizing rabbits (28, 29). The polyclonal rabbit antibodies raised against recombinant TbiscU were commercially prepared (Seva-Imuno, Prague, Czech Republic). Rabbit γ-globulins were purified from sera by affinity chromatography in a Prosep®, a high capacity column (Bioprocessing Ltd., Consett, UK).

Total cell lysates and subcellular fractions of noninduced and induced trypanosomes were separated on SDS-PAGE gels, blotted, and probed with polyclonal antibodies against TbisS2, TbiscU, aconitase (Ref. 40; provided by M. Boshart), Hsp60 (provided by P. A. M. Michels), mitochondrial RNA-binding protein 2 (MRP2) (28), and the La protein (29). Secondary anti-rabbit or anti-mouse antibodies coupled to alkaline phosphatase (MP Biomedicals) were visualized with 5-bromo-4-chloro-3-indolyl phosphate (Sigma-Aldrich).

Digitonin Fractionation—Digitonin fractionation of procyclics was performed as described elsewhere (30) with the following modifications. The cells were washed twice and resuspended in ice-cold SHE buffer (25 mM Hepes, pH 7.4, 250 mM sucrose, 1 mM EDTA) at $\sim 5 \times 10^9$ cells/ml. Aliquots containing 1 mg of protein were resuspended in 350 μl of Hanks' balanced salt solution buffer (Invitrogen) and incubated for 4 min at 25 °C with increasing concentrations of digitonin (Merck) dissolved in dimethylformamide and centrifuged at 14,000 $\times$ *g* for 2 min. Whole cell lysates were prepared by incubating the same aliquots in 350 μl of Hanks' balanced salt solution buffer containing 0.1% Triton X-100 for 5 min on ice and centrifuged as above. The resulting supernatants were immediately assayed for the presence of the cytosolic (pyruvate kinase) and mitochondrial (threonine dehydrogenase) marker enzymes. To obtain cytosolic and mitochondria-rich fractions, the concentration of digitonin was used that released the maximum pyruvate kinase activity and no threonine dehydrogenase into the supernatant. This supernatant was considered to represent the

cytosolic fraction. Pelleted intact mitochondria were washed once and then resuspended in 350 μl of Hanks' balanced salt solution buffer and incubated with 0.1% Triton X-100 for 5 min on ice. After centrifugation, the supernatant containing mitochondrial matrix proteins was collected (the mitochondrial fraction).

Enzyme Assays and Determination of Metabolic End Products—The activities of pyruvate kinase and threonine dehydrogenase were monitored spectrophotometrically at 340 nm as a rate of NADH oxidation or NAD reduction, respectively (31, 32). The activity of aconitase was measured as the production of *cis*-aconitate, monitored at 240 nm (33). Ubiquinol-cytochrome-*c* reductase activity (complex III) was measured in QCR buffer (40 mM sodium phosphate buffer, pH 7.4, 0.5 mM EDTA, 20 mM sodium malonate, 50 μM horse heart cytochrome *c* (Sigma-Aldrich), 0.005% dodecylmaltoside) as the rate of 2,3-dimethoxy-5-methyl-6-decyl-1,4-benzoquinol oxidation monitored at 550 nm (prior to use, decylubiquinone (Sigma-Aldrich) was reduced as described elsewhere (34)). KCN was added to a final concentration of 200 μM as an inhibitor of interfering oxidase activity.

To determine the metabolic end products, ~8×10^7 cells were washed once with phosphate-buffered saline, resuspended in 200 μl of incubation buffer (phosphate-buffered saline buffer supplemented with 11 mM glucose and 24 mM $NaHCO_3$, pH 7.3), and incubated for 2 h at 27 °C. After centrifugation for 10 min at 1,400 × *g*, the supernatant was analyzed by HPLC in a PL Hi-Plex H column as described elsewhere (35).

ATP Production in Isolated Mitochondria—Intact mitochondria were prepared from cell aliquots containing 1 mg of protein by digitonin fractionation as described above. The mitochondrial pellet was resuspended in 750 μl of the buffer for *in organello* ATP production assay (20 mM Tris-HCl, pH 7.4, 15 mM KH_2PO_4, 0.6 M sorbitol, 10 mM $MgSO_4$, 2.5 mg/ml bovine serum albumin), and 75-μl aliquots were used for each measurement. ATP production was induced by the addition of substrates as published elsewhere (36). The concentration of ATP was determined by a luminometer using the ATP Bioluminiscence assay kit CLS II (Roche Applied Science).

Measurement of Mitochondrial Membrane Potential—Tetramethylrodamine ethyl ester (Molecular Probes, Eugene, OR) uptake was used as a measure of the mitochondrial membrane potential (37).

EPR Analysis of FeS Clusters—EPR spectra were recorded on a Bruker Elexsys E580 spectrometer operating in X-band continuous-wave mode, with an Oxford Instruments ESR9000 liquid helium flow cryostat. The measurement conditions were: temperature, 12 K; microwave power, 20 milliwatts; frequency, 9.38 GHz; and modulation amplitude, 1 millitesla.

RESULTS

Genes Coding for TbiscS and TbiscU—The *T. brucei* genome project data base (www.sanger.ac.uk/) was searched for homologs of IscS and IscU using *S. cerevisiae* Nfs1p and Isu1p as queries. A BLAST search for IscS identified two homologs in the *T. brucei* genome, here named TbiscS1 and TbiscS2, with calculated molecular weights of 48,991 and 48,150, respectively. Alignment of their deduced amino acid sequences

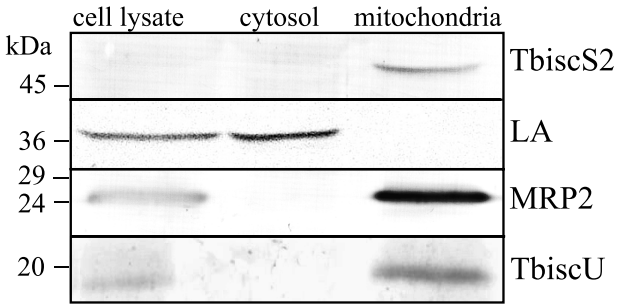

FIGURE 1. **Subcellular localization of TbiscS2 and TbiscU by immunoblot analysis in whole cell lysates, cytosol, and mitochondrion of the parental 29-13 cells.** MRP2 and La proteins were used as mitochondrial and cytosolic marker proteins, respectively.

together with Nfs1p revealed significant differences between the two trypanosome genes (supplemental material). Similar to Nfs1p, TbiscS2 possesses conserved residues corresponding to the active site loop that are responsible for the targeted delivery of sulfur to IscU (38), as well as the conserved C terminus essential for specific interaction with IscU (39). In contrast, TbiscS1 lacks these regions. Phylogenetic analysis of the two *T. brucei* proteins indicated that TbiscS2 is closely related to other mitochondrial IscS homologs, whereas TbiscS1 clusters together with putative selenocysteine lyases (data not shown). Thus, TbiscS2 was selected for further studies. To prove that TbiscS2 is transcribed, the spliced leader RNA and primers from the 5′ end of the gene were used for reverse transcription-PCR. In three clones with identical sequences, the splice acceptor site was mapped to 25 bp upstream of the initial methionine, resulting in a very short 5′-untranslated region (data not shown).

A BLAST search for Isu1p identified a single IscU homolog (TbiscU) in the *T. brucei* genome data base with a calculated molecular weight of 19,435. Alignment of the deduced TbiscU amino acid sequence with yeast Isu1p revealed that all three conserved cysteine residues required for the assembly of the transient FeS cluster are present in TbiscU (supplemental material).

TbiscS2 and TbiscU Are Localized in the Mitochondrion—PsortII analysis (psort.nibb.ac.jp/) of TbiscS2 and TbiscU predicted N-terminal leader sequences for targeting the proteins into mitochondria as well as putative cleavage sites with the characteristic arginine at the −2 position that is recognized by mitochondrial processing peptidase (supplemental material). To verify the predicted cellular localization of these proteins in procyclic *T. brucei*, specific polyclonal antibodies were raised against recombinant TbiscS2 and TbiscU and used for immunoblot analysis. In subcellular fractions obtained by differential permeabilization of the cell membranes by increasing concentrations of digitonin (30), both TbiscS2 and TbiscU were detected in the mitochondrial fractions, whereas no signals were observed in the cytosol (Fig. 1). Antibodies against the MRP2 (28) and the cytosolic La protein (29) were used as controls in cell fractionation experiments. The low cellular abundance of TbiscS2 is probably responsible for difficulty in identifying the protein in the whole cell lysate (40).

Inhibition of TbiscS2 and TbiscU Gene Expression by RNAi—A 424-bp-long fragment of TbiscS2 and a 484-bp-long fragment of TbiscU (supplemental material) were cloned into the

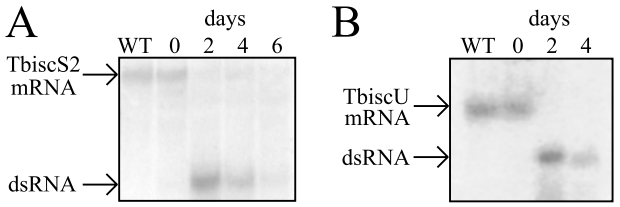

FIGURE 2. **Effect of TbiscS2 (*A*) and TbiscU (*B*) RNAi on mRNA levels.** TbiscS2 and TbiscU mRNA levels were analyzed by Northern blot analysis in extracts from parental strain 29-13 (WT), noninduced cells (day 0) and in extracts isolated 2, 4, and 6 days after RNAi induction (*A*, TbiscS RNAi cells) or 2 and 4 days after RNAi induction (*B*, TbiscU RNAi cells). The positions of the targeted mRNAs and the double-stranded RNAs synthesized after induction are indicated with *arrows*. *WT*, wild type.

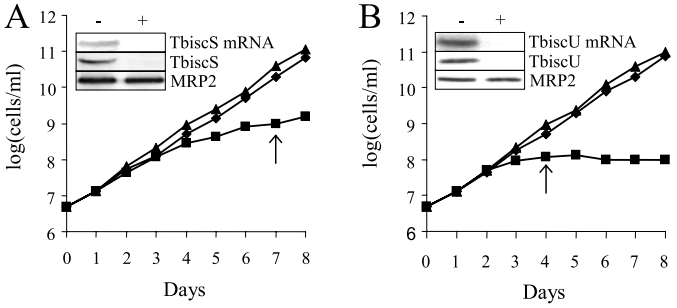

FIGURE 3. **Effect of TbiscS2 (*A*) and TbiscU (*B*) RNAi on cell growth.** The cell density of the parental 29-13 cells (*triangles*), noninduced cells (*diamonds*), and cells induced with 2 μg/ml of tetracycline (*squares*) are indicated. The *y* axis is a log scale and represents the product of the measured cell densities and total dilution. The *arrows* indicate the time points chosen for biochemical experiments. The *insets* show a Northern blot of the total RNA (*top panels*) and immunoblots of mitochondrial fractions (*middle* and *bottom panels*) before (−) and after (+) RNAi induction by tetracycline. The mitochondrial protein MRP2 was used as a protein loading control.

pZJM (25) and p2T7-177 (26) RNAi vectors, respectively. Transfection of both constructs into the procyclics resulted in stable integration into the trypanosome genome as confirmed by Southern hybridization of the digested total DNA (data not shown). Phleomycin-resistant transfectants were cloned by limiting dilution, and RNAi was induced by the addition of tetracycline into the SDM-79 medium. Total RNA was isolated from the noninduced and induced clonal cell lines at different time points and analyzed on Northern blots (Fig. 2). The analysis showed that in the TbiscS2 and TbiscU knock-downs, the corresponding mRNA was almost completely eliminated after 2–3 days of induction, followed by growth inhibition of both mutants. Although the growth of the parental strain 29-13 and noninduced RNAi cells were almost identical, the growth of TbiscS2 knock-down cells gradually slowed down, and the growth of the TbiscU-induced cells was completely inhibited (Fig. 3). The observed phenotypes indicate that both components of the mitochondrial FeS cluster assembly machinery are essential for the viability of the procyclics. Based on the growth curves, days 4 and 7 after RNAi induction were selected for all subsequent biochemical experiments. At these time points, the levels of TbiscS2 and TbiscU mRNA and corresponding proteins in the mitochondria of their respective knock-downs became undetectable by Northern and immunoblot analyses (Fig. 3).

Mitochondrial FeS Cluster Assembly Machinery Is Required for FeS Proteins in Mitochondria and Cytosol—Aconitase was chosen as a marker FeS protein to test whether TbiscS2 and

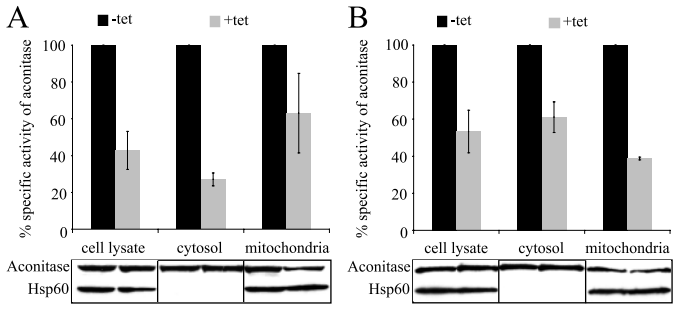

FIGURE 4. **Decrease in activity of marker FeS enzyme aconitase in TbiscS2 (*A*) and TbiscU (*B*) RNAi cells.** The percentages of specific activity of aconitase in total cell lysate, cytosol, and mitochondria in cells before (−*tet*) and after 7 (TbiscS2) or 4 (TbiscU) days (+*tet*) of RNAi induction by tetracycline are shown by *black* and *gray columns*, respectively. Immunoblot analyses of aconitase apoprotein in the respective fractions are shown below the *bars*. The mitochondrial non-FeS protein Hsp60 was used as a protein loading control. The *bars* indicate standard deviations ($n = 3$).

TbiscU are required for FeS cluster assembly in the trypanosome organelle and whether the mitochondrial FeS cluster assembly machinery is also involved in the maturation of cytosolic FeS proteins. In procyclic trypanosomes, aconitase has dual localization, with 70 and 30% of its total active form being distributed in the mitochondrion and cytosol, respectively (33). After RNAi induction, the activity of aconitase was reduced in both cellular compartments (Fig. 4). The TbiscS2 knock-down cells displayed higher inhibition of the cytosolic aconitase activity, which was down to ~30% of that in the noninduced cells, than mitochondrial aconitase, which retained ~70% of its activity (Fig. 4*A*). The down-regulation of TbiscU resulted in a considerably higher inhibition of aconitase activity in the mitochondrion than in the cytosol (Fig. 4*B*). In contrast, the activity of pyruvate kinase, a cytosolic enzyme that does not require an FeS cluster for its activity, remained unaffected (data not shown).

In addition to the impaired FeS cluster assembly, this inhibition of aconitase activity could be caused by affecting the expression of the corresponding protein or by oxidation of the [4Fe4S] cluster of the active aconitase to its inactive [3Fe4S] form (41). To exclude these possibilities, the protein level and presence of aconitase clusters in the subcellular fractions of TbiscS2-induced cells were verified by immunoblot analysis (Fig. 4) and EPR (Fig. 5). No decrease in the aconitase level in the cytosol of the induced cells was observed on immunoblots. The EPR analysis unequivocally confirmed that the decrease in the cytosolic aconitase activity was a consequence of decreased FeS cluster formation. Because the [4Fe4S] cluster is highly susceptible to conversion to [3Fe4S] upon exposure to oxygen, we assumed that in the samples prepared under aerobic conditions, all of the aconitase clusters were present in the [3Fe4S] form. The signal corresponding to total [3Fe4S] clusters of cytosolic aconitase in the induced cells was only 20% of that in the noninduced cells (Fig. 5*A*).

The level of mitochondrial aconitase detected on immunoblots of TbiscS2 knock-downs was slightly decreased in comparison to noninterfered cells. This effect is most likely caused by the degradation of apo-aconitase, which was observed in yeast mitochondria (42). The mitochondrial EPR spectra comprise contributions from the [3Fe4S] clusters of aconitase (peak at

$g = 2.03$) and succinate dehydrogenase (peak at $g = 2.02$) (43, 44). As expected, the intensity of the combined signals in the mitochondria of induced cells was decreased, accounting for about 30% of that in noninduced cells (Fig. 5*B*). These results indicate that TbiscS2 and TbiscU, both mitochondrial components of the FeS cluster assembly machinery, are essential for the maturation of FeS proteins operating in the mitochondrion as well as in the cytosol of *T. brucei* procyclics.

Metabolic Changes Mimic Interstagial Transformation—FeS proteins are involved in critical steps of mitochondrial energy metabolism, which is substantially down-regulated in the bloodstream stages. Similar metabolic changes might be induced in cells with impaired FeS cluster formations, which in turn affect the function of FeS proteins. To test this hypothesis, we compared mitochondrial ATP synthesis, membrane potential, and the end products of glucose metabolism in FeS cluster assembly-competent cells and procyclics in which TbiscS2 and TbiscU were down-regulated.

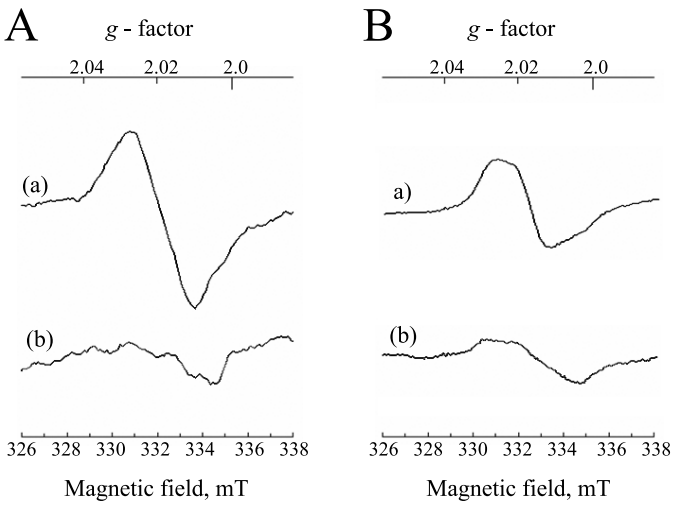

FIGURE 5. **Electron paramagnetic resonance analysis of the cytosolic (*A*) and mitochondrial (*B*) fractions of noninduced cells (*line a*) and cells after 7 days of TbiscS2 RNAi induction (*line b*).** The signals in the cytosol and mitochondria belong to aconitase ($g = 2.03$) and aconitase with succinate dehydrogenase ($g = 2.02$ and 2.03), respectively.

The mitochondrial ATP of the procyclic stage is produced via three different pathways that can be assayed in the isolated intact mitochondria (36): (i) Succinate is the main substrate for oxidative phosphorylation. A respiratory chain loaded with electrons by succinate dehydrogenase generates a proton gradient that drives mitochondrial F_0F_1 ATP synthetase (45). This pathway involves at least two FeS proteins, namely succinate dehydrogenase and the Rieske protein of ubiquinol-cytochrome-*c* reductase. In TbiscS2 knock-downs, succinate dehydrogenase-dependent ATP production was completely lost (Fig. 6*A*). The residual succinate-dependent ATP synthesis was insensitive to malonate, a competitive inhibitor of succinate dehydrogenase. Accordingly, the specific activity of ubiquinol-cytochrome-*c* reductase in mitochondrial lysates of the parental strain and noninduced cells fluctuated around 750 milliunits/mg, whereas the level of FeS cluster assembly-impaired cells was reduced by about 50% in three independent experiments. (ii) α-Ketoglutarate induces ATP production by substrate level phosphorylation occurring in the citric acid cycle. (iii) Pyruvate and succinate induce ATP production by substrate level phosphorylation occurring in the acetate-succinate CoA transferase/succinyl-CoA synthetase cycle. Interestingly, both pyruvate-succinate- and α-ketoglutarate-induced ATP synthesis was moderately decreased upon down-regulation of TbiscS2, although no FeS proteins are directly involved in these pathways (Fig. 6, *B* and *C*). However, both pyruvate and α-ketoglutarate metabolism are indirectly dependent on the maintenance of the mitochondrial redox balance, for which FeS proteins are required.

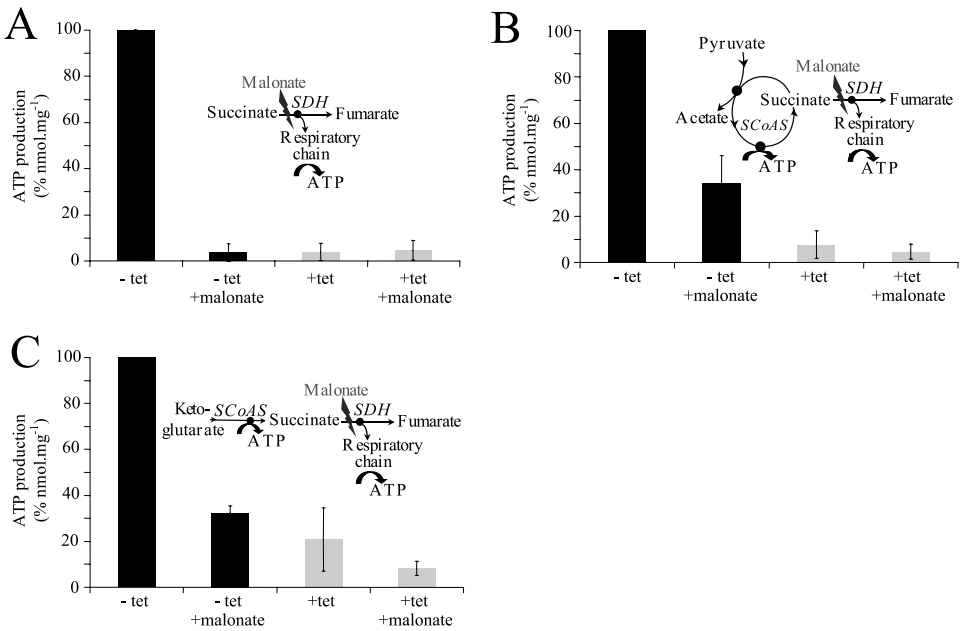

FIGURE 6. **ATP production is severely affected in the mitochondrion of TbiscS2 RNAi cells.** The three ATP-producing pathways are indicated. ATP production in the mitochondria isolated from noninduced and tetracycline-induced cells (7 days post-induction) was triggered by the addition of succinate (*A*), pyruvate and succinate (*B*), or ketoglutarate (*C*).

Previous experiments indicated a malfunction of FeS protein-dependent components of the proton generating respiratory chain in FeS cluster assembly-impaired cells. Thus, changes in mitochondrial membrane potential can be expected. To study the mitochondrial membrane potential in *T. brucei*, tetramethylrodamine ethyl ester has been evaluated as a sensitive fluorescence probe (37). Indeed, cytofluorometric profiles of trypanosomes using tetramethylrodamine ethyl ester in this study indicated a decreased membrane potential in the iron-sulfur cluster assembly-impaired mitochondria of *T. brucei* interfered against TbiscS2 and TbiscU in comparison with the noninterfered cells (supplemental material).

All of these results indicate that the involvement of mitochondria in energetic metabolism is decreased

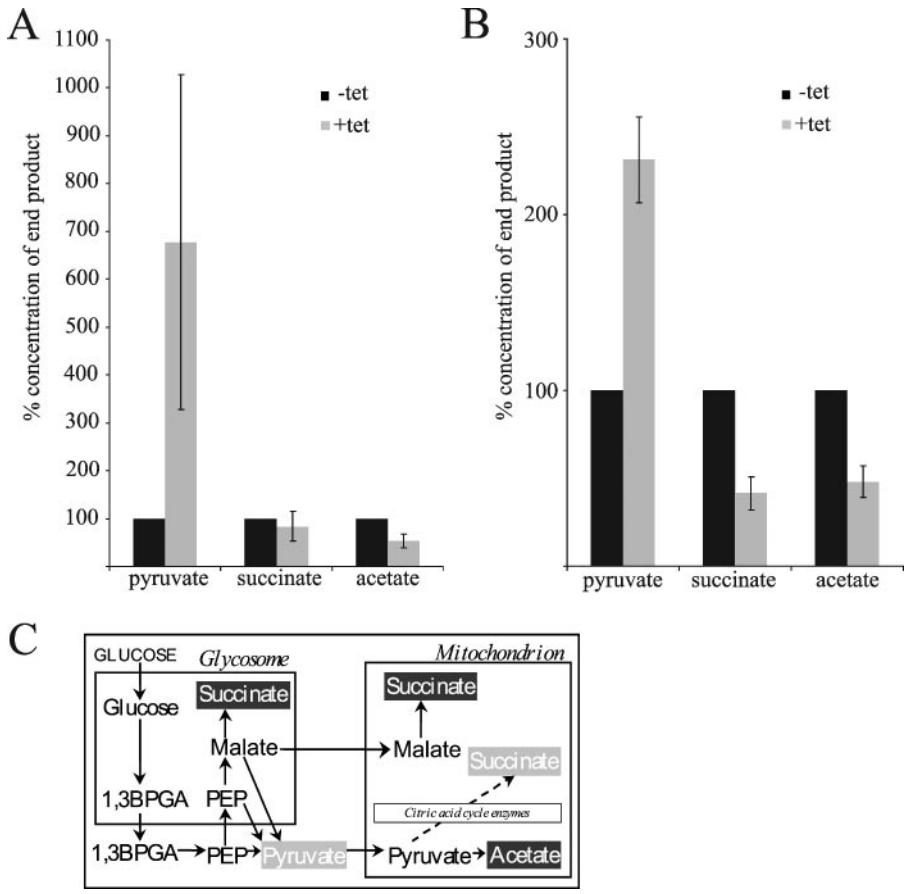

FIGURE 7. **Effect of TbiscS2 (*A*) and TbiscU (*B*) RNAi on end products of glucose metabolism.** Graph shows relative concentration of glucose metabolism end products detected by HPLC in the incubation buffer after removal of intact cells. Metabolites of noninduced cells (−*tet*) are represented by *black columns*, and end products of the cells in which RNAi was induced (+*tet*) for 7 (TbiscS2) or 4 (TbiscU) days are represented by *gray columns*. *C*, the schematic diagram shows glucose metabolism in noninduced cells with indication of major (*black*) and minor (*gray*) end products.

in TbiscS2 and TbiscU knock-downs. In the bloodstream stages, the inactivation of mitochondria is compensated by glycolysis producing pyruvate as a major metabolic end product. A similar trend was observed in FeS cluster assembly-impaired cells. The production of succinate decreased to 84 and 41% after induction of RNAi in TbiscS2 and TbiscU knock-down cells, respectively. The acetate production decreased to 54% after TbiscS2 and to 48% after TbiscU knock-down. In contrast, the production of pyruvate was 8-fold and more than 2-fold increased in TbiscS2 and TbiscU knock-down cells, respectively, when compared with wild-type trypanosomes (Fig. 7).

DISCUSSION

In this paper, we have demonstrated that TbiscS2 and TbiscU, homologs of the bacterial and yeast cysteine desulfurase IscS/Nfs, and the scaffold protein IscU/Isu are indispensable for FeS cluster formation and consequently the viability of the procyclic stage of *T. brucei.* Although both proteins were specifically localized to the mitochondrion, their deficient expression affected the maturation of FeS proteins operating not only in the mitochondrion, but also in the cytosol.

The mitochondria isolated from knock-down cells displayed decreased enzymatic activities of FeS proteins including aconitase and Rieske protein-containing ubiquinol-cytochrome-*c* reductase, undetectable succinate-induced ATP synthesis mediated by succinate dehydrogenase (complex II), and decreased mitochondrial membrane potential. In addition, the cells expressing the interfering RNA had decreased cytochrome-dependent respiration via complex IV and partially switched to the trypanosome alternative oxidase.[3]

The dual localization of aconitase in the mitochondrion and cytosol of *T. brucei*, with both forms being products of a single-copy gene (33) provides a convenient system to examine whether TbiscS2 and TbiscU are required for FeS cluster formation outside of the organelle. Indeed, the enzymatic activity of cytosolic aconitase was markedly decreased upon RNAi induction in both TbiscS2 and TbiscU knock-downs. Control immunoblot and EPR analyses confirmed that the reduction of aconitase activity in both mitochondria and cytosol was due to the lack of FeS clusters.

The analysis of subcellular fractions using specific antibodies raised against recombinant proteins revealed the confinement of TbiscS2 and TbiscU to the mitochondria-rich fractions of *T. brucei*. Accordingly, both proteins possess putative N-terminal presequences required for protein targeting into the mitochondrion. Moreover, TbiscS2 lacks an alternative initiation codon required for synthesizing the cytosolic IscS form identified in humans (21). Although we cannot exclude the possibility that a low level of TbiscS2 and/or TbiscU is present in the cytosol below the detection limit of immunoblot analysis, our experimental data suggest that the trypanosome mitochondrion is essential for the maturation of FeS proteins inside as well as outside the organelle, as was observed in yeast (42, 46). In addition to mitochondria, components of the FeS cluster assembly machinery were recently localized to the mitochondrion-related hydrogenosomes and mitosomes of the parasitic protists *Trichomonas vaginalis* and *Giardia intestinalis*, respectively (14, 15, 47, 48). Based on these findings from evolutionarily distant organisms, it seems that the formation of cellular FeS clusters is a general role of mitochondria in eukaryotic cells and that this role was probably inherited from a premitochondrial endosymbiont (14, 49, 50). Further studies are required to elucidate why the FeS cluster-producing pathway was transferred to another cellular com-

[3] V. Vilímová, E. Horáková, A. Horváth, J. Lukeš, and J. Tachezy, unpublished data.

partment in humans, a pattern that is currently under debate (11, 24), and if so, at which step of evolution this pattern appeared.

In *T. brucei*, one of the major differences between the procyclic stage of the insect vector and the blood stage parasitizing mammals is the way they generate energy, in particular the use of the mitochondrion in the process (10, 51). Remarkably, the overall metabolic changes observed in the FeS cluster-impaired cells resulted in a phenotype that mimics the interstagial transition of the organelle. The mitochondrion of the TbiscS2 and TbiscU procyclic knock-downs resembled its counterpart in the blood stages by decreasing its production of ATP and acetate and by partially redirecting its electron flow from the FeS cluster-containing respiratory complexes, which pass those electrons on to cytochrome *c* oxidase, to cytochrome-independent trypanosome alternative oxidase. Moreover, the impaired cells produce less succinate, which could be ascribed to the decreased activity of fumarase, another putative FeS protein. Consequently, the production of pyruvate was increased in these cells. The molecular events responsible for the transformation from one life stage to the other remain poorly understood in *T. brucei* (52). However, it is apparent that the cyclic transformation of procyclics into blood stages and vice versa is associated with the down- and up-regulation of the FeS protein-dependent metabolic pathways, which are involved in the mitochondrial components of the citric acid cycle and respiratory chain.

In conclusion, our study provides experimental evidence that FeS cluster assembly machinery is one of the fundamental cell components that are shared throughout the eukaryotes, from fungi and animals (Opisthokonta) to the most distant unicellular organisms represented by *T. brucei* (Excavata). Specifically in *T. brucei*, we postulate that the function of ISC assembly machinery is critical for the interstagial changes in the *T. brucei* life cycle. A challenging question will be to establish whether this machinery is developmentally regulated in this parasitic protist and what factor triggers FeS protein biogenesis during the cyclic changes of its host.

Acknowledgments—We are grateful to The Institute for Genomic Research and the Wellcome Trust Sanger Institute for the sequences accessible in the T. brucei genome database. We thank I. Šlapetová for contributions in the early stages of this project, P. A. M. Michels for help with cell fractionation experiments and biochemical studies, and S. E. J. Rigby and P. Heathcote for providing the EPR facilities. P. A. M. Michels and M. Boshart kindly provided antibodies. We also thank T. M. Embley for critical reading of the manuscript.

REFERENCES

1. Berriman, M., Ghedin, E., Hertz-Fowler, C., Blandin, G., Renauld, H., Bartholomeu, D. C., Lennard, N. J., Caler, E., Hamlin, N. E., Haas, B., Bohme, W., Hannick, L., Aslett, M. A., Shallom, J., Marcello, L., Hou, L. H., Wickstead, B., Alsmark, U. C. M., Arrowsmith, C., Atkin, R. J., Barron, A. J., Bringaud, F., Brooks, K., Carrington, M., Cherevach, I., Chillingworth, T. J., Churcher, C., Clark, L. N., Corton, C. H., Cronin, A., Davies, R. M., Doggett, J., Djikeng, A., Feldblyum, T., Field, M. C., Fraser, A., Goodhead, I., Hance, Z., Harper, D., Harris, B. R., Hauser, H., Hostetter, J., Ivens, A., Jagels, K., Johnson, D., Johnson, J., Jones, K., Kerhornou, A. X., Koo, H., Larke, N., Landfear, S., Larkin, C., Leech, V., Line, A., Lord, A., MacLeod, A., Mooney, P. J., Moule, S., Martin, D. M. A., Morgan, G. W., Mungall, K., Norbertczak, H., Ormond, D., Pai, G., Peacock, C. S., Peterson, J., Quail, M. A., Rabbinowitsch, E., Rajandream, M. A., Reitter, C., Salzberg, S. L., Sanders, M., Schobel, S., Sharp, S., Simmonds, M., Simpson, A. J., Talton, L., Turner, C. M. R., Tait, A., Tivey, A. R., Van Aken, S., Walker, D., Wanless, D., Wang, S. L., White, B., White, O., Whitehead, S., Woodward, J., Wortman, J., Adams, M. D., Embley, T. M., Gull, K., Ullu, E., Barry, J. D., Fairlamb, A. H., Opperdoes, F., Barret, B. G., Donelson, J. E., Hall, N., Fraser, C. M., Melville, S. E., and El-Sayed, N. M. (2005) *Science* **309,** 416–422
2. Motyka, S. A., and Englund, P. T. (2004) *Curr. Opin. Microbiol.* **7,** 362–368
3. Simpson, A. G., and Roger, A. J. (2004) *Curr. Biol.* **14,** R693–R696
4. Cavalier-Smith, T. (2004) *Proc. Biol. Sci.* **271,** 1251–1262
5. Lukeš, J., Hashimi, H., and Ziková, A. (2005) *Curr. Genet.* **48,** 277–299
6. Michels, P. A., Moyersoen, J., Krazy, H., Galland, N., Herman, M., and Hannaert, V. (2005) *Mol. Membr. Biol.* **22,** 133–145
7. Clayton, C. E., and Michels, P. (1996) *Parasitol. Today* **12,** 465–471
8. Chaudhuri, M., Ajayi, W., and Hill, G. C. (1998) *Mol. Biochem. Parasitol.* **95,** 53–68
9. van Hellemond, J. J., Opperdoes, F. R., and Tielens, A. G. M. (1998) *Proc. Natl. Acad. Sci. U. S. A.* **95,** 3036–3041
10. Besteiro, S., Barrett, M. P., Riviere, L., and Bringaud, F. (2005) *Trends Parasitol.* **21,** 185–191
11. Lill, R., and Mühlenhoff, U. (2005) *Trends Biochem. Sci.* **30,** 133–141
12. Johnson D., Dean, D., Smith, A. D., and Johnson, M. K. (2004) *Annu. Rev. Biochem.* **74,** 247–281
13. Lill, R., and Kispal, G. (2000) *Trends Biochem. Sci.* **25,** 352–356
14. Sutak, R., Dolezal, P., Fiumera, H. L., Hrdy, I., Dancis, A., Delgadillo-Correa, M., Johnson, P. J., Müller, M., and Tachezy, J. (2004) *Proc. Natl. Acad. Sci. U. S. A.* **101,** 10368–10373
15. Tovar, J., Léon-Avila, G., Sánchez, L. B., Sutak, R., Tachezy, J., van der Giezen, M., Hernández, M., Müller, M., and Lucocq, J. M. (2003) *Nature* **426,** 172–176
16. LaGier, M. J., Tachezy, J., Stejskal, F., Kutisová, K., and Keithly, J. S. (2003) *Microbiology* (*UK*) **149,** 3519–3530
17. Katinka, M. D., Duprat, S., Cornillot, E., Metenier, G., Thomarat, F., Prensier, G., Barbe, V., Peyretaillade, E., Brottier, P., Wincker, P., Delbac, F., El Alaoui, H., Peyret, P., Saurin, W., Gouy, M., Weissenbach, J., and Vivares, C. P. (2001) *Nature* **414,** 450–453
18. Balk, J., and Lobreaux, S. (2005) *Trends Plant Sci.* **10,** 324–331
19. Kispal, G., Sipos, K., Lange, H., Fekete, Z., Bedekovics, T., Janaky, T., Bassler, J., Aguilar Netz, D. J., Balk, J., Rotte, C., and Lill, R. (2005) *EMBO J.* **24,** 589–598
20. Yarunin, A., Panse, V. G., Petfalski, E., Dez, C., Tollervey, D., and Hurt, E. C. (2005) *EMBO J.* **24,** 580–588
21. Land, T., and Rouault, T. A. (1998) *Mol. Cell* **2,** 807–815
22. Tong, W. H., Jameson, G. N. L., Huynh, B. H., and Rouault, T. A. (2003) *Proc. Natl. Acad. Sci. U. S. A.* **100,** 9762–9767
23. Tong, W. H., and Rouault, T. (2000) *EMBO J.* **19,** 5692–5700
24. Li, K., Tong, W. H., Hughes, R. M., and Rouault, T. A. (2006) *J. Biol. Chem.* **281,** 12344–12351
25. Wang, Z., Morris, J. C., Drew, M. E., and Englund, P. T. (2000) *J. Biol. Chem.* **275,** 40174–40179
26. Wickstead, B., Ersfeld, K., and Gull, K. (2002) *Mol. Biochem. Parasitol.* **125,** 211–216
27. Wirtz, E., and Clayton, C. (1995) *Science* **268,** 1179–1183
28. Vondrušková, E., van den, B. J., Ziková, A., Ernst, N. L., Stuart, K., Benne, R., and Lukeš, J. (2005) *J. Biol. Chem.* **280,** 2429–2438
29. Foldynová-Trantírková, S., Paris, Z., Sturm, N. R., Campbell, D. A., and Lukeš, J. (2005) *Int. J. Parasitol.* **35,** 359–366
30. Moyersoen, J., Choe, J., Kumar, A., Voncken, F. G., Hol, W. G., and Michels, P. A. (2003) *Eur. J. Biochem.* **270,** 2059–2067
31. Callens, M., and Opperdoes, F. R. (1992) *Mol. Biochem. Parasitol.* **50,** 235–243
32. Heise, N., and Opperdoes, F. R. (1999) *Mol. Biochem. Parasitol.* **99,** 21–32
33. Saas, J., Ziegelbauer, K., von, H. A., Fast, B., and Boshart, M. (2000) *J. Biol. Chem.* **275,** 2745–2755
34. Trumpower, B. L., and Edwards, C. A. (1979) *J. Biol. Chem.* **254,**

8697–8706
35. Vanacova, S., Rasoloson, D., Razga, J., Hrdý, I., Kulda, J., and Tachezy, J. (2001) *Microbiology* (*UK*) **147,** 53–62
36. Bochud-Allemann, N., and Schneider, A. (2002) *J. Biol. Chem.* **277,** 32849–32854
37. Horváth, A., Horáková, E., Dunajciková, P., Verner, Z., Pravdová, E., Šlapetová, I., Cuninková, L., and Lukeš, J. (2005) *Mol. Microbiol.* **58,** 116–130
38. Lauhon, C. T., Skovran, E., Urbina, H. D., Downs, D. M., and Vickery, L. E. (2004) *J. Biol. Chem.* **279,** 19551–19558
39. Urbina, H. D., Silberg, J. J., Hoff, K. G., and Vickery, L. E. (2001) *J. Biol. Chem.* **276,** 44521–44526
40. Panigrahi, A. K., Schnaufer, A., Carmean, N., Igo, R. P., Jr., Gygi, S. P., Ernst, N. L., Palazzo, S. S., Weston, D. S., Aebersold, R., Salavati, R., and Stuart, K. D. (2001) *Mol. Cell Biol.* **21,** 6833–6840
41. Flint, D. H., Tuminello, J. F., and Emptage, M. H. (1993) *J. Biol. Chem.* **268,** 22369–22376
42. Kispal, G., Csere, P., Prohl, C., and Lill, R. (1999) *EMBO J.* **18,** 3981–3989
43. Ackrell, B. A., Kearney, E. B., Mims, W. B., Peisach, J., and Beinert, H. (1984) *J. Biol. Chem.* **259,** 4015–4018
44. Beinert, H., Emptage, M. H., Dreyer, J. L., Scott, R. A., Hahn, J. E., Hodgson, K. O., and Thomson, A. J. (1983) *Proc. Natl. Acad. Sci. U. S. A.* **80,** 393–396
45. Tielens, A. G. M., and van Hellemond, J. J. (1998) *Biochim. Biophys. Acta.* **1365,** 71–78
46. Gerber, J., Mühlenhoff, U., and Lill, R. (2003) *EMBO Rep.* **4,** 906–911
47. Dolezal, P., Smid, O., Rada, P., Zubacova, Z., Bursac, D., Sutak, R., Nebesarova, J., Lithgow, T., and Tachezy, J. (2005) *Proc. Natl. Acad. Sci. U. S. A.* **102,** 10924–10929
48. Regoes, A., Zourmpanou, D., Leon-Avila, G., van der Giezen, M., Tovar, J., and Hehl, A. B. (2005) *J. Biol. Chem.* **280,** 30557–30563
49. Tachezy, J., Sánchez, L. B., and Müller, M. (2001) *Mol. Biol. Evol.* **18,** 1919–1928
50. Embley, T. M., and Martin, W. (2006) *Nature* **440,** 623–630
51. van Weelden, S. W., van Hellemond, J. J., Opperdoes, F. R., and Tielens, A. G. (2005) *J. Biol. Chem.* **280,** 12451–12460
52. Hendriks, E., van Deursen, F. J., Wilson, J., Sarkar, M., Timms, M., and Matthews, K. R. (2000) *Biochem. Soc. Trans.* **28,** 531–536

REDUCTIVE EVOLUTION OF THE MITOCHONDRIAL PROCESSING PEPTIDASES OF UNICELLULAR PARASITES

Ondřej Šmíd[1], Anna Matušková[2], Simon R. Harris[3], Tomáš Kučera[2], Marián Novotný[1], Lenka Horváthová[1], Ivan Hrdý[1], Eva Kutejová[4], Robert P. Hirt[3], T. Martin Embley[3], Jiří Janata[2], and Jan Tachezy[1]

[1]Department of Parasitology, Faculty of Science, Charles University in Prague, Vinicna 7, 128 44 Prague, Czech Republic.

[2]Institute of Microbiology, Academy of Sciences of the Czech Republic, Videnska 1083, 14220 Prague, Czech Republic.

[3]Institute for Cell and Molecular Biosciences, Catherine Cookson Building, Framlington Place, Newcastle University, Newcastle upon Tyne, NE2 4HH, UK.

[4]Institute of Molecular Biology, Slovak Academy of Sciences, Dubravska cesta 21, 845 51 Bratislava, Slovak Republic.

Corresponding author:

Prof. Jan Tachezy, Ph.D.
Charles University in Prague, Faculty of Science
Department of Parasitology
Vinicna 7, 128 44 Prague
Czech Republic
Phone: +420-221-951-811
FAX: +420-224-919-704
E-mail: tachezy@natur.cuni.cz

ABSTRACT

Mitochondrial processing peptidases (MPP) are heterodimeric enzymes (α/βMPP) that play an essential role in mitochondrial biogenesis, by recognizing and cleaving the targeting presequences of nuclear-encoded mitochondrial proteins. The two subunits are paralogues that probably evolved by duplication of a gene for a monomeric metallopeptidase from the endosymbiotic ancestor of mitochondria. Here we characterize the MPP-like proteins from two highly reduced versions of mitochondria, the mitosomes of *Giardia intestinalis* and the hydrogenosomes of *Trichomonas vaginalis*. We demonstrate that the *Trichomonas* processing peptidase (HPP) functions efficiently as a α/β heterodimer. By contrast, and so far uniquely among eukaryotes, the *Giardia* processing peptidase (GPP) functions as a monomer comprising a single βMPP-like protein (βGPP). The structure and surface charge distribution of βGPP appear to have co-evolved with the properties of *Giardia* mitosomal targeting sequences, which, unlike classic mitochondrial targeting signals, are typically short and depauperate in positively-charged residues. The majority of hydrogenosomal presequences resemble those of mitosomes, but longer, positively-charged mitochondrial-type presequences were also identified, consistent with the retention of the *T. vaginalis* αHPP. Our phylogenetic analyses suggest that MPP and the divergent α/βHPP and βGPP evolved from an ancestral heterodimeric α/βMPP metallopeptidase, implying that the monomeric structure of GPP, resembling the putative ancestral state of the mitochondrial enzyme, is the product of reductive evolution.

INTRODUCTION

The acquisition of the mitochondrial endosymbiont and its evolution into the mitochondrion were key events in the evolution of eukaryotes (1). During this process, most of the protomitochondrial genome was either lost or transferred to the nucleus of the host cell (2). As a consequence, most mitochondrial proteins are host-nuclear encoded and must be specifically targeted to the organelle where they function. In the best understood system, N-terminal extensions attached to mitochondrial matrix proteins are specifically recognised by receptors on the mitochondrial surface, and the preproteins are subsequently imported by translocases of the outer and inner mitochondrial membranes (3). A final step in the import process is the removal of the N-terminal extension, by the mitochondrial processing peptidase (MPP) (4), to prevent it from interfering with protein function and/or stability (5). The MPP comprises a catalytic βMPP subunit that binds a zinc cation using amino acid residues of the conserved motif H*XX*EHX_{76}E (6), and a regulatory αMPP subunit with a flexible glycine-rich loop that is important for substrate recognition (7). The two subunits together form a negatively charged cavity that accommodates and immobilizes presequences during processing (6). The activity of MPP thus requires the cooperative action of both subunits; neither subunit is functional alone (6, 8).

Mitochondrial targeting presequences are characterized by the ability to form a positively-charged amphipathic alpha helix, but otherwise show little primary sequence conservation (6). Their most prominent common feature is the presence of a cleavage motif, which determines the peptide bond to be cleaved by the processing peptidase. The cleavage motif includes a positively-charged residue, typically arginine, at the -2 or -3 position from the cleavage site (P_2 or P_3), which is followed by hydrophobic (P_1') and hydrophilic (P_2', P_3') residues (9). Mutational analyses indicate that the P_2 (P_3)

arginine plays a key role in the recognition of the processing site by MPP and interacts with the glutamate of the βMPP active site (9). In addition, there are one or more basic amino acid residue(s) N-terminally distal from the processing site that bind to acidic residues of the MPP cavity and stabilize the substrate-MPP complex (10).

Mitosomes and hydrogenosomes are highly reduced versions of mitochondria that are found in diverse parasitic or free-living unicellular eukaryotes inhabiting oxygen-poor or intracellular niches (1). The *Giardia* and *Trichomonas* organelles lack a genome so all of their proteins are encoded by the nuclear genome and must be imported (1). Some hydrogenosomal and mitosomal proteins have N-terminal extensions that are reminiscent of the presequences that direct proteins into mitochondria and they contain distinguishable cleavage motifs (11, 12). This suggests that the *Giardia* and *Trichomonas* organelles may also contain an MPP-like enzyme. A single gene coding for a putative processing peptidase has been found in the genome of *G. intestinalis* (13) and the gene product has been shown to localize in mitosomes (14). The primary structure of GPP is highly divergent from mitochondrial homologues, with only 13.1% identity and 29.7% similarity to the βMPP of *Saccharomyces cerevisiae*. A single gene for a βMPP homologue (20.9% identity and 42.9% similarity to *S. cerevisiae* βMPP) was also recently identified in the genome of *T. vaginalis* (15). In this case, functional data were presented suggesting that the hydrogenosomal processing peptidase (βHPP) functioned as a homodimeric enzyme (15). No αMPP homologue was detected, although a protein rich in glycine amino acid residues (GRLP), that shares a limited similarity with the glycine-rich loop of αMPP, was located to *T. vaginalis* hydrogenosomes. However, GRLP was reported not to stimulate βHPP activity *in vitro* (15).

The progenitor of MPP was probably a monomeric α-proteobacterial peptidase, similar to the recently described *R. prowazekii* processing peptidase (RPP) (16). During the evolution of mitochondria, gene duplication and subunit specialization gave rise to the heterodimeric α/βMPP, which is now present in the mitochondrial matrix or integrated as the core I and II subunits of the cytochrome *bc1* complex in the inner mitochondrial membrane (6). The single subunit structure of GPP and HPP (15) may thus reflect retention of the ancestral form of organization, or reductive evolution from the classic MPP heterodimer. It has also been suggested that the *Giardia* protein may have had a separate origin by lateral gene transfer from a bacterium other than the mitochondrial endosymbiont (13). Here we show that GPP functions as a monomer consisting of a single βMPP homologue while HPP, like classical MPP, is fully active only upon heterodimerization of an α and β subunit. Based upon phylogenetic and functional analyses we infer that the unique monomeric structure of the *Giardia* mitosomal processing peptidase GPP, is the result of reductive, substrate-driven evolution from a heterodimeric progenitor enzyme.

RESULTS AND DISCUSSION

Phylogenetic analyses of GPP, βHPP and GRLP. To investigate the origins of the MPP-like proteins of *Giardia* and *Trichomonas* and the *Trichomonas* GRLP we carried out a phylogenetic analysis. As these proteins are heterogeneous for their amino acid compositions, and because a failure to accommodate such heterogeneity can lead to incorrect trees (17), we used a recently described node-discreet-compositional-heterogeneity method to analyze the data (17). A heterogeneous model comprising 10 composition vectors was found sufficient to produce data of similar composition to the original sequences, as judged by Bayesian posterior predictive simulation (17) (Fig. S1). Phylogenetic analyses using this model support the hypotheses that GPP, βHPP and βMPP share a common origin. The position of the GPP among βMPP, together with the presence of the catalytic motif H*XX*EHX_{76}E , are consistent with the protein being a βMPP-like peptidase (βGPP), and not an αMPP-like protein as currently annotated (13). This result contrasts with a previous analysis, using a poorly fitting composition homogeneous model, when GPP was reported to have no phylogenetic affinity with either MPP or the α-proteobacteria (13). Our results suggest that αMPP and βMPP probably arose once by a primordial gene duplication at the base of eukaryotes, and that all MPP-like proteins share common ancestry with single subunit enzymes from α-proteobacteria, consistent with an origin from the mitochondrial endosymbiont (Fig. 1A). Notably, our analyses also show that GRLP is part of the αMPP clade, suggesting that, contrary to previous claims (15), *T. vaginalis* may possess a functional homologue (GRLP) of αMPP (henceforth αHPP).

GPP Functions As a β Monomer While HPP forms an α/β Heterodimer. To investigate the functionality of the βGPP, βHPP and αHPP-like proteins, we expressed

them in *E. coli*. The recombinant βGPP processed the N-terminal extensions of *Giardia* mitosomal ferredoxin (Gifdx) and the iron-sulphur cluster scaffold proteins (GiiscU and GiiscA). The processing activity was demonstrated as a shift in the substrate gel mobility and the cleavage sites were identified by N-terminal amino acid sequencing of the cleaved products (Fig. 2). The activity of the recombinant βGPP was inhibited by the chelator EDTA, and activity was also lost when the first glutamate of the H*XX*EHX_{76}E motif was mutated to glutamine (Fig. 3). These data indicate that the βGPP is an active metallopeptidase with a similar cleavage mechanism to MPP (6). Like the rickettsial homologue of MPP (16), βGPP was active as a monomer, which was demonstrated by size exclusion chromatography of recombinant βGPP as well as by analysis of βGPP from a mitosome-rich fraction separated on a sucrose gradient under native conditions (Fig. 1B, C). Importantly, kinetic parameters of monomeric βGPP (V_{max}=0.27 μM/min; K_m=8.4 μM, Fig. S3) were comparable to those published for the heterodimeric MPP of *Neurospora crassa* (8). It has recently been suggested that the *T. vaginalis* HPP functions as a homodimer of two identical βHPP subunits (15), so we investigated the activity of βHPP with- and without αHPP. Unlike for βGPP, no activity for βHPP alone could be detected by gel shift assay (Fig. 1D), but a small amount of activity was observed when a highly sensitive fluorometric assay was used (15) (Fig. 1E). However, the processing activity measured by this assay increased by almost two orders of magnitude when the βHPP was associated with the αHPP-like protein, indicating that – like classic MPP – the *T. vaginalis* HPP functions most efficiently as a heterodimer (Fig. 1E).

Mitosomal and Some Hydrogenosomal Targeting Presequences Lack Distal Positively-Charged Residues. To further investigate the structure-function

relationships of the GPP, HPP and MPP, we screened *in silico* the *G. intestinalis* and *T. vaginalis* proteomes for putative mitosomal and hydrogenosomal N-terminal presequences (Tables S1 and S2), which were then analyzed for structural elements known to mediate substrate-MPP interactions. In particular, we searched for the positively-charged residues proximal to the cleavage site (P_2 or P_3), and those which are N-terminally distal from the processing site. The distance between the proximal and distal group was defined to be at least 3 amino acid residues (18, 19). *Giardia* mitosomal presequences were predicted in three of nine putative mitosomal proteins (Table S2). All of these presequences possess the proximal P_2 arginine within a conserved cleavage motif (Fig. 4), but the distal positively-charged residues are absent (Table S2). The lengths of the *Giardia* mitosomal presequences that have been experimentally verified are 10, 12 and 18 amino acid residues. The majority of the *in silico* predicted *Trichomonas* hydrogenosomal presequences (147) resemble the *Giardia* pattern; having a length of 4 to 21 amino acid residues, possessing a P_2 arginine within a cleavage motif (Fig. 4), and lacking the distal positively-charged residues. However, we also detected 79 putative hydrogenosomal presequences, of 10 to 24 amino acids, that – like classic mitochondrial sequences – do contain distal arginines or lysines at position $P_6 – P_{22}$.

Properties of MPP, GPP and HPP Reflect the Character of their Respective Substrates. To compare the specificities of the βGPP, α/βHPP and yeast α/βMPP in vitro, we tested their activity on a selection of mitosomal, hydrogenosomal and mitochondrial substrates (Fig. 2). The βGPP cleaved only its own mitosomal substrates. By contrast, the α/βHPP cleaved the hydrogenosomal presequences, and the presequences of mitosomal ferredoxin and two mitochondrial substrates. The yeast

α/βMPP processed all of the mitochondrial substrates and the two mitochondrial-like hydrogenosomal substrates that possess distal positively-charged residues.

To gain further insights into the structure-function basis of these different substrate spectra, we modelled each of the different proteins (Fig. 5 and Fig. S4), using the yeast MPP structure as a guide (10). For yeast MPP, the substrate is first recognized by the glycine-rich loop of αMPP (6, 7) and then moved to the active site of βMPP which interacts with the substrate cleavage motif including the proximal arginine. The distal positive residues of the presequence help to stabilize the substrate-MPP complex by binding to negatively charged residues within the large polar cavity formed by the α/βMPP subunits (10). The part of the substrate-binding cavity formed by βMPP thus displays an evenly distributed negative charge to accommodate both proximal and distal positively-charged residues of mitochondrial presequences. The αMPP interacts only with the distal positive residues of longer (> 20 amino acid residues) mitochondrial presequences (9, 10).

As the βGPP functions as a monomer we predict that its substrates, including the proximal arginine, interact directly with the negatively charged region of its catalytic site (Fig. 5). The rest of the predicted βGPP cavity is, unlike βMPP, positively-charged, although its predicted overall fold structure still resembles that of βMPP (Fig. S4). The difference in βGPP charge distribution is compatible with the absence of distal positively-charged residues in the mitosomal presequences, and, along with the absence of an αMPP-like subunit, explains the inability of βGPP to process mitochondrial-type presequences. The simplicity of GPP is consistent with the highly reduced function of mitosomes and likely reflects the paucity of proteins that are targeted to this organelle when compared with mitochondria. As shown above (Table S2), only nine mitosomal proteins have been identified so far and these are involved either in organelle

biogenesis (Gipam18, GiHsp70, GiCpn60, GPP) or the formation of Fe-S clusters (GiiscS, GiiscU, GiiscA, Gigrx, Gifdx), which is currently the only known mitosomal function for *G. intestinalis*. Other than these, no other homologues of mitochondrial proteins have been recognized in the genome of *G. intestinalis* (13).

The *T. vaginalis* HPP represents an intermediate stage between GPP and MPP in terms of charge distribution and enzymatic activity. Thus, it can process presequences with- or without distal positive residues, but can only cleave the shorter mitochondrial presequences (Fig. 2). The presence of mitochondrial type presequences on hydrogenosomal proteins is consistent with the retention of the αHPP, which is likely involved in their recognition via its glycine-rich loop and/or their docking at the cleavage site.

Our phylogenetic and functional analyses show that the *Giardia* GPP is a striking example of reductive evolution from a heterodimeric to a monomeric enzyme, with properties resembling the putative ancestral α-proteobacterial enzyme, rather than the highly specialized MPP heterodimer found in well characterized mitochondria. While the principal selective pressure for the evolution of the processing peptidases is probably the ability to efficiently process their substrates, the differences in properties of the substrate presequences may also reflect the mode of their translocation across the organelle membranes (20). In mitochondria from species across the phylogenetic tree (21), the positive residues of N-terminal presequences are recognized by the outer membrane TOM system and then the inner membrane translocase complex TIM23 (3). Interestingly, no receptors (Tom20, Tom 22, Tom70) or components of the translocation channel of the TOM complex (Tom40, Tom5, Tom6, Tom7) have so far been identified for *G. intestinalis* (13) or *T. vaginalis* (22). Putative core components of the TIM23 translocase (Tim23, Tim17) as well as Pam18 involved in protein transfer to

the matrix have been found in *T. vaginalis*, but only Pam18 was found in *G. intestinalis* (14). It thus appears that reductive evolution of the organelles has dramatically affected both the processing peptidases and the protein import pathway (21), with important implications for general models of mitochondrial biosynthesis, structure and function.

MATERIALS AND METHODS

Phylogenetic analysis. Complete sequences of βGPP, βHPP, and βMPP were aligned with Muscle (23) to calculate sequence identity and similarity values. MPP, GPP and HPP sequences were aligned with Muscle (23) and analysed with Gblocks (24) to remove ambiguously aligned sites. Bayesian phylogenetic analyses were conducted using P_4 (http://www.nhm.ac.uk/research-curation/projects/P4/index.html). The optimal substitution model for Bayesian analyses was identified by ProtTest (25) (WAG + Gamma), a polytomy prior (26), and one or more base composition vectors, which were free to vary during the chain under the NDCH model (17). MCMC chains were run for 1,000,000 generations, sampling trees and parameters every 200 generations. Model parameter proposal tuning values were determined using the P_4 "autoTune" method. The burn-in was identified using the method of Beiko and co-workers (27). The base composition component of the model was tested by simulation of the base composition X^2statistic (17) at each sampling point, resulting in a posterior predictive distribution (28) against which the statistic of the original data could be tested using tail-area probability. Composition vectors were successively added until adequate fitting of the observed data to the model was identified (see Fig. S1).

Preparation of recombinant proteases and substrate proteins. The βGPP (NCBI accession: XP_001707100), αHPP (XP_001276882) and βHPP (XP_001316822) subunits and their substrates were expressed with hexahistidine tags in *E. coli.* An α/βHPP heterodimer was assembled from βHPP-His and non-tagged αHPP subunits by incubation of lysates of *E. coli* expressing the respective proteins for 30 min on ice in 20 mM Tris, 20 mM NaCl (pH 8.6), 1 mM $MnCl_2$. All recombinant proteins were purified by nickel column chromatography (HiTrap Chelating) under native (βGPP-His, αHPP-

His, βHPP-His, and α/βHPP-His) or denaturing (substrate proteins) conditions. An α/βMPP heterodimer was prepared as published (18).

***In vitro* protease activity assays.** The GPP reactions were carried out in 20 mM Tris (pH 8.0), 100 mM NaCl, 1mM $MnCl_2$, 30 min at 37°C, the HPP reactions in 20 mM Tris-HCl (pH 8.6), 20 mM NaCl, 2 mM $MnCl_2$, 30 min at 37°C and activity of MPP was determined in 50 mM HEPES (pH 7.4), 20 mM NaCl, 1 mM $MnCl_2$, 30 min at 30°C. To identify the cleavage sites, all substrates processed by the three proteases were subjected to N-terminal protein sequencing by Edman degradation. The kinetics of GPP was determined using the method published by Arretz and co-workers (8). For determination of the activity of the HPP subunits, purified αHPP-His and βHPP-His were incubated on ice for 30 min either alone, or mixed together with 1 mM $MnCl_2$. After addition of TviscU, the reaction was allowed to proceed at 37°C for 60 min. The specific activity of HPP with a fluorescent substrate based on the presequence of TvAK [Abz-MLST LAKRF AY(NO_2)GKKDRM] (Bachem, Switzerland) was measured at 420 nm, with an excitation wavelength of 315 nm (Infinite M200, Tecan).

Size exclusion chromatography of purified GPP. A pre-calibrated Superdex 200 column was used to determine the molecular mass of *E. coli* produced GPP, under native conditions. Affinity purified βGPP-His in buffer of 50 mM CHES (pH 9.5), 150 mM NaCl was loaded on the column and washed (0.5 ml/min), collecting 1 ml fractions. Protein-containing fractions were assayed for βGPP activity.

Sucrose gradient centrifugation of a *Giardia* mitosome-enriched fraction. The molecular mass of GPP expressed in *G. intestinalis* with a hemagglutinin (HA) tag was

estimated under native conditions by sucrose gradient centrifugation (15). The mitosome-enriched fraction was isolated from a *G. intestinalis* homogenate using a published method (14). The proteins in the mitosomal-enriched fraction were then separated on a calibrated sucrose gradient (15). Fractions were analysed by immunoblot using anti-HA antibodies. Bands visualized by alkaline phosphatase were quantified by densitometry (GS-800 Calibrated Densitometer, BioRad).

Hydrogenosomal and mitosomal presequence identification. An application based on the NetBeans Platform (http://platform.netbeans.org) was developed to search for proteins containing N-terminal hydrogenosomal and mitosomal presequences in the predicted *T. vaginalis* (http://www.trichdb.org/trichdb/) and *G. intestinalis* (http://www.giardiadb.org/giardiadb/) proteomes, respectively. Hydrogenosmal presequences were predicted based on two main parameters extracted from 21 known hydrogenosomal presequences: (i) the cleavage site motif, specified as RXF/(ILFSAGQ) or R(FNESG)/(ILFSAGQ) (the slash indicates the cleavage site and brackets mean one residue position), and the presequence start motif defined as ML(STACGR) or MTL or MSL. In addition, tryptophan was forbidden from the presequence, the maximum presequence length was optimized to 25 residues. Any presequences with overall negative charges were excluded (the approximate presequence charge at pH7 was counted according to the Henderson-Hasselbalch equation using the following pKa values: N-terminus 8.0, lysine 10.0, arginine 12.0, histidine 6.5, glutamic acid 4.4, aspartic acid 4.4, tyrosine 10.0, and cysteine 8.5). The *G. intestinalis* proteome was searched for N-terminal presequences based on three experimentally verified mitosomal presequences of known mitosomal proteins (13) (Table S2). The parameters defined for the search were as follows: the cleavage site

motif was defined as R(FS)/(IL)T, the presequence start motif as M(SLT), the maximum presequence length was set up to 20 residues, tryptophan was forbidden from the presequence. A search using parameters for prediction of hydrogenosomal presequences did not reveal additional mitosomal protein candidates.

Protein structure prediction. The MODELLER program (29) version 9.2 was used to build 3-D models of αHPP, βHPP and βGPP. Alignments of the βGPP and βHPP with the βMPP (pdbid 1HR6) (10) and of the αHPP with the αMPP (pdbid 1HR6) (10) were carried out using the PROBCONS web service (30) and manually edited. The quality of the final model was checked using the ProCheck (31) and WhatCheck (32) programs. The electrostatic properties of the model were evaluated using APBS version 0.5.1 (33).

ACKNOWLEDGEMENTS

We thank M. Marcincikova for technical support, Z. Voburka for protein N-terminal sequencing, J. Horvath for the development of the presequences identification software and DeLano Scientific LLC. for PyMol. The project was funded by the Grant Agency of the Academy of Sciences of the CR IIA501110631 (J.T.), Ministry of Education, Youth and Sports of the CR MSM0021620858 and LC07032 (J.T.) and the Grant Agency of Charles University B-Bio166/2006 (O.S.). S.H., R.P.H. and T.M.E. were supported by a grant from the Biotechnology and Biological Sciences Research Council (UK) and funding from the Royal Society (UK) to T.M.E.

REFERENCES

1. Embley TM, Martin W (2006) Eukaryotic evolution, changes and challenges. *Nature* 440:623-630.

2. Timmis JN, Ayliffe MA, Huang CY, Martin W (2004) Endosymbiotic gene transfer: organelle genomes forge eukaryotic chromosomes. *Nature Rev Genet* 5:123-135.

3. Neupert W, Herrmann JM (2007) Translocation of proteins into mitochondria. *Annu Rev Biochem* 76:723-749.

4. Yaffe MP, Ohta S, Schatz G (1985) A yeast mutant temperature-sensitive for mitochondrial assembly is deficient in a mitochondrial protease activity that cleaves imported precursor polypeptides. *EMBO J* 4:2069-2074.

5. Mukhopadhyay A, Yang CS, Wei B, Weiner H (2007) Precursor protein is readily degraded in mitochondrial matrix space if the leader is not processed by mitochondrial processing peptidase. *J Biol Chem* 282:37266-37275.

6. Gakh O, Cavadini P, Isaya G (2002) Mitochondrial processing peptidases. *Biochim Biophys Acta* 1592:63-77.

7. Nagao Y, Kitada S, Kojima K, Toh H, Kuhara S, Ogishima T, Ito A (2000) Glycine-rich region of mitochondrial processing peptidase alpha-subunit is essential for binding and cleavage of the precursor proteins. *J Biol Chem* 275:34552-34556.

8. Arretz M, Schneider H, Guiard B, Brunner M, Neupert W (1994) Characterization of the mitochondrial processing peptidase of *Neurospora crassa*. *J Biol Chem* 269:4959-4967.

9. Kitada S, Yamasaki E, Kojima K, Ito A (2003) Determination of the cleavage site of the presequence by mitochondrial processing peptidase on the substrate binding scaffold and the multiple subsites inside a molecular cavity. *J Biol Chem* 278:1879-1885.

10. Taylor AB, Smith BS, Kitada S, Kojima K, Miyaura H, Otwinowski Z, Ito A, Deisenhofer J (2001) Crystal structures of mitochondrial processing peptidase reveal the mode for specific cleavage of import signal sequences. *Structure* 9:615-625.

11. Bradley PJ, Lahti CJ, Plumper E, Johnson PJ (1997) Targeting and translocation of proteins into the hydrogenosome of the protist *Trichomonas*: similarities with mitochondrial protein import. *EMBO J* 16:3484-3493.

12. Tovar J, Leon-Avila G, Sanchez LB, Sutak R, Tachezy J, van der Giezen M, Hernandez M, Müller M, Lucocq JM (2003) Mitochondrial remnant organelles of *Giardia* function in iron-sulphur protein maturation. *Nature* 426:172-176.

13. Morrison HG, McArthur AG, Gillin FD, Aley SB, Adam RD, Olsen GJ, Best AA, Cande WZ, Chen F, Cipriano MJ *et al.* (2007) Genomic minimalism in the early diverging intestinal parasite *Giardia lamblia*. *Science* 317:1921-1926.

14. Dolezal P, Smid O, Rada P, Zubacova Z, Bursac D, Sutak R, Nebesarova J, Lithgow T, Tachezy J (2005) *Giardia* mitosomes and trichomonad

hydrogenosomes share a common mode of protein targeting. *Proc Natl Acad Sci U S A* 102:10924-10929.

15. Brown MT, Goldstone HM, Bastida-Corcuera F, Delgadillo-Correa MG, McArthur AG, Johnson PJ (2007) A functionally divergent hydrogenosomal peptidase with protomitochondrial ancestry. *Mol Microbiol* 64:1154-1163.

16. Kitada S, Uchiyama T, Funatsu T, Kitada Y, Ogishima T, Ito A (2007) A protein from a parasitic microorganism, *Rickettsia prowazekii*, can cleave the signal sequences of proteins targeting mitochondria. *J Bacteriol* 189:844-850.

17. Foster PG (2004) Modeling compositional heterogeneity. *Syst Biol* 53:485-495.

18. Janata J, Hola K, Kubala M, Gakh O, Parkhomenko N, Matuskova A, Kutejova E, Amler E (2004) Substrate evokes translocation of both domains in the mitochondrial processing peptidase alpha-subunit during which the C-terminus acts as a stabilizing element. *Biochem Biophys Res Commun* 316:211-217.

19. Kojima K, Kitada S, Ogishima T, Ito A (2001) A proposed common structure of substrates bound to mitochondrial processing peptidase. *J Biol Chem* 276:2115-2121.

20. Dyall SD, Brown MT, Johnson PJ (2004) Ancient invasions: from endosymbionts to organelles. *Science* 304:253-257.

21. Dolezal P, Likic V, Tachezy J, Lithgow T (2006) Evolution of the molecular machines for protein import into mitochondria. *Science* 313:314-318.

22. Carlton JM, Hirt RP, Silva JC, Delcher AL, Schatz M, Zhao Q, Wortman JR, Bidwell SL, Alsmark UC, Besteiro S *et al.* (2007) Draft genome sequence of the sexually transmitted pathogen *Trichomonas vaginalis*. *Science* 315:207-212.

23. Edgar RC (2004) MUSCLE: multiple sequence alignment with high accuracy and high throughput. *Nucleic Acids Res* 32:1792-1797.

24. Talavera G, Castresana J (2007) Improvement of phylogenies after removing divergent and ambiguously aligned blocks from protein sequence alignments. *Syst Biol* 56:564-577.

25. Abascal F, Zardoya R, Posada D (2005) ProtTest: selection of best-fit models of protein evolution. *Bioinformatics* 21:2104-2105.

26. Lewis PO, Holder MT, Holsinger KE (2005) Polytomies and Bayesian phylogenetic inference. *Syst Biol* 54:241-253.

27. Beiko RG, Keith JM, Harlow TJ, Ragan MA (2006) Searching for convergence in phylogenetic Markov chain Monte Carlo. *Syst Biol* 55:553-565.

28. Bollback JP (2002) Bayesian model adequacy and choice in phylogenetics. *Mol Biol Evol* 19:1171-1180.

29. Sali A, Blundell TL (1993) Comparative protein modelling by satisfaction of spatial restraints. *J Mol Biol* 234:779-815.

30. Do CB, Mahabhashyam MS, Brudno M, Batzoglou S (2005) ProbCons: Probabilistic consistency-based multiple sequence alignment. *Genome Res* 15:330-340.

31. Laskowski RA, Moss DS, Thornton JM (1993) Main-chain bond lengths and bond angles in protein structures. *J Mol Biol* 231:1049-1067.

32. Rodriguez R, Chinea G, Lopez N, Pons T, Vriend G (1998) Homology modeling, model and software evaluation: three related resources. *Bioinformatics* 14:523-528.

33. Baker NA, Sept D, Joseph S, Holst MJ, McCammon JA (2001) Electrostatics of nanosystems: application to microtubules and the ribosome. *Proc Natl Acad Sci U S A* 98:10037-10041.

34. Crooks GE, Hon G, Chandonia JM, Brenner SE (2004) WebLogo: a sequence logo generator. *Genome Res* 14:1188-1190.

FIGURE LEGENDS

Fig. 1. Phylogenetic and functional characterization of βGPP and α/βHPP. (**A**) Bayesian phylogenetic analysis of MPP-like protein sequences using a model (17) that allows for across-tree changes in protein amino acid composition. Scale bar indicates estimated substitutions per site. Posterior probabilities of 100% are shown as black dots on nodes, and those greater than 95% are shown as values. Bacterial MPP homologues are shown in black, αMPP in red and βMPP in blue. *Trichomonas* α- and βHPPs and *Giardia* βGPP are highlighted in green. Only α-proteobacterial relationships are shown for bacteria. The fit between the model and the data is shown in Fig. S1 and the full tree with additional details are shown in Fig. S2. (**B**) Protein size exclusion chromatography of purified βGPP showing that it elutes as a single peak between 17 and 44 kDa. The activity of βGPP was assayed for cleavage of the targeting presequence of GiiscU for each fraction and the products were separated by SDS-PAGE. Shift in protein mobility indicates cleavage of a presequence. βGPP activity was only detected in fractions from the central peak. (**C**) Separation of proteins from a mitosome-rich fraction on a sucrose gradient along with molecular size markers. Bands on the immunoblot and SDS-PAGE were quantified by densitometry. The calculated molecular mass of the βGPP monomer is 44.5 kDa. (**D**) Processing activity of the αHPP-His (lane 1), βHPP-His (lane 2) and corresponding α/βHPP heterodimer (lane 3) with TviscU, showing that the α- and β-subunits are both required for activity. (**E**) Specific activities were also determined for the βHPP subunit and the α/βHPP heterodimer with a fluorescent substrate based on the *T. vaginalis* adenylate kinase presequence (n=3, mean values with s.d.) The activity of the βHPP subunit by itself is at the limit of detection for this assay.

Fig. 2. Comparative processing of mitosomal, hydrogenosomal and mitochondrial proteins by βGPP, α/βHPP and α/βMPP. The sequence of the demonstrated N-terminal mitochondrial, mitosomal or hydrogenosomal targeting presequences is indicated for each substrate protein with / indicating the cleavage site. Processing of *Giardia intestinalis* mitosomal presequences (Gifdx, [2Fe2S] ferredoxin; GiiscA and GiiscU, metallochaperones involved in FeS cluster assembly), *Trichomonas vaginalis* hydrogenosomal presequences (Tvfdx, [2Fe2S] ferredoxin; TvAK, adenylate kinase; Tvhsp70, heat shock protein 70; TviscU, metallochaperone involved in FeS cluster assembly) and mitochondrial presequences (ScMDH, *Saccharomyces cerevisiae* malate dehydrogenase; MmMDH, *Mus musculus* MDH; ClMDH, *Citrullus lanatus* MDH) was tested. Reaction products were separated by SDS-PAGE. Shift in protein mobility indicates cleavage of a targeting presequence. The sites of cleavage indicated by slashes in left column were determined by N-terminal amino acid sequencing. Substrates were incubated with (+) or without (-) the corresponding protease.

Fig. 3. The βGPP is a metallopeptidase with a similar cleavage mechanism to α/βMPP. (**A**) Alignment of βGPP and βMPP subunit showing the conserved zinc-binding motif. (**B**) Effect of protease inhibitors and mutation of E37 on the activity of βGPP. Lane 1: βGPP + GiiscU showing cleavage to produce the mature protein; lane 2: βGPP + GiiscU + serine and cysteine protease inhibitors showing no inhibition; lane 3: βGPP + GiiscU + EDTA showing inhibition of cleavage; lane 4: Mutant βGPP in which E37 was mutated to glutamine + GiiscU, showing that the mutation of a key residue for βMPP activity also eliminates βGPP activity.

Fig. 4. Sequence logos (34) of substrate cleavage sites of α/βHPP and βGPP. Logos were compiled using the WebLogo web based application (http://weblogo.berkeley.edu/logo.cgi) and consist of stacks of amino acids, one stack for each position in the sequence. The overall height of the stack indicates the sequence conservation at that position, while the height of symbols within the stack indicates the relative frequency of each amino acid at that position. (**A**) The α/βHPP substrate logo was created from predicted hydrogenosomal presequences listed in Table S1. (**B**) The three known mitosomal presequences (listed in Table S2) were used to compile a substrate logo for βGPP.

Fig. 5. Comparative distribution of charge polarity between mitochondrial, hydrogenosomal and mitosomal peptidases. (**A**) Predicted charge polarity distribution of the βHPP subunit and βGPP based on the known structure and charge distribution of the *Saccharomyces cerevisiae* βMPP subunit (10). Red and blue colours denote negative and positive charge (±5 kT/e where kT is thermal energy and e is unit charge), respectively, whereas white denote relatively non-polar regions. The yellow asterisk marks the Zn-binding region in the active site of the enzyme (shown in b). The negative charges are distributed evenly in the cavity of βMPP while in the cavity of βGPP the negative charges are concentrated mainly around the active site. (**B**) Alignment of key segments where negatively charged residues of βMPP are located and known to interact with the substrate. Numbered residues are those of yeast βMPP. E_{160} and D_{164} make a salt bridge with substrate residue R-2 (P_2) and F_{77} interacts with P_1' which is also often a F residue. H_{70}-H_{74} is the conserved motif of the active site (Fig. S5).

FIGURES

Fig. 1

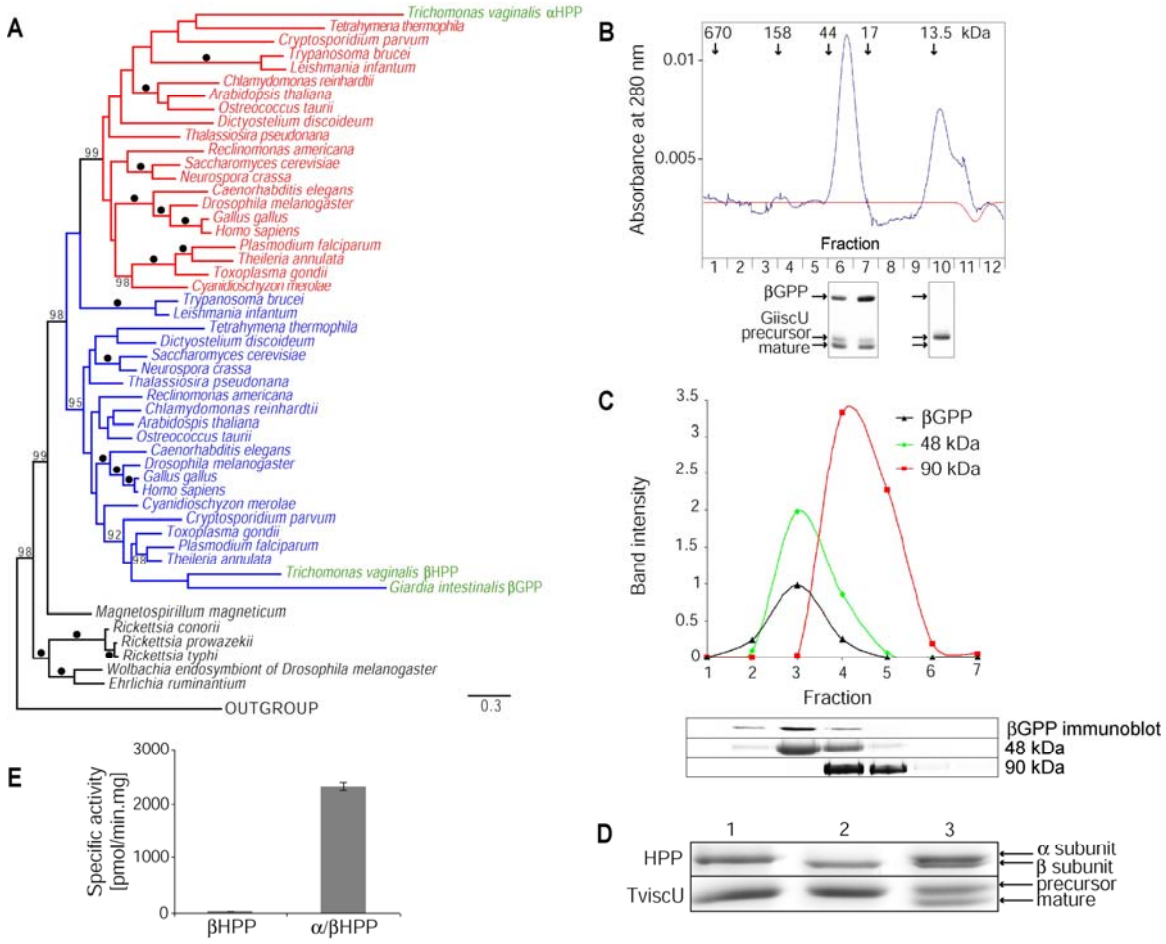

Fig. 2

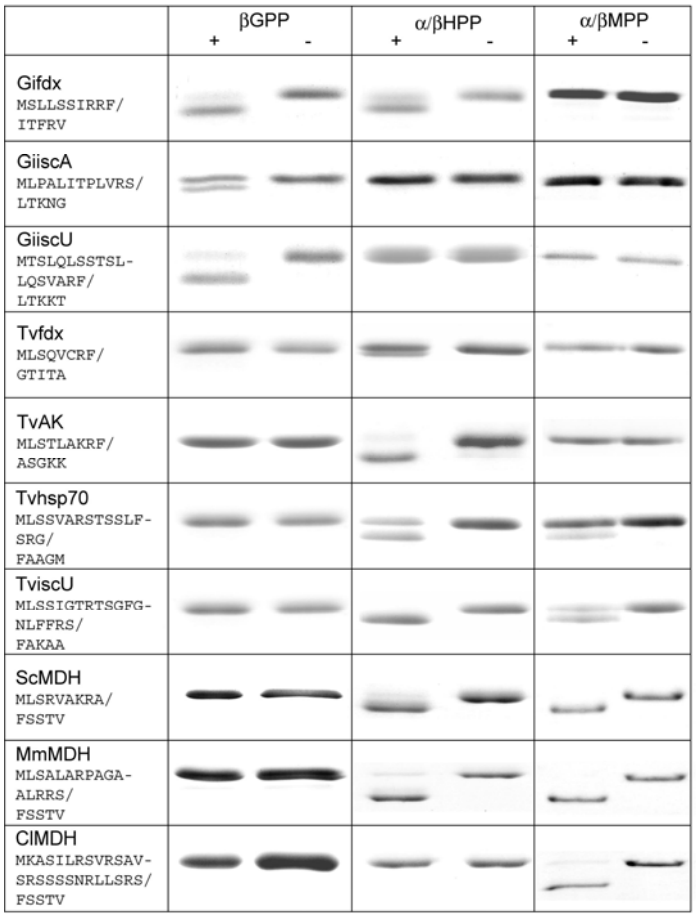
βGPP
+
-
α/βHPP
+
-
α/βMPP
+
-
Gifdx
MSLLSSIRRF/
ITFRV
GiiscA
MLPALITPLVRS/
LTKNG
GiiscU
MTSLQLSSTSL-
LQSVARF/
LTKKT
Tvfdx
MLSQVCRF/
GTITA
TvAK
MLSTLAKRF/
ASGKK
Tvhsp70
MLSSVARSTSSLF-
SRG/
FAAGM
TviscU
MLSSIGTRTSGFG-
NLFFRS/
FAKAA
ScMDH
MLSRVAKRA/
FSSTV
MmMDH
MLSALARPAGA-
ALRRS/
FSSTV
ClMDH
MKASILRSVRSAV-
SRSSSSNRLLSRS/
FSSTV

Fig. 3

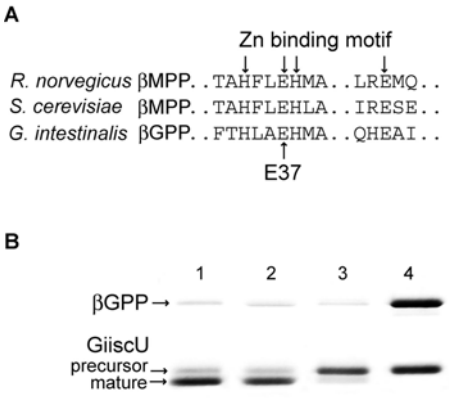
A
Zn binding motif
R. norvegicus βMPP. .TAHFLEHMA..LREMQ..
S. cerevisiae βMPP. .TAHFLEHLA..IRESE..
G. intestinalis βGPP. .FTHLAEHMA..QHEAI..
E37
B
1
2
3
4
βGPP→
GiiscU
precursor→
mature→

Fig. 4

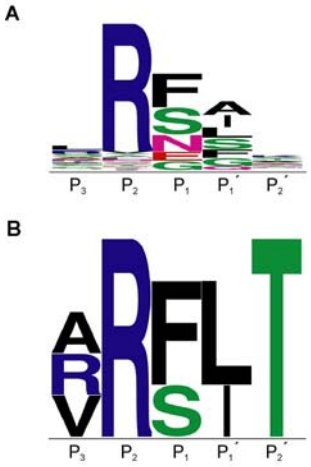
A
B
P3 P2 P1 P1´ P2´
P3 P2 P1 P1´ P2´

Fig. 5

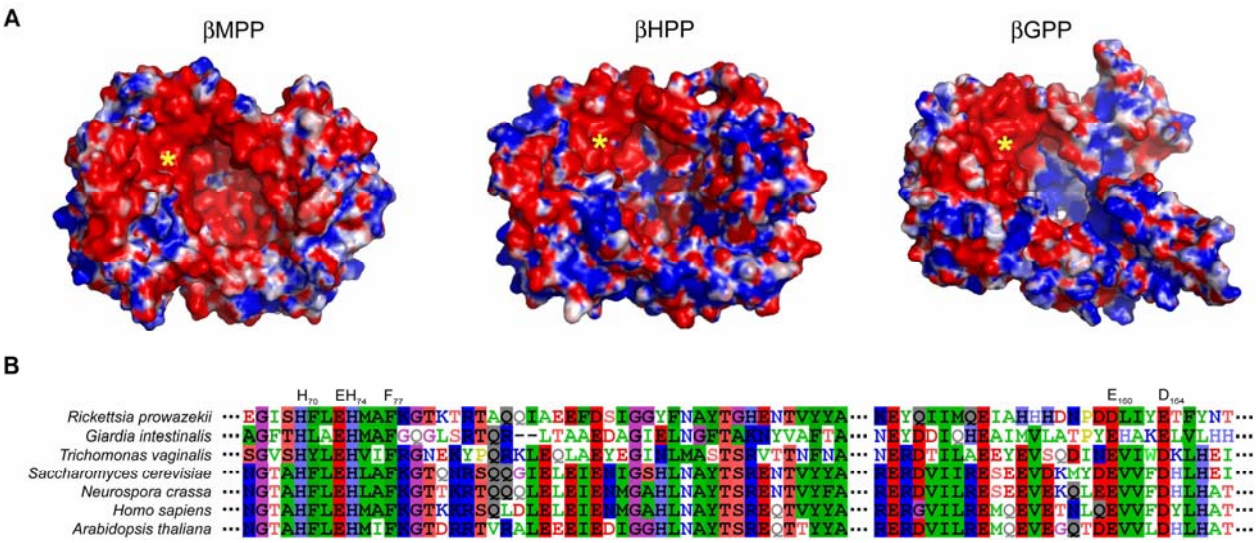
A
βMPP
βHPP
βGPP
B
H70 EH74 F77
E100 D164
Rickettsia prowazekii
Giardia intestinalis
Trichomonas vaginalis
Saccharomyces cerevisiae
Neurospora crassa
Homo sapiens
Arabidopsis thaliana

SUPPORTING INFORMATION

Fig. S1. Bayesian model composition fit to the data assessed by posterior predictive simulation. Bars show the posterior distribution of X^2 for the homogeneous composition model (red) and the heterogeneous composition (NDCH) model with 10 composition vectors (green) in comparison to the statistic from the observed data. The simulated data for the NDCH model include the X^2 statistic from the observed data whereas the simulated data from the homogeneous model do not, the NDCH model thus provides a much better fit to the data. The original X^2 statistic for the data was 1292. In the simulations from the homogeneous analysis, this statistic ranged between 617 and 933 (mean =763), while in the heterogeneous analysis (10 composition vectors) the statistic ranged between 877 and 1487 (mean =1132).

Fig. S2. Bayesian phylogenetic analysis of MPP-like protein sequences using the NDCH model (1) that allows for across-tree changes in protein amino acid composition. The tree is a majority rule consensus of 3,500 trees sampled from the posterior probability distribution of an MCMC with 10 across-tree composition vectors. Scale bar indicates estimated substitutions per site. Values on branches are posterior probabilities. Bacterial MPP homologues are shown in black, αMPP in red and βMPP in blue. *Trichomonas* α- and βHPPs and *Giardia* βGPP are highlighted in green.

Fig. S3. The enzyme kinetics of the monomeric βGPP are comparable to those of *Neurospora crassa* heterodimeric α/βMPP. The Lineweaver-Burk double reciprocal plot of reaction velocity, calculated as concentration of processed GiiscU in μM per minute versus concentration of GiiscU precursor. The least square fit line through the data intercepts x and y axes at $-1/K_m$ and $1/V_{max}$, respectively. The kinetic parameters V_{max}=1.7 μM/min; K_m= 8.4 μM; *k*cat=17 min^{-1} of βGPP are of similar magnitude to

published values for *Neurospora crassa* heterodimeric α/βMPP (2): V_{max}= 0.27 μM/min; K_m=1.27 μM; k_{cat}=6.75 min^{-1}**.**

Fig. S4. Tertiary structures of MPP, HPP and GPP. Homology models of βHPP and βGPP were built using the known structure of *Saccharomyces cerevisiae* βMPP, αHPP was modelled using *S. cerevisiae* αMPP. β-sheets are shown in yellow, α-helices in red, loops in grey. The glycine-rich loop of the α subunits and the zinc-biding motif of β subunits are highlighted in green.

Table S1

N-terminal presequences of hydrogenosomal proteins predicted in *T. vaginalis* proteome. *T. vaginalis* proteins with (A) presequences containing proximal arginine only, (B) presequences with both proximal and distal positive residues. Slash indicates predicted cleavage sites. Experimentally verified hydrogenosomal presequences are highlighted in bold.

A

Protein ID NCBI	N-terminal presequence	Presequence length	Presequence charge at pH 7.0	Annotation
TVAG_045480	MLRF/GD	4	1.909	high molecular weight subunit PW212 precursor-related protein
TVAG_336890	MLRF/GV	4	1.909	conserved hypothetical protein
TVAG_333710	MLRF/SD	4	1.909	conserved hypothetical protein
TVAG_368750	MLRG/IK	4	1.909	conserved hypothetical protein
TVAG_165200	MLRG/IK	4	1.909	neurofilament protein, putative
TVAG_165200	MLRG/IK	4	1.909	neurofilament protein, putative
TVAG_090770	MLRG/IV	4	1.909	conserved hypothetical protein
TVAG_475700	MLRN/AF	4	1.909	conserved hypothetical protein
TVAG_337780	MLRN/AL	4	1.909	conserved hypothetical protein
TVAG_495580	MLRN/FT	4	1.909	conserved hypothetical protein
TVAG_015120	MLRN/LD	4	1.909	conserved hypothetical protein
TVAG_214000	MLRN/QD	4	1.909	hypothetical protein
TVAG_499270	MLRN/QE	4	1.909	hypothetical protein
TVAG_035490	MLRS/AL	4	1.909	conserved hypothetical protein
TVAG_131910	MLRS/FT	4	1.909	conserved hypothetical protein
TVAG_465120	MLRS/IE	4	1.909	conserved hypothetical protein
TVAG_136750	MLRS/IF	4	1.909	clathrin coat adaptor ap3 medium chain, putative
TVAG_184410	MLRS/LA	4	1.909	hypothetical protein
TVAG_304640	MLRS/LG	4	1.909	beige/BEACH domain containing protein
TVAG_106590	MLRS/SI	4	1.909	conserved hypothetical protein

TVAG_254890	MLRNF/GK	5	1.909	pyruvate:ferredoxin oxidoreductase E
TVAG_242960	MLRNF/GK	5	1.909	pyruvate:ferredoxin oxidoreductase B2 (3)
TVAG_230580	**MLRNF/SK**	**5**	**1.909**	**pyruvate:ferredoxin oxidoreductase B1 (4)**
TVAG_210030	MLRSF/AK	5	1.909	OsmC-like protein
TVAG_198110	**MLRSF/GK**	**5**	**1.909**	**pyruvate:ferredoxin oxidoreductase A (4)**
TVAG_441970	MLGRF/IT	5	1.909	von Willebrand factor type A domain containing protein
TVAG_593050	MLGRS/SD	5	1.909	hypothetical protein
TVAG_266350	MLRRN/IK	5	2.909	conserved hypothetical protein
TVAG_045030	MLSRE/GI	5	0.912	conserved hypothetical protein
TVAG_223970	MLSRG/LG	5	1.909	conserved hypothetical protein
TVAG_178120	MLSRS/II	5	1.909	protein phosphatase-7, putative
TVAG_146620	MLSRS/IL	5	1.909	protein phsophatase-2A, putative
TVAG_459960	MLSRS/IL	5	1.909	protein phosphatase-1, putative
TVAG_316160	MLSRS/IL	5	1.909	protein phosphatase-5, putative
TVAG_153840	MLSRS/LS	5	1.909	conserved hypothetical protein
TVAG_252470	MTLRF/QN	5	1.909	conserved hypothetical protein
TVAG_252480	MTLRF/QN	5	1.909	conserved hypothetical protein
TVAG_252460	MTLRF/QS	5	1.909	conserved hypothetical protein
TVAG_339330	MLSRIF/GK	6	1.909	conserved hypothetical protein
TVAG_457260	MLSRLF/ST	6	1.909	conserved hypothetical protein
TVAG_099790	MLSRVF/SL	6	1.909	conserved hypothetical protein
TVAG_069270	MLTRQF/ST	6	1.909	CMGC family protein kinase
TVAG_437150	MLTPRS/LR	6	1.909	conserved hypothetical protein
TVAG_205530	MSLKRG/AG	6	2.908	conserved hypothetical protein
TVAG_043080	MSLVRS/GR	6	1.909	conserved hypothetical protein
TVAG_163820	MSLYRF/SV	6	1.908	hypothetical protein
TVAG_485180	MTLPRS/SI	6	1.909	conserved hypothetical protein
TVAG_424100	MLSSIRF/AI	7	1.909	conserved hypothetical protein
TVAG_266800	MSLARRN/QL	7	2.909	conserved hypothetical protein
TVAG_377880	MTLGKRE/IR	7	1.911	hypothetical protein
TVAG_267050	MSLMHRVF/GK	8	2.149	conserved hypothetical protein
TVAG_432650	MLAAVSRS/SA	8	1.909	NifU-like protein, putative

TVAG_191660	MLALTSRN/FA	8	1.909	groes chaperonin, putative
TVAG_154730	MLASASRF/AT	8	1.909	Iron-sulfur flavoprotein
TVAG_078730	MLASISRS/AV	8	1.909	Ferredoxin 7
TVAG_099490	MLASLSRN/FG	8	1.909	ROK family protein
TVAG_041340	MLATFARN/FA	8	1.909	chaperonin, 10 kDa family protein
TVAG_183850	MLCSIQRS/IT	8	1.878	amidinotransferase family protein
TVAG_182150	MLSGFSRS/IM	8	1.909	frataxin(5)
TVAG_114560	MLSGFSRS/LM	8	1.909	frataxin(5)
TVAG_158970	MLSGIYRS/FS	8	1.908	protein phosphatase 2C, putative
TVAG_421060	MLSISSRS/GS	8	1.909	C-MYB, putative
TVAG_253010	MLSKVERS/AA	8	1.911	conserved hypothetical protein
TVAG_003900	**MLSQVCRF/GT**	**8**	**1.878**	**Ferredoxin 1 (Tvfdx)(6)**
TVAG_076230	MLSQVGRF/FA	8	1.909	mrp, putative
TVAG_393850	MLSSAARS/IA	8	1.909	Acetyl-CoA hydrolase, putative
TVAG_164890	MLSSASRS/IA	8	1.909	Acetyl-CoA hydrolase, putative
TVAG_381290	MLSSIARS/LS	8	1.909	Hsp20/alpha crystallin family protein
TVAG_456770	MLSSIIRS/FA	8	1.909	HesB-like domain containing protein
TVAG_412560	MLSSISRS/IT	8	1.909	OsmC-like protein
TVAG_444140	MLSSTSRF/AT	8	1.909	Iron-sulfur flavoprotein
TVAG_299570	MLSYVHRF/IC	8	2.148	conserved hypothetical protein
TVAG_373690	MLTQAFRS/FS	8	1.909	HesB-like domain containing protein
TVAG_071030	MSLKAKRN/IY	8	3.907	hypothetical protein
TVAG_361540	MLSQAFRAF/AQ	9	1.909	HesB-like domain containing protein
TVAG_205390	MLTSIGRYF/AK	9	1.908	small GTP-binding protein, putative
TVAG_133030	**MLAAYGHRF/QT**	**9**	**2.148**	**hydrogenosomal NADH dehydrogenase 51 kDa subunit**
TVAG_318670	**MLAGDFSRN/LH**	**9**	**0.912**	**succinate thiokinase alpha-chain (7)**
TVAG_392320	MLASFGLRF/AT	9	1.909	groes chaperonin, putative
TVAG_449080	MLSILLARF/SL	9	1.909	conserved hypothetical protein
TVAG_152030	MLSILLARF/SL	9	1.909	conserved hypothetical protein
TVAG_040870	MLSLALFRF/GS	9	1.909	Clan CA, family C1, papain-like cysteine peptidase
TVAG_213140	MLSLCQTRF/AS	9	1.878	Ferredoxin 3

TVAG_393380	MLSLFLTRF/SS	9	1.909	conserved hypothetical protein
TVAG_211590	MLSSCAKRG/LK	9	2.877	protein ssnA, putative
TVAG_066380	MLSSQFVRF/AD	9	1.909	metallo-beta-lactamase superfamily protein
TVAG_259190	**MLSSSFARN/FN**	**9**	**1.909**	**succinate thiokinase beta-chain (8)**
TVAG_047890	**MLSSSFERN/LH**	**9**	**0.912**	**succinate thiokinase alpha-chain (7)**
TVAG_165340	**MLSSSFERN/LH**	**9**	**0.912**	**succinate thiokinase alpha-chain (7)**
TVAG_146730	MLSSVGSRF/AA	9	1.909	Iron-sulfur flavoprotein
TVAG_040030	MLSSVGSRF/AA	9	1.909	Iron-sulfur flavoprotein
TVAG_489800	**MLSTLAKRF/AS**	**9**	**2.908**	**TvAK (9)**
TVAG_036010	MLSTSSARSFS/AL	9	1.909	hydrogenosomal oxygen reductase
TVAG_217870	MLTSAFKRF/AG	9	2.908	mrp, putative
TVAG_370510	MLTSIPSRF/AA	9	1.909	multimeric flavodoxin domain containing protein, putative
TVAG_096520	MTLNQTTRF/AS	9	1.909	pyruvate:ferredoxin oxidoreductase D
TVAG_205570	MLSHLTNRPF/IN	10	2.149	conserved hypothetical protein
TVAG_215080	MLSSFLSRTF/AN	10	1.909	conserved hypothetical protein
TVAG_242760	MLSSFLSRTF/AN	10	1.909	conserved hypothetical protein
TVAG_589340	MSLSKSEREF/II	10	0.913	conserved hypothetical protein
TVAG_068150	MLCSFSNSRF/FK	10	1.878	Ferredoxin 6
TVAG_292710	MLCSVSNYRF/FK	10	1.877	Ferredoxin 4
TVAG_354390	MLGTSKSYRN/LY	10	2.907	conserved hypothetical protein
TVAG_144730	**MLSNGSFARN/FN**	**10**	1.909	**succinate thiokinase beta-chain (8)**
TVAG_399860	MLSQCSPLRF/GS	10	1.878	Ferredoxin 2
TVAG_329120	MLTQNIPQRF/GK	10	1.909	CAMK family protein kinase
TVAG_125860	MSLIATPSRS/FA	10	1.909	conserved hypothetical protein
TVAG_132440	MSLQSKNVRS/SS	10	2.908	alanine aminotransferase, putative
TVAG_113640	MTLPARQLRN/GL	10	2.909	alcohol dehydrogenase, putative
TVAG_302980	MTLPQRQIRN/GL	10	2.909	alcohol dehydrogenase, putative
TVAG_236210	MTLPQRQIRN/GL	10	2.909	conserved hypothetical protein
TVAG_296220	**MLASVNTSRFF/AR**	**11**	**1.909**	**hydrogenosomal NADH dehydrogenase 24 kDa subunit**
TVAG_183500	MLSASSNFARN/FN	11	1.909	succinate thiokinase beta-chain (3)
TVAG_062660	MLSFFFSLSRS/AC	11	1.909	hypothetical protein

TVAG_112950	MLSLFISLSRS/AD	11	1.909	conserved hypothetical protein
TVAG_385350	MLSSISSFARF/AL	11	1.909	thioredoxin family protein
TVAG_086470	MLSSISSFSRF/AL	11	1.909	thioredoxin family protein
TVAG_412220	**MLTSVSLPVRN/IC**	**11**	**1.909**	**malic enzyme D (10)**
TVAG_416100	**MLTSVSYPVRN/IC**	**11**	**1.908**	**malic enzyme C (10)**
TVAG_491540	MLSIELQIGRQF/QD	12	0.912	conserved hypothetical protein
TVAG_183790	MLASSVAAPVRN/IC	12	1.909	malic enzyme (3)
TVAG_094800	MLSILFTECLRS/SR	12	0.881	conserved hypothetical protein
TVAG_009360	MLSLLLITLSRS/AV	12	1.909	dnaK protein
TVAG_445730	MLTSLNTFGLRF/SF	12	1.909	chaperonin, 10 kDa family protein
TVAG_238830	**MLTSSVNFPARE/LS**	**12**	**0.912**	**malic enzyme B (10)**
TVAG_340290	**MLTSSVSLPARE/LS**	**12**	0.912	**malic enzyme H (11)**
TVAG_267870	**MLTSSVSVPVRN/IC**	**12**	**1.909**	**malic enzyme A (10)**
TVAG_485280	MLGIFFSIASCRS/LR	13	1.878	3D domain containing protein
TVAG_150360	MLSHISHSSFLRF/FS	13	2.39	thiogalactoside transacetylase, putative
TVAG_453700	MSLTTSDAQKLRE/LF	13	0.913	EF hand family protein
TVAG_335420	MLSSSSPLIVVLRS/LN	14	1.909	TolA protein, putative
TVAG_269160	MSLSCSVGLSEKRN/SN	14	1.88	hypothetical protein
TVAG_458080	MSLSPQQFFEIIRG/GK	14	0.912	conserved hypothetical protein
TVAG_037570	MLASTGINSTANILRN/IT	16	1.909	64kDa iron hydrogenase, putative
TVAG_010180	MLSFLSYFALSAVTRN/GK	16	1.908	DnaJ domain containing protein
TVAG_019190	MLTISHSGLPSSFLRF/LT	16	2.149	DnaJ domain containing protein
TVAG_000350	MTLPFLPFLLYNKYRF/LE	16	2.906	conserved hypothetical protein
TVAG_361590	MLATASASTSNILRN/IT	17	1.909	64kDa iron hydrogenase, putative
TVAG_393400	MLSLLFAQLAVSIRG/QK	17	1.909	conserved hypothetical protein
TVAG_269930	MLSVFIHTTNRSFRN/LI	17	3.149	conserved hypothetical protein
TVAG_107350	MLCQLTVIQSLLQNRVF/IN	17	1.878	conserved hypothetical protein
TVAG_382990	MLANPGTNGLLPMIVRF/LN	17	1.909	conserved hypothetical protein
TVAG_216970	MLSCLFLIGVLQSLERN/GL	17	0.881	conserved hypothetical protein
TVAG_182340	MLSSLDCLPSTFMRTF/AE	18	0.881	co-chaperone GrpE family protein
TVAG_553580	MLGACIMTGMPYTKGARF/LS	18	2.876	conserved hypothetical protein
TVAG_486320	MLSIILSHIACETDPQQIIRN/ID	21	0.124	conserved hypothetical protein

TVAG_424790	MLSILLNHITCETDPQQILRN/ID	21	0.124	conserved hypothetical protein

B

Protein ID NCBI	N-terminal presequence	Presequence length	Presequence charge at pH 7.0	Annotation
TVAG_379550	MSLKTISRLF/AY	10	2.908	tyrosine aminotransferase, putative
TVAG_480640	MLSVRKGERF/LI	10	2.911	conserved hypothetical protein
TVAG_361080	MTLRTLCERF/AA	10	1.881	hypothetical protein
TVAG_026600	MLRSVCISSRG/GF	11	2.878	conserved hypothetical protein
TVAG_321030	MLSALKSGIRF/SS	11	2.908	CoA binding domain containing protein
TVAG_060450	MLRHLTVRPGRF/SD	12	4.149	conserved hypothetical protein
TVAG_088050	MLSKASSAFVRS/FV	12	2.908	chaperonin, putative
TVAG_277380	MLTTFGKHFARG/FA	12	3.148	mrp, putative
TVAG_542680	MLAAEFKKRYGRE/LI	13	2.911	conserved hypothetical protein
TVAG_213670	MLALFLQRANLRE/SS	13	1.912	conserved hypothetical protein
TVAG_070600	MLGKVMMSKVERS/AA	13	2.91	conserved hypothetical protein
TVAG_203620	MLSKQASSAFIRS/FV	13	2.908	chaperonin 60 putative
TVAG_475950	MSLRIHKLSNYRF/GA	13	4.147	hydrolase, NUDIX family protein
TVAG_492000	MLRKLCFKAPVPRS/QS	14	4.876	conserved hypothetical protein
TVAG_090870	MLRSLQLSFRQLRG/IN	14	3.909	beige/BEACH domain containing protein
TVAG_167250	**MSLIEAAKHFTRAF/AK**	**14**	**2.151**	**Hsp60(12)**
TVAG_204990	MSLFCEPFRYEICRF/AN	15	0.852	conserved hypothetical protein
TVAG_399620	MLALAFLASSRTLHRS/IV	16	3.149	conserved hypothetical protein
TVAG_433130	MLATCGRHLNSSFARSF/AK	16	3.119	heat shock protein, putative
TVAG_277950	MLGLRTPPEHKSSVRS/GV	16	3.151	conserved hypothetical protein
TVAG_237140	**MLSSVARSTSSLFSRG/FA**	**16**	**2.909**	**Tvhsp70**
TVAG_340390	MLSSVGKTSGSLFFRS/FQ	16	2.908	heat shock protein 70 (HSP70)-4, putative
TVAG_030930	MSLKHINLTRYDERRS/SN	16	3.152	conserved hypothetical protein
TVAG_135950	MLSTKTSPFFPGYDFRS/AT	17	1.91	ef-hand domain (C-terminal) containing protein, putative
TVAG_308130	MLTLVPHRRIPMSKERS/QS	17	4.151	WD repeat-containing protein slp1, putative

TVAG_143400	MLSQPQPRKKTVRQCGRF/SI	18	5.876	conserved hypothetical protein
TVAG_356810	MLSSICRFGHSMRRHERE/IK	18	3.364	nitroimidazole resistance protein, putative
TVAG_005890	MLSSISRLGHVMRRGDRE/IK	18	3.154	nitroimidazole resistance protein, putative
TVAG_478310	MLTSKHDIHPNKYNELRS/IY	18	2.392	conserved hypothetical protein
TVAG_494010	MSLFSFNSMKHYLLKFRYF/IL	19	4.145	HEAT repeat family protein
TVAG_559350	MSLSKSERESIILNDARG/IQ	18	0.916	conserved hypothetical protein
TVAG_466520	MSLSKSERESIILNNARG/IQ	18	1.913	conserved hypothetical protein
TVAG_471430	MSLSKSERKDVVLNDARG/IQ	18	1.915	conserved hypothetical protein
TVAG_352770	MSLSKSERKSIILNDARG/IQ	18	2.912	conserved hypothetical protein
TVAG_104990	MSLSKSERQSIILHDARG/IQ	18	2.153	conserved hypothetical protein
TVAG_504860	MSLSKSKRESIILNDARG/IQ	18	2.912	conserved hypothetical protein
TVAG_250290	MSLSKSKRESIILNDARG/IQ	18	2.912	conserved hypothetical protein
TVAG_106920	MTLSKSERESIILNDARG/IQ	18	0.916	conserved hypothetical protein
TVAG_146780	MLAAVKNSTFGFGNFFIRS/FA	19	2.908	conserved hypothetical protein
TVAG_322470	MLALIAFARNPNYYNLFRF/IK	19	2.907	conserved hypothetical protein
TVAG_270230	MLRTLCQVRQNLPRYIQRS/FD	19	4.877	conserved hypothetical protein
TVAG_352670	MLRTLYQVRQNLPRNIQRS/FD	19	4.908	conserved hypothetical protein
TVAG_161150	MLRTLYQVRQNLPRSIQRS/FD	19	4.908	conserved hypothetical protein
TVAG_148060	MLRTLYQVRQNLPRSIQRS/FD	19	4.908	conserved hypothetical protein
TVAG_103700	MLRTLYQVRQNLPRYIQRS/FD	19	4.907	conserved hypothetical protein
TVAG_418580	MLRTLYQVRQNLPRYMQRS/FD	19	4.907	conserved hypothetical protein
TVAG_008840	**MLSSIGTRTSGFGNLFFRS/FA**	**19**	**2.909**	**TviscU**
TVAG_074640	MLTSLCMSNLGPHREGFRG/LP	19	2.121	glucosylceramidase, putative
TVAG_421230	MSLFKLIFALFISVISERG/IF	19	1.911	conserved hypothetical protein
TVAG_163470	MSLQEANGRLLEARAKQRE/LK	19	1.916	conserved hypothetical protein
TVAG_385950	MSLSSYIIHSFKHLLDPRF/GE	19	2.39	protein phosphatase-1, putative
TVAG_053240	MTLLSHLLLKNREQDMCRN/LK	19	2.123	conserved hypothetical protein
TVAG_010980	MTLVFLSLLLTDARSFRRE/AL	19	1.914	hypothetical protein
TVAG_460050	MLAKLLSFITNASPAKEYRN/IE	20	2.909	conserved hypothetical protein
TVAG_300690	MLSFLFLFISGKNITISKRG/ST	20	3.907	conserved hypothetical protein
TVAG_007300	MLTARGSTVMIRIKRTTGRS/FI	20	5.908	ubiquitin family protein
TVAG_425510	MLTKKLYRTRSTSTSSAVRG/SQ	20	5.906	conserved hypothetical protein

TVAG_140830	MSLPRQFDRNGRIHQSGSRG/SL	20	4.152	conserved hypothetical protein
TVAG_207600	MSLRSSRSSTKSTKSQVSRS/IT	20	5.907	hypothetical protein
TVAG_291910	MSLSSQTSSRRSSTNSVTRS/ST	20	3.909	conserved hypothetical protein
TVAG_072420	MSLYDEYAIHIPKSPHRRRS/AI	20	3.392	conserved hypothetical protein
TVAG_258310	MTLYRYNSQKQIVEVNLKRG/SY	20	3.908	conserved hypothetical protein
TVAG_449880	MLRSRKSSKDPQNNRRRVTRHF/LS	22	8.15	conserved hypothetical protein
TVAG_327760	MLSSPQKFAANVLLFNASARN/SG	21	2.908	Iron-sulfur flavoprotein
TVAG_452330	MSLTPRIGQLYLSGIKKRERN/SN	21	4.909	conserved hypothetical protein
TVAG_090660	MLRRSTCDANHIRQFFLSKHRYF/AR	23	5.359	conserved hypothetical protein
TVAG_085490	MLRRSTCDANHIRQFFLSKHRYF/AR	23	5.359	conserved hypothetical protein
TVAG_000900	MLRRSTCDANHIRQFFLSKHRYF/AR	23	5.359	conserved hypothetical protein
TVAG_228260	MLSSCATRRLKTIVGNGKLIRS/LN	22	5.876	amidohydrolase family protein
TVAG_160480	MSLGVSHPKLSPAQQVNQLGRN/ID	22	3.148	conserved hypothetical protein
TVAG_160860	MSLKEENEKLRNKIQQLSLQRN/QE	22	2.914	conserved hypothetical protein
TVAG_199590	MTLSKAFSAPDSVEVASYMIRS/SI	22	0.912	conserved hypothetical protein
TVAG_447950	MTLSKAFSAPDSVEVASYMIRS/SI	22	0.912	conserved hypothetical protein
TVAG_304780	MLSNIIAISFAMKSQENIKHIRE/SD	23	2.152	conserved hypothetical protein
TVAG_197430	MLTGIDLIIHCCKNDNVKILNRE/LM	23	1.094	ankyrin repeat-cotaining protein, putative
TVAG_130280	MLGIKFGNSTIVVHHIADTRRERN/AI	24	3.394	heat shock protein 70kD, putative
TVAG_174040	MLGIKFGNSTIVVHHISDTRSERN/AI	24	2.394	heat shock protein, putative
TVAG_111940	MLRTLYQVRQNLPRYIQRSFDKRN/AE	24	5.909	conserved hypothetical protein
TVAG_049690	MLRYPFTPNKPYTALALNFTFPRF/FD	24	3.906	thiamin pyrophosphokinase, putative

Table S2

N-terminal presequences of mitosomal proteins found in *G. intestinalis* proteome.

Protein ID NCBI	N-terminal presequence	presequence length	presequence charge at pH 7.0	Annotation
gi:157815925	MSLLSSIRRF/IT	10	2.997	Gifdx (13)
gi:159115366	MLPALITPLVRS/LT	12	1.997	GiiscA†
gi:159117498	MTSLQLSSTSLLQSVARF/LT	18	1.997	GiiscU (13)
gi:159119780		0		GiiscS (13)
gi:159113748		0		GPP (13)
gi:159119748		0		Gihsp70 (14)
ctg02_23-5-32114-31794*		0		Gipam18 (13)
gi:159110554		0		Gicpn60 (14)
gi:159117945		0		Gigrx†

***** Open reading frame ID from GiardiaDB database (http://giardiadb.org/giardiadb/).
† Experimentally verified (data not shown).

SUPPORTING REFERENCES

1. Foster PG (2004) Modeling compositional heterogeneity. *Syst Biol* 53:485-495.

2. Arretz M, Schneider H, Guiard B, Brunner M, Neupert W (1994) Characterization of the mitochondrial processing peptidase of *Neurospora crassa*. *J Biol Chem* 269:4959-4967.

3. Hirt RP, Noel CJ, Sicheritz-Ponten T, Tachezy J, Fiori PL (2007) *Trichomonas vaginalis* surface proteins: a view from the genome. *Trends Parasitol* 23:540-547.

4. Hrdy I, Müller M (1995) Primary structure and eubacterial relationships of the pyruvate:ferredoxin oxidoreductase of the amitochondriate eukaryote *Trichomonas vaginalis*. *J Mol Evol* 41:388-396.

5. Dolezal P, Dancis A, Lesuisse E, Sutak R, Hrdy I, Embley TM, Tachezy J (2007) Frataxin, a conserved mitochondrial protein, in the hydrogenosome of *Trichomonas vaginalis*. *Eukaryot Cell* 6:1431-1438.

6. Johnson PJ, Doliveira CE, Gorrell TE, Müller M (1990) Molecular analysis of the hydrogenosomal ferredoxin of the anaerobic protist *Trichomonas vaginalis*. *Proc Natl Acad Sci U S A* 87:6097-6101.

7. Lahti CJ, Bradley PJ, Johnson PJ (1994) Molecular Characterization of the Alpha-Subunit of *Trichomonas vaginalis* Hydrogenosomal succinyl-CoA synthetase. *Mol Biochem Parasitol* 66:309-318.

8. Lahti CJ, Doliveira CE, Johnson PJ (1992) Beta-succinyl-coenzyme-A synthetase from *Trichomonas vaginalis* is a soluble hydrogenosomal protein

with an amino-terminal sequence that resembles mitochondrial presequences. *J Bacteriol* 174:6822-6830.

9. Lange S, Rozario C, Müller M (1994) Primary structure of the hydrogenosomal adenylate kinase of *Trichomonas vaginalis* and its phylogenetic relationships. *Mol Biochem Parasitol* 66:297-308.

10. Hrdy I, Müller M (1995) Primary structure of the hydrogenosomal malic enzyme of *Trichomonas vaginalis* and its relationship to homologous enzymes. *J Eukaryot Microbiol* 42:593-603.

11. Dyall SD, Yan W, Delgadillo-Correa MG, Lunceford A, Loo JA, Clarke CF, Johnson PJ (2004) Non-mitochondrial complex I proteins in a hydrogenosomal oxidoreductase complex. *Nature* 431:1103-1107.

12. Bui ETN, Bradley PJ, Johnson PJ (1996) A common evolutionary origin for mitochondria and hydrogenosomes. *Proc Natl Acad Sci U S A* 93:9651-9656.

13. Dolezal P, Smid O, Rada P, Zubacova Z, Bursac D, Sutak R, Nebesarova J, Lithgow T, Tachezy J (2005) *Giardia* mitosomes and trichomonad hydrogenosomes share a common mode of protein targeting. *Proc Natl Acad Sci U S A* 102:10924-10929.

14. Regoes A, Zourmpanou D, Leon-Avila G, van der GM, Tovar J, Hehl AB (2005) Protein import, replication, and inheritance of a vestigial mitochondrion. *J Biol Chem* 280:30557-30563.

Fig. S1

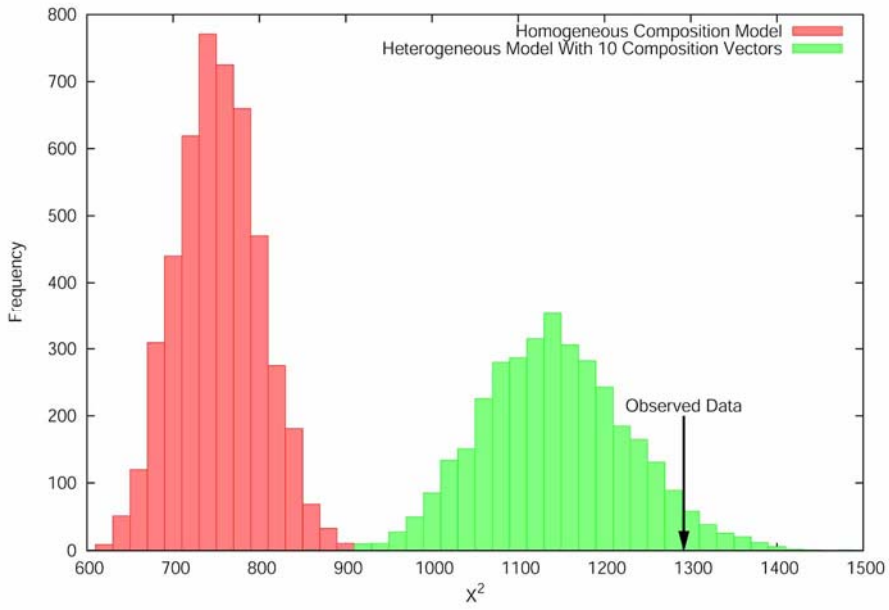
Homogeneous Composition Model
Heterogeneous Model With 10 Composition Vectors
Observed Data
Frequency
X2
800
700
600
500
400
300
200
100
0
600
700
800
900
1000
1100
1200
1300
1400
1500

Fig. S2

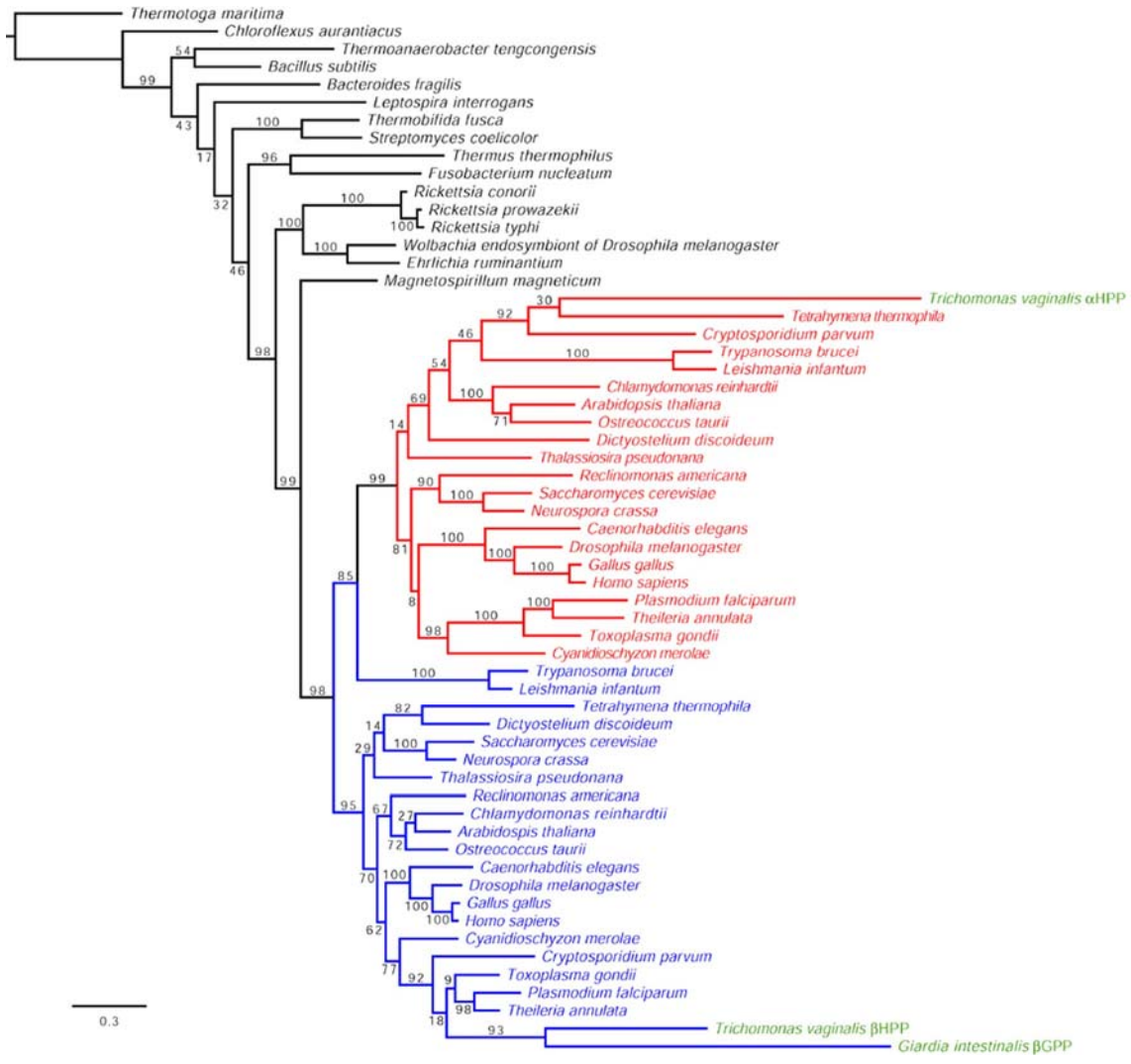
Thermotoga maritima
Chloroflexus aurantiacus
Thermoanaerobacter tengcongensis
Bacillus subtilis
Bacteroides fragilis
Leptospira interrogans
Thermobifida fusca
Streptomyces coelicolor
Thermus thermophilus
Fusobacterium nucleatum
Rickettsia conorii
Rickettsia prowazekii
Rickettsia typhi
Wolbachia endosymbiont of Drosophila melanogaster
Ehrlichia ruminantium
Magnetospirillum magneticum
Trichomonas vaginalis αHPP
Tetrahymena thermophila
Cryptosporidium parvum
Trypanosoma brucei
Leishmania infantum
Chlamydomonas reinhardtii
Arabidopsis thaliana
Ostreococcus taurii
Dictyostelium discoideum
Thalassiosira pseudonana
Reclinomonas americana
Saccharomyces cerevisiae
Neurospora crassa
Caenorhabditis elegans
Drosophila melanogaster
Gallus gallus
Homo sapiens
Plasmodium falciparum
Theileria annulata
Toxoplasma gondii
Cyanidioschyzon merolae
Trypanosoma brucei
Leishmania infantum
Tetrahymena thermophila
Dictyostelium discoideum
Saccharomyces cerevisiae
Neurospora crassa
Thalassiosira pseudonana
Reclinomonas americana
Chlamydomonas reinhardtii
Arabidopsis thaliana
Ostreococcus taurii
Caenorhabditis elegans
Drosophila melanogaster
Gallus gallus
Homo sapiens
Cyanidioschyzon merolae
Cryptosporidium parvum
Toxoplasma gondii
Plasmodium falciparum
Theileria annulata
Trichomonas vaginalis βHPP
Giardia intestinalis βGPP
0.3

Fig. S3

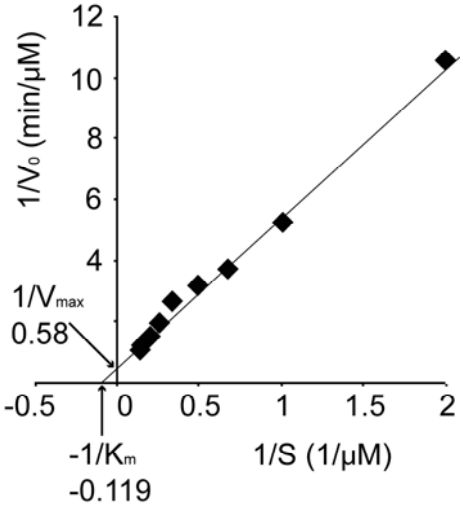

Fig. S4

	α	β	α/β
MPP			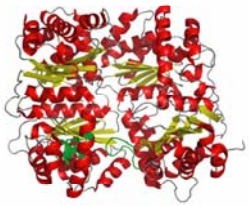
HPP	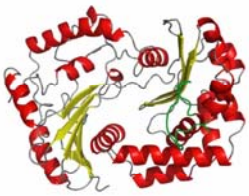		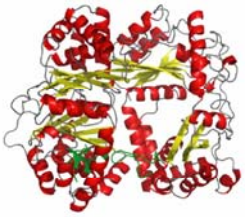
GPP	not present	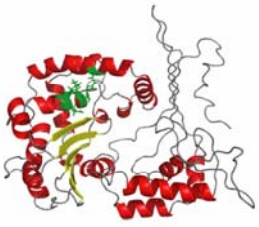	not present

THE MONOTHIOL GLUTAREDOXIN IN THE MITOSOMES OF *GIARDIA INTESTINALIS*

Ondrej Smid, Robert Sutak, and Jan Tachezy

Department of Parasitology, Faculty of Science, Charles University, Vinicna 7, Prague 2, 128 44, Czech Republic

Corresponding author:

Prof. Jan Tachezy, Ph.D.
Charles University in Prague, Faculty of Science
Department of Parasitology
Vinicna 7, 128 44 Prague
Czech Republic
Phone: +420-221-951-811
FAX: +420-224-919-704
E-mail: tachezy@natur.cuni.cz

ABSTRACT

Mitosomes of *G. intestinalis* are recently discovered organelles that were demonstrated to function in iron-sulfur (FeS) cluster biogenesis. However, so far only an incomplete set of FeS cluster assembly machinery components was localized to mitosomes. By proteomic analysis of mitosome-rich fraction, we identified a novel mitosomal protein homologous to monothiol glutaredoxins. In addition to the conserved CXXS motif-containing glutaredoxin domain, Gigrx possesses a non-conserved N-terminal extension. This region is devoid of homology to any known protein and is not required for import into mitosomes. The result of Neighbor-Net analysis of sequence similarities shows that Gigrx is closely related to the single glutaredoxin domain-containing mitochondrial proteins involved in FeS cluster assembly. Same as other monothiol glutaredoxins, the purified Gigrx binds an FeS cluster and glutathione. The identification of a mitochondrial-type monothiol glutaredoxin in mitosomes of *G. intestinalis* provides further evidence that mitosomes and mitochondria share a common ancestor.

INTRODUCTION

Giardia intestinalis is a parasitic protist that was considered amitochondrial until recently. Even though mitochondria are not present, related organelles of endosymbiotic origin, the mitosomes, were discovered in this organism (1). Apparent similarities, notably double membrane that limits the organelles (1), a common mode of protein import (2) and maturation (3) and compartmentalization of a key part of the FeS cluster assembly process (1) suggest common ancestry of mitosomes and mitochondria, even though alternative evolutionary scenarios are still discussed (4). Interestingly, the FeS cluster biosynthesis is the only metabolic function of *G. intestinalis* mitosomes known to date.

FeS clusters are cofactors of a number of proteins. Most importantly, they are indispensable for the activity of the essential proteins Rad3 and Pri2 involved in DNA metabolism and Rli1 participating in translation initiation (5). Thus, the biogenesis of FeS clusters is an essential process for a cell (5). In most non-plant eukaryotes including *G. intestinalis*, the crucial part of this biosynthetic pathway occurs exclusively in the mitochondrion or a related organelle (1, 5, 6). The FeS cluster assembly is centered around IscU, a metallochaperone that serves as a scaffold for a new FeS cluster. The cysteine desulphurase IscS catalyzes mobilization of sulphur for the FeS cluster being assembled from a cysteine molecule and delivers it to IscU. Iron is delivered to IscS/IscU complex most likely by the protein frataxin. At some point during the process of FeS cluster biogenesis, electrons are required. The mitochondrial [2Fe2S] ferredoxin and its NADH-dependent reductase form a short electron-transport chain that ends on the FeS cluster being assembled. After the assembly on IscU, the FeS cluster is transferred to apoproteins by the action of the Hsp70 (Ssq1), and Hsp40 (Jac1) chaperones, proteins IscA, Iba57 and monothiol glutaredoxin (5).

Glutaredoxins are evolutionarily conserved oxidoreductases that use glutathione as a reducing agent (7). The number of cysteine residues in the active site was used to define two major groups of glutaredoxins. Dithiol glutaredoxins contain a CXXC motif while the active site of monothiol glutaredoxins is characterized by the presence of a conserved CXXS motif. Dithiol glutaredoxins mantain and regulate biological activity of proteins by reducing protein disulfide bonds or deglutathionylation (7). The function and mode of action of monothiol glutaredoxins is less understood. They seem to lack the protein disulfide reduction activity, but they are able to reduce the mixed protein-

glutathione disulfides, at least *in vitro* (7, 8). The best studied monothiol glutaredoxin, mitochondrial Scgrx5 of *S. cerevisiae*, is the glutaredoxin involved in FeS cluser assembly (9).

Structurally, monothiol glutaredoxins are either proteins with a single glutaredoxin domain or modular proteins with glutaredoxin domain(s) N-terminally linked by a non-conserved region to an additional (Trx)-like domain. Prokaryotic organisms possess only the single domain type. In eukaryotes, mitochondrial and plastid monothiol glutaredoxins are of the single-domain type while the Trx-Grx fusion proteins are present in other compartments (10, 11). Recently, it has been demonstrated that the yeast glutaredoxin Scgrx5 and other monothiol glutaredoxins bind 2Fe2S cluster bridging two subunits of a homodimer, coordinated by a cysteine residue of the active site of each monomer and cysteines of two glutathione molecules (12).

Of the *Giardia* FeS cluster assembly machinery, only the proteins IscS, IscU (1), ferredoxin (2), and Hsp70 (13) were identified thus far. Here we report identification of a mitosomal glutaredoxin of *G. intestinalis* and demonstrate that it is a monothiol glutaredoxin homologous to the yeast Scgrx5 with the conserved CXXS motif of the active site co-ordinating an FeS cluster.

MATERIALS AND METHODS

Cell cultivation

G. intestinalis strain WB (American Type Culture Collection) was grown in TYI-S-33 medium supplemented with 10% heat-inactivated bovine serum, 0.1% bovine bile and antibiotics (2).

Preparation of mitosome-rich fractions

Trophozoites detached from the wall of the growth vessels were harvested, washed twice in ST buffer (250 mM sucrose, 0.5 mM KCl, 10 mM Tris pH 7.2), and suspended in ST buffer with 50 μg/ml Nα-tosyl-l-lysine chloromethyl ketone and 10 μg/ml of leupeptin. The cells were disrupted by sonication and centrifuged at 680 × *g* for 10 min and at 2,760 × *g* for 20 min to remove unbroken cells, nuclei, and cytoskeletar residues. The resulting supernatant was centrifuged at 50,000 × g for 30 min. Acquired high-speed pellet was resuspended in 0.5 ml of ST buffer and layered onto a discontinuous sucrose gradient consisting of 1 ml each of 25%, 30%, 35%, 40%, 45%, 50%, 55%, and 60% of a sucrose solution with 25 mM Tris pH 7.2. The gradient was centrifuged for 22 h in a Beckman SW 40 rotor at 120,000 × *g* at 4°C. The 1 ml fractions were analysed by immunoblot using anti-GiiscU antibody (1).

2D polyacrylamide gel electrophoresis (2D PAGE)

The mitosome-rich fraction prepared as described above was washed with ST buffer, solubilised in 7 M urea, 2 M thiourea, 4% CHAPS, 0.5% Bio-Lyte Ampholyte (Bio-Rad), 100 mM DTT, bromophenol blue, 40 mM Tris pH 8.8 and subjected to IEF on 17-cm pH 3 to 10 and pH 4 to 7 immobilized pH gradient strips (Bio-Rad). After focusing, gel strips were equilibrated for 2x15 min with 6 M urea, 20% glycerol, 50 mM Tris pH 8.2, 2% SDS, 65 mM DTT and bromophenol blue. The second dimension was run on 13.5% SDS-PAGE gels. Gels were stained with Coomassie Brilliant Blue G250 and imaged on the GS-800 calibrated densitometer. Images were analysed using PDQuest 2-D Analysis Software (Bio-Rad).

Trypsin digestion and mass spectrometry

The spots were manually excised from the gel, washed twice with 25 mM NH_4HCO_3, dehydrated in acetonitrile (ACN), dried in a Speed vac, and subjected to in-gel digestion by rehydration with 10 ng/μL trypsin (Sigma-Aldrich), 25 mM NH_4HCO_3, 5 mM

$CaCl_2$. Digestion was performed at 37°C overnight. Tryptic peptides were extracted by subsequent washing in 0.1% TFA, 50% ACN and 100% ACN, desalted using C18 ZipTip (Millipore) and analysed in a Voyager-DE PRO MALDI-TOF mass spectrometer (Applied Biosystems). A saturated solution of α-cyano-4-hydroxycinnamic acid in 50% acetonitrile and 0.1% TFA was used as matrix. The spectra were analysed using Mascot engine search (Matrix Science, London, UK).

Selectable transformation of *G. intestinalis* and immunofluorescence analysis

For overexpression with HA-tag in *G. intestinalis*, the glutaredoxin sequence (http://www.giardiadb.org/giardiadb/) was amplified from *Giardia* cDNA prepared as described (2) and inserted to the plasmid pONDRA (2). Electroporation and selection for stable transfectants was performed as published by Sun et al. (14). *G. intestinalis* cells for immunofluorescent microscopy were prepared and the image processed as published (2).

Protein expression and purification

Full-length Gigrx was inserted into the pET42b vector for overexpression with C-terminal hexahistidine tag in *E. coli*. The protein expression and purification was performed as described (3). The active mitosomal processing peptidase was prepared as published (3). C-terminal part of Gigrx (Gigrx-C) was inserted into the pQE30 (Qiagen) for overexpression with N-terminal hexahistidine tag in *E. coli*. After induction of Gigrx-C expression by 0.5 mM isopropylthiogalactoside, the medium was supplemented with 0.5 mM $(NH_4)_2Fe(SO_4)_2$ and the bacteria were grown at 20°C overnight. Gigrx-C with hexahistidine tag was purified by nickel column chromatography under native conditions.

Analytical methods

UV-vis spectra were monitored between 260 and 700 nm by Shimadzu UV-1601 spectrophotometer. Glutathione was detected fluorometrically in the fraction containing purified GigrxC (15). After incubation with 2 mM EDTA, 100 μM monochlorobimane (MCB) (Fluka) was added together with glutathione S-transferase (Sigma). The concentration of the fluorescent GSH-MCB conjugate was measured after 2 hour incubation at 470 nm, with an excitation wavelength of 380 nm (Infinite M200, Tecan).

Sequence analyses

Protein isoelectric point (pI), molecular weight (MW) and identity/similarity values were calculated with Sequence Manipulation Suite tools (http://www.bioinformatics.org/sms2/). Glutaredoxin and glutaredoxin-related sequences were identified by BLAST searches (http://blast.ncbi.nlm.nih.gov/Blast.cgi, http://toxodb.org/toxo/) and aligned using ClustalX (16). After removal of unaligned positions, the sequences were analysed by SplitsTree4 application (17) with default settings including the UncorrectedP method for distance estimation, the NeighborNet method for computing the phylogenetic network and the EqualAngle algorithm for network visualization.

RESULTS

Purification of mitosome-rich fraction

To obtain the mitosome-rich subcellular fraction from *Giardia*, we performed discontinual sucrose gradient centrifugation of high-speed sediment fraction of sonicated cells. As proven by immunoblot analysis using antibody against the mitosomal protein GiiscU, mitosomes were distributed mainly in the upper part of the gradient (Fig 1). Results obtained from other tested methods of cell disruption and fractionation were not reproducible. The mechanical cell disruption resulted in the generation of various aggregates which were unsuitable for further separation, while fractionation using other gradients such as continuous percoll or metrizamide resulted in rather protracted distribution of GiiscU among the fractions (data not shown).

Proteomic analysis of mitosomal fraction and cellular localization of *G. intestinalis* glutaredoxin

From duplicate experiments, using both 3-10 and 4-7 pH gradient strips we identified a monothiol glutaredoxin homologous to the yeast Scgrx5. Fig. 2 shows the representative 3-10 pH gradient 2D gel with marked proteins with confirmed mitosomal localization. To verify subcellular localization of *Giardia* glutaredoxin (Gigrx), we overexpressed its hemagglutinin (HA)-tagged version in *G. intestinalis*. A single band of approximately 25 kDa was detected by immunoblot analysis of Gigrx-HA-expressing cells using anti-HA antibody (data not shown). Immunofluorescent microscopy demonstrates that Gigrx-HA co-localizes with GiiscU to mitosomes (Fig. 3).

Characterization of the *G. intestinalis* glutaredoxin

Gigrx is a monothiol glutaredoxin containing the conserved CXXS motif of the active site (Fig. 4). The cysteine Cys117 suggested to be essential for the catalytic activity of the yeast monothiol Scgrx5 (7) is not conserved in Gigrx. However, Gigrx possesses a cysteine residue at the position 198 that might have a function similar to the Cys117 of Scgrx. Gigrx was predicted to be a 202 amino acid residues (AA) long protein (http://www.giardiadb.org/giardiadb/) of 22.1 kDa and pI=8.03. Interestingly, the N-terminal part of Gigrx comprising first 98 AA of the protein (Fig. 4) shares homology with neither thioredoxins nor any other known protein. A cleavable presequence resembling mitochondrial targeting peptide was predicted by MitoProt (http://ihg2.helmholtz-muenchen.de/ihg/mitoprot.html) on the N-terminus of Gigrx,

indicating that the extension may be required for mitosomal targeting of the protein (Fig. 4).

To evaluate the accuracy of the presequence prediction, we expressed the full-length Gigrx with hexahistidine (His) tag in *E. coli* and incubated the purified Gigrx-His with the mitosomal processing peptidase (3) *in vitro*. Cleavage of the predicted N-terminal presequence of Gigrx was not observed (data not shown). To examine the function of the first 98 AA of Gigrx, we overexpressed the truncated version (Gigrx-C, Fig. 4) with HA-tag in *G. intestinalis*. The shortened Gigrx was detected in mitosomes by immunofluorescence analysis (data not shown), indicating that the N-terminal extension is not required for mitosomal targeting.

For the assessment of the relationships of Gigrx to glutaredoxins from other organisms, Neighbor-Net analysis was performed. The Neighbor-Net method is a modification of the Neighbor-Joining algorithm and is often used for one-graph visualization of alternative topologies of phylogenetic trees. It allows to explore the data by depicting the conflicting signals connecting one sequence to different neighbors by boxes in the resulting graph (18, 19). The Neighbor-Net network of glutaredoxin sequences demonstrates that Gigrx clusters with mitochondrial monothiol glutaredoxins (Fig 5). Accordingly, Gigrx exhibits 40.5% identity and 55.4% similarity to the yeast monothiol glutaredoxin Scgrx5.

Gigrx contains all amino acid residues that were shown to be essential for coordination of an FeS cluster and binding of glutathione by a single-domain monothiol gluateroxin (12) (Fig. 4). To investigate whether Gigrx contains an FeS cluster, we expressed Gigrx-C with His-tag in *E. coli* and analyzed the UV-visible spectrum of the purified protein. Same as in the spectrum of Scgrx5, absorption peaks 320 nm, 410 nm, 510 nm and 590 nm sensitive to the chelator EDTA could be identified (Fig 6), indicating the presence of an FeS cluster on Gigrx. To address the question whether the FeS cluster of Gigrx is co-ordinated by glutathione, we employed the monochlorobimane fluorometric method for glutathione detection (15). By this approach, we detected 6,9 nmol of glutathione per mg of the purified Gigrx-C.

DISCUSSION

Only a limited amount of information is available concerning the function of *G. intestinalis* mitosomes. After development of the method for purification of mitosome-rich fraction, we have used proteomic and transfection methods to identify proteins localized in the organelle. By this approach we identified a glutaredoxin-related protein and confirmed its mitosomal localization. The *Giardia* glutaredoxin Gigrx belongs to the monothiol glutaredoxin family that is characterized by the presence of the conserved CXXS motif of the active site. Sequence and biochemic analyses indicate that Gigrx is closely related to the mitochondrial single-domain monothiol glutaredoxins shown to be involved in FeS cluster assembly (9, 20, 21). Identification of the monothiol glutaredoxin as a component of the FeS cluster assembly machinery in the reduced mitochondria of *Giardia* suggests the importance of the enzyme for the process of FeS cluster biogenesis.

The *S. cerevisiae* monothiol glutaredoxin Scgrx5 contains an N-terminal presequence that is essential for import into mitochondrial matrix (9). By contrast, the N-terminal extension of Gigrx is not required for translocation of Gigrx into mitosomes, indicating that, unlike the yeast homologue, Gigrx possesses targeting information within the conserved part of the protein. Similarly, the cysteine desulfurase GiiscS is targeted to mitosomes in the absence of an N-terminal targeting presequence (2). These findings suggest that mitosomal protein import apparatus can employ an alternative mechanism for import of matrix proteins that is not dependent on the cleavabe N-terminal presequence.

Glutaredoxins are glutathione-dependent enzymes. Even though *Giardia* was shown to lack glutathione (22) and our attempts to detect the molecule in the mitosomal fraction of *Giardia* were unsuccessful (data not shown), homologues of enzymes involved in the synthesis of glutathione were identified in the genome of the parasite, namely glutamate-cysteine ligase (NCBI gi: 159111616) and glutathione synthase (NCBI gi: 159119420). Moreover, genes coding for putative homologues of glutathione-S-transferase (NCBI gi: 159116102) and glutathione reductase (NCBI gi: 159115502) could be detected in the *Giardia* genome. These findings may indicate that free glutathione is present in the *Giardia* cell in concentration below the detection limit of the assays used (HPLC, MCB-GST). The major low-molecular weight thiol of *G. intestinalis* being cysteine (22), glutathione in such a low concentration is most likely not involved in the reactions controlling cellular redox state but may only be required

for the activity of Gigrx. The presence of gluathione in the purified Gigrx-C favors this hypothesis.

Apart from the components of the FeS cluster assembly machinery, no other set of proteins typical for mitochondria or hydrogenosomes have been identified in the mitosome-rich fraction of *Giardia*. This may indicate that the function of the mitochondrial remnant in *G. intestinalis* is restricted to the production of FeS clusters. It was clearly demonstrated that mitochondrial FeS cluster assembly machinery is essential for the formation of mitochondrial as well as cytosolic and nuclear FeS cluster proteins. The reason for such compartmentalization is unknown, but the low oxygen concentration inside the mitochondrial matrix may be favorable for the oxygen-sensitive process of FeS cluster biosynthesis.

FIGURE LEGENDS

Fig. 1. Purification of mitosome-rich fraction of Giardia. (a) Separation of high-speed pellet of sonicated cells on discontinual sucrose gradient. (b) Anti-GiiscU immunoblot analysis of revealed fractions.

Fig. 2. 2D electrophoresis of mitosome-rich fraction. A representative 3-10 pH gradient 2D gel is shown with marked proteins with confirmed mitosomal localization.

Fig. 3. Cellular localization of Gigrx. *G. intestinalis* cells expressing HA-tagged Gigrx were stained for immunofluorescence microscopy with mouse anti-hemagglutinine (HA) antibody (green). The mitosomal marker protein GiiscU was detected by polyclonal rabbit anti-GiiscU antibody (red). The merged image is given for immunofluorescent staining, the nuclei (blue) stained with DAPI.

Fig. 4. Alignment Gigrx, the mitochondrial monothiol glutaredoxin of *S. cerevisiae* (ScGrx5) and the monothiol glutaredoxin of *Rickettsia prowazekii* (RpGrx2). The single line denotes the N-terminal extension of Gigrx while the double line indicates the predicted Gigrx targeting presequence. Boxed is the conserved CXXS motif of monothiol glutaredoxins. Arrowhead marks the processing site of ScGrx5. The amino acid residues involved in glutathione binding are indicated by asterisks. The cysteine residue that coordinates an FeS cluster is highlighted by a dot.

Fig. 5. Neighbor-Net analysis of glutaredoxins and related proteins. Gigrx clusters with mitochondrial single-domain monothiol glutaredoxins. Glutaredoxin and glutaredoxin-related sequences of *Arabidopsis thaliana* (AtGrx1 NCBI gi: 15241374, AtGrx2 NCBI gi: 15223928, AtGrx3 NCBI gi: 4218125, AtGrx4 NCBI gi: 15225333, AtGrx5 NCBI gi: 18424656, AtGrx6 NCBI gi: 186527928, AtGrx7 NCBI gi: 15242674, AtGrx8 NCBI gi: 15218675, AtGrx9 NCBI gi: 15229353, AtGrx10 NCBI gi: 15234680, AtGrx11 NCBI gi: 15234673, AtGrx12 NCBI gi: 15234671, AtGrx13 NCBI gi: 15234675, AtGrx14 NCBI gi: 15238885, AtGrx15 NCBI gi: 116830287, AtGrx16 NCBI gi: 15227150, AtGrx17 NCBI gi: 15241297, AtGrx18 NCBI gi: 21537203, AtGrx19 NCBI gi: 15229356, AtGrx20 NCBI gi: 7573360, AtGrx21 NCBI gi: 15218686, AtGrx22 NCBI gi: 15234516, AtGrx23 NCBI gi|15233118, AtGrx24 NCBI gi: 18404699), *Chlamydomonas reinhardtii* (Crgrx1 NCBI gi: 159490044,

Crgrx2 NCBI gi: 159471714, Crgrx3 NCBI gi: 159489795, Crgrx4 NCBI gi: 159491488, Crgrx5 NCBI gi: 159485728, Crgrx6 NCBI gi: 159463028), *Cryptosporidium parvum* (CpGrx1 NCBI gi: 66475834, CpCrx2 NCBI gi: 66358556), *Dictyostelium discoideum* (DdGrx1 NCBI gi: 66804263, DdGrx2 NCBI gi: 66826841, DdGrx3 NCBI gi: 66821301, DdGrx4 NCBI gi: 66819631), *Drosophila melanogaster* (DmGrx1 NCBI gi: 24666486, DmGrx2 NCBI gi: 19922712, DmGrx3 NCBI gi: 24642023, DmGrx4 NCBI gi: 19921242), *Gallus gallus* (GgGrx1 NCBI gi: 170671712, GgGrx2 NCBI gi: 118094049, GgGrx3 NCBI gi: 45384038, GgGrx4 NCBI gi: 50749993, GgGrx5 NCBI gi: 56605958), *Neurospora crassa* (NcGrx1 NCBI gi: 85103722, NcGrx3 NCBI gi: 85117048, NcGrx2 NCBI gi: 85099869, NcGrx4 NCBI gi: 85111703), *Plasmodium falciparum* (PfGrx1 NCBI gi: 124504793, PfGLP1 NCBI gi: 124504757, PfGLP2 NCBI gi: 86170662, PfGLP3 NCBI gi: 124511746), *Rickettsia prowazekii* (RpGrx1 NCBI gi: 15604077, RpGrx2 NCBI gi: 15604579), *Synechocystis* sp. (SspGrx1 NCBI gi: 16329670, SspGrx2 NCBI gi: 16330124, SspGrx3 NCBI gi: 16332161), *Tetrahymena thermophila* (TtGrx1 NCBI gi: 118372064, TtGrx2 NCBI gi: 118399637, TtGrx3 NCBI gi: 118366013, TtGrx4 NCBI gi: 118351420), *Toxoplasma gondii* (TgGrx1 ToxoDB gi: 69.m00142, TgGrx2 ToxoDB gi: 76.m01670, TgGrx3 ToxoDB gi: 49.m00010, TgGrx4 ToxoDB gi: 540.m00198, TgGrx5 ToxoDB gi: 59.m06121, TgGrx6 ToxoDB gi: 42.m03554, TgGrx7 ToxoDB gi: 38.m02359, TgGrx8 ToxoDB gi: 50.m03182), and *Trypanosoma brucei* (Tb2CGrx1 NCBI gi: 71754627, Tb2CGrx2 NCBI gi: 115504173, Tb1CGrx1 NCBI gi: 83763891, Tb1CGrx2 NCBI gi: 71748416, Tb1CGrx3 NCBI gi: 72388948) were included in the analysis.

Fig. 6. UV-visible spectrum of Gigrx without the N-terminal extension (Gigrx-C). Spectra of purified Gigrx-C before (straight line) and after incubation with EDTA (dashed line) were analysed. Absorption peaks and shoulders indicating the presence of an FeS cluster are marked by arrows.

REFERENCES

1. Tovar J, Leon-Avila G, Sanchez LB, Sutak R, Tachezy J, van der Giezen M, Hernandez M, Muller M, Lucocq JM (2003) *Nature* 426**:**172-176.

2. Dolezal P, Smid O, Rada P, Zubacova Z, Bursac D, Sutak R, Nebesarova J, Lithgow T, Tachezy J (2005) *Proc Natl Acad Sci U S A* 102**:**10924-10929.

3. Smid O, Matuskova A, Harris S, Kucera T, Novotny M, Horvathova L, Hrdy I, Kutejova E, Hirt RP, Embley TM *et al.* (2008) *in review*.

4. Morrison HG, McArthur AG, Gillin FD, Aley SB, Adam RD, Olsen GJ, Best AA, Cande WZ, Chen F, Cipriano MJ *et al.* (2007) *Science* 317**:**1921-1926.

5. Lill R, Muhlenhoff U (2008) *Annu Rev Biochem* 77**:**669-700.

6. Sutak R, Dolezal P, Fiumera HL, Hrdy I, Dancis A, Delgadillo-Correa M, Johnson PJ, Muller M, Tachezy J (2004) *Proc Natl Acad Sci U S A* 101**:**10368-10373.

7. Tamarit J, Belli G, Cabiscol E, Herrero E, Ros J (2003) *J Biol Chem* 278**:**25745-25751.

8. Zaffagnini M, Michelet L, Massot V, Trost P, Lemaire SD (2008) *J Biol Chem* 283**:**8868-8876.

9. Rodriguez-Manzaneque MT, Tamarit J, Belli G, Ros J, Herrero E (2002) *Mol Biol Cell* 13**:**1109-1121.

10. Vilella F, Alves R, Rodriguez-Manzaneque MT, Belli G, Swaminathan S, Sunnerhagen P, Herrero E (2004) *Comp Funct Genomics* 5**:**328-341.

11. Herrero E, de la Torre-Ruiz MA (2007) *Cell Mol Life Sci* 64**:**1518-1530.

12. Picciocchi A, Saguez C, Boussac A, Cassier-Chauvat C, Chauvat F (2007) *Biochemistry* 46**:**15018-15026.

13. Regoes A, Zourmpanou D, Leon-Avila G, van der GM, Tovar J, Hehl AB (2005) *J Biol Chem* 280**:**30557-30563.

14. Sun CH, Chou CF, Tai JH (1998) *Mol Biochem Parasitol* 92**:**123-132.

15. Kamencic H, Lyon A, Paterson PG, Juurlink BH (2000) *Anal Biochem* 286**:**35-37.

16. Thompson JD, Gibson TJ, Plewniak F, Jeanmougin F, Higgins DG (1997) *Nucleic Acids Res* 25**:**4876-4882.

17. Huson DH (1998) *Bioinformatics* 14**:**68-73.

18. Bryant D, Moulton V (2004) *Mol Biol Evol* 21**:**255-265.

19. Gelius-Dietrich G, Henze K (2004) *J Eukaryot Microbiol* 51**:**456-463.

20. Molina-Navarro MM, Casas C, Piedrafita L, Belli G, Herrero E (2006) *FEBS Lett* 580**:**2273-2280.

21. Wingert RA, Galloway JL, Barut B, Foott H, Fraenkel P, Axe JL, Weber GJ, Dooley K, Davidson AJ, Schmid B *et al.* (2005) *Nature* 436**:**1035-1039.

22. Brown DM, Upcroft JA, Upcroft P (1993) *Mol Biochem Parasitol* 61**:**155-158.

FIGURES

Fig. 1

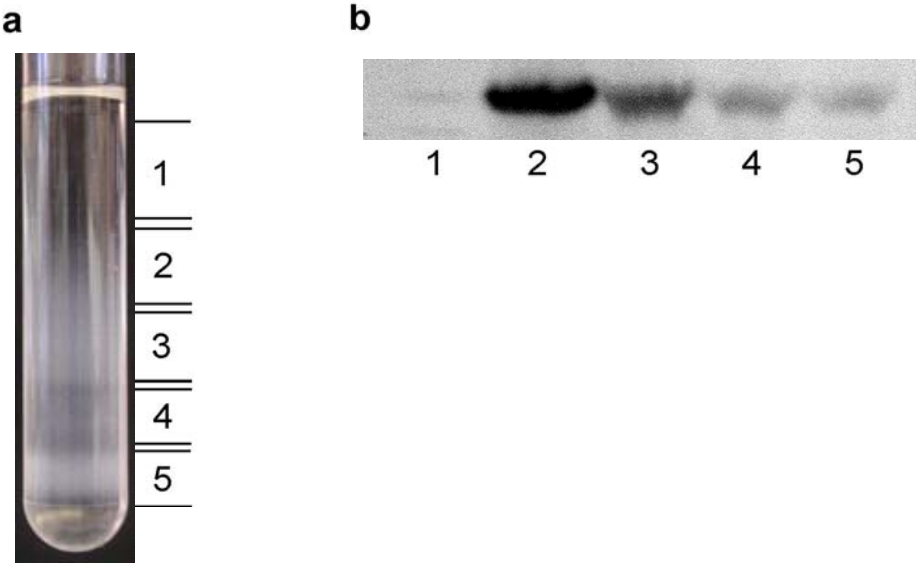

Fig. 2

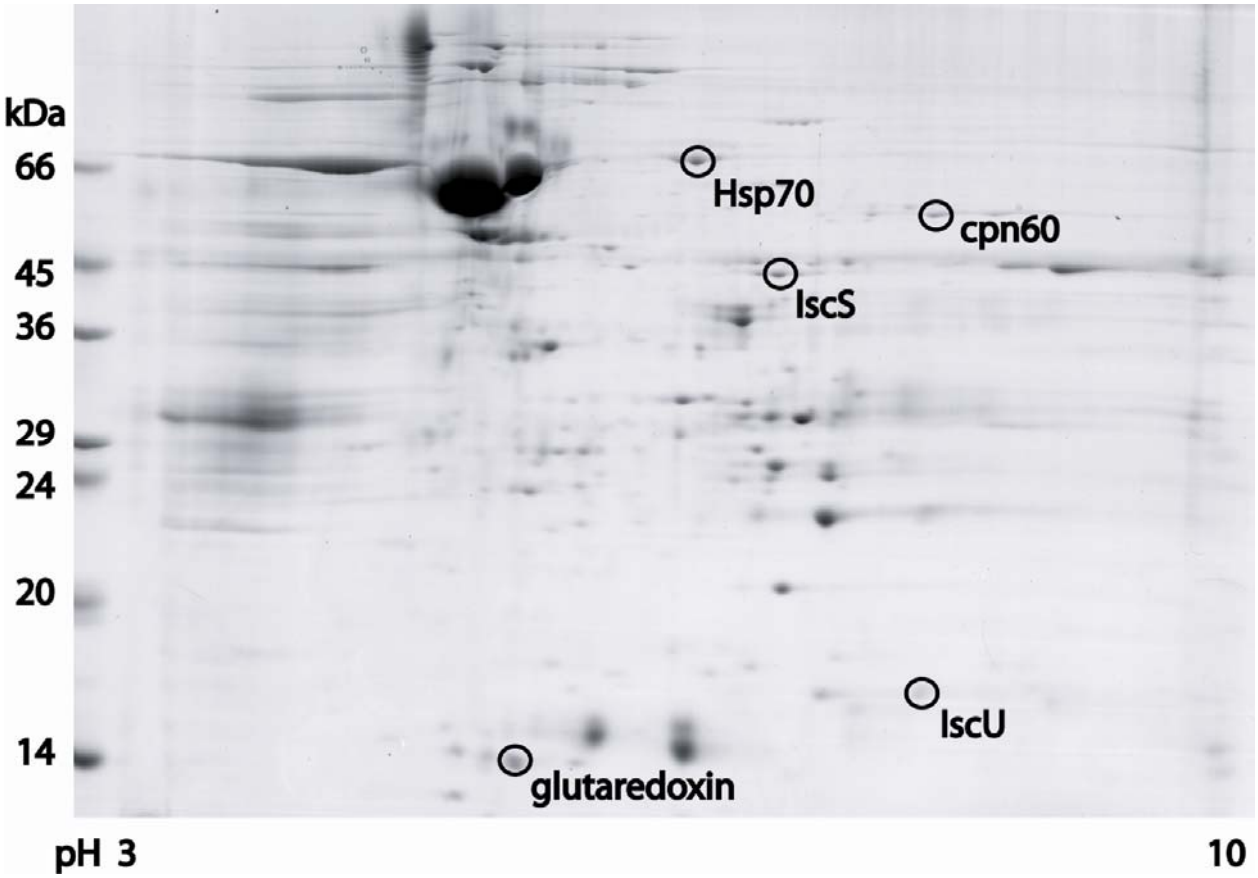

Fig. 3

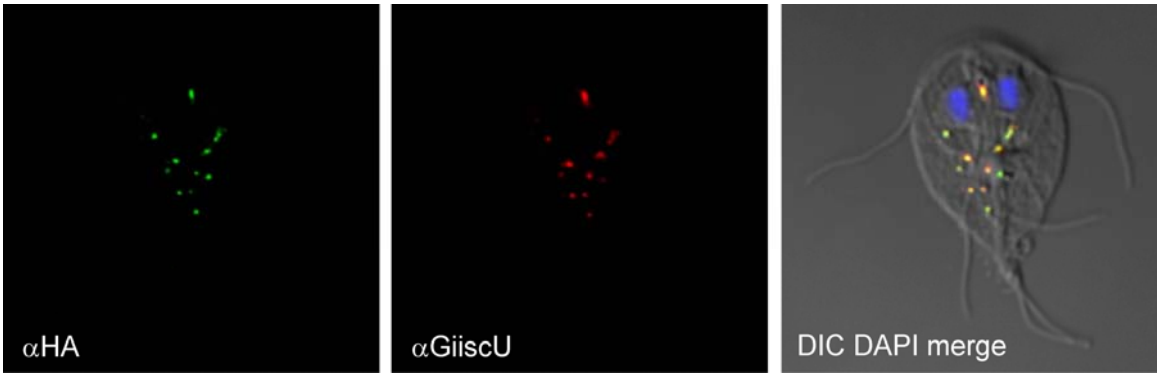

Fig. 4

```
ScGrx5  ------------------------------------------------------------------MF
Gigrx   MDQINGGLFPKALALTRYASRGLILGIISAAGAELENQLAGFLTRRYPRSLFLPNAQNSVSRFLMPVCAP
RpGrx2  ------------------------------------------------------------------

ScGrx5  LPKFNPIRSFSPILRAKTLLRYQNRMYLSTEIRKAIEDAIESAPVVLFMKGTPEFPKCGFSRATIGLLGN
Gigrx   LATVSRGLERTSDLNATLAQSESIKQELKMFILPQIRELLAENPVVLFMKGTPDSPECGFSKFASMLLKY
RpGrx2  --------------------------MTKNKNLEFIQNAIKKNKVVLFMKGTKEMPACGFSGTVVAILNK

ScGrx5  QGVDPAKFAAYNVLEDPELREGIKEFSEWPTIPQLYVNKEFIGGCDVITSMARSGELADLLEEAQALVPE
Gigrx   NNIS---FVGVDVLDDPALRQGIKLYGNWPTIPQLYVKGELIGGSDIIQQLHESGELRKVCGLPD-----
RpGrx2  LGVE---FSDINVLFDTALREDLKKFSDWPTFPQLYINGVLVGGCDIAKELYQNGELEKMLKDVVV----

ScGrx5  EEEETKDR
Gigrx   --------
RpGrx2  --------
```

Fig. 5

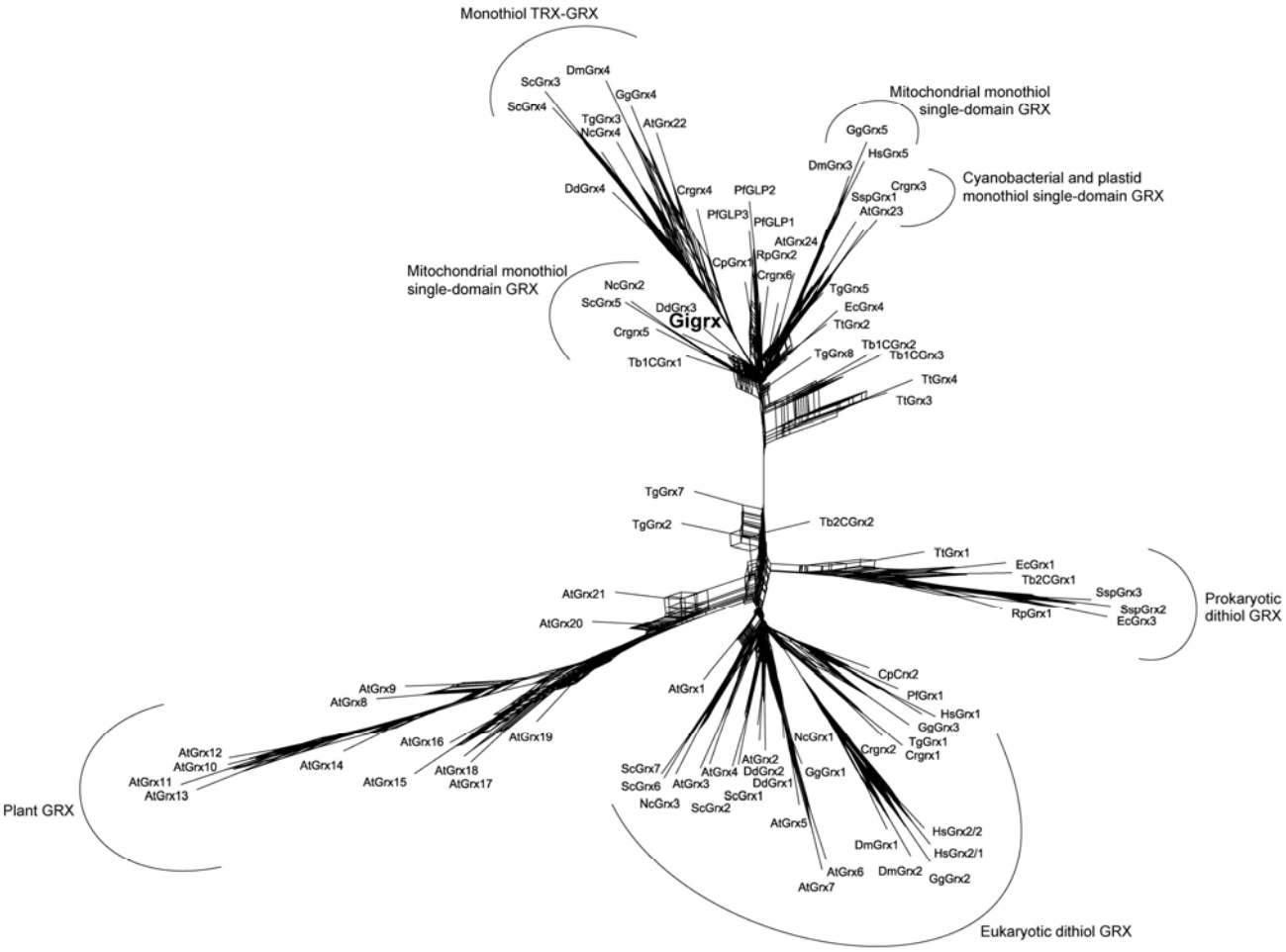
Monothiol TRX-GRX
Mitochondrial monothiol single-domain GRX
Cyanobacterial and plastid monothiol single-domain GRX
Mitochondrial monothiol single-domain GRX
Gigrx
Prokaryotic dithiol GRX
Plant GRX
Eukaryotic dithiol GRX
DmGrx4
ScGrx3
GgGrx4
ScGrx4
TgGrx3
NcGrx4
AtGrx22
GgGrx5
HsGrx5
DmGrx3
Crgrx3
SspGrx1
AtGrx23
DdGrx4
Crgrx4
PfGLP2
PfGLP3
PfGLP1
AtGrx24
RpGrx2
CpGrx1
Crgrx6
NcGrx2
ScGrx5
DdGrx3
Crgrx5
Tb1CGrx1
TgGrx5
EcGrx4
TtGrx2
TgGrx8
Tb1CGrx2
Tb1CGrx3
TtGrx4
TtGrx3
TgGrx7
TgGrx2
Tb2CGrx2
TtGrx1
EcGrx1
Tb2CGrx1
SspGrx3
SspGrx2
EcGrx3
RpGrx1
AtGrx21
AtGrx20
AtGrx9
AtGrx8
AtGrx1
CpCrx2
PfGrx1
HsGrx1
GgGrx3
TgGrx1
Crgrx1
Crgrx2
NcGrx1
AtGrx12
AtGrx10
AtGrx11
AtGrx13
AtGrx14
AtGrx16
AtGrx15
AtGrx18
AtGrx17
AtGrx19
ScGrx7
ScGrx6
NcGrx3
AtGrx3
AtGrx4
AtGrx2
DdGrx2
DdGrx1
ScGrx1
ScGrx2
GgGrx1
AtGrx5
HsGrx2/2
HsGrx2/1
DmGrx1
AtGrx6
AtGrx7
DmGrx2
GgGrx2

Fig. 6

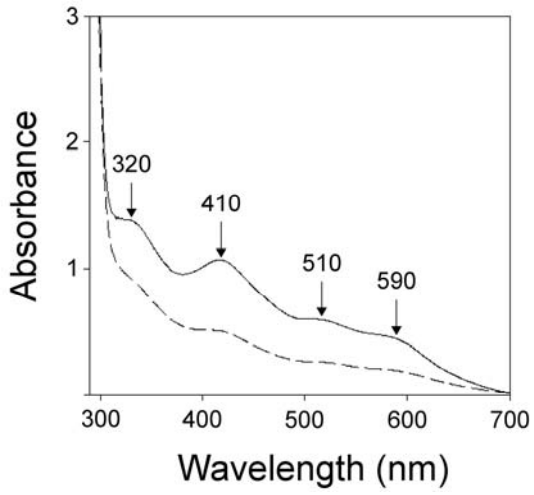
Absorbance
Wavelength (nm)
320
410
510
590
1
2
3
300
400
500
600
700

CONCLUSIONS

Mitochondria appear to be vital organelles for all eukaryotic organisms known to date. A large body of evidence strongly indicates that hydrogenosomes and mitosomes, the organelles of anaerobic or intracellular parasitic protists lacking the „typical“ mitochondria, are only a variation on the mitochondrial theme. However, even though the three organelles are evolutionarily the same entity, remarkable differences exist between them that reflect the adaptation of the organisms to their specific niches. In the thesis I tried to unravel some aspects of the essential mitochondrial processes of FeS cluster assembly and mitochondrial protein import in parasitic protists *T. brucei* and *G. intestinalis*.

We investigated the function of the *T. brucei* cysteine desulfurase IscS and the scaffold protein IscU. We demonstrated that the two proteins are essential for FeS cluster formation and consequently the viability of the procyclic stage of *T. brucei*. Even though both IscS and IscU were specifically localized to the mitochondrion, their deficient expression affected the maturation of FeS proteins operating not only in the mitochondrion, but also in the cytosol. This indicates that a crucial part of FeS cluster assembly is localized to the mitochondrion of *T. brucei*. One of the major differences between the *T. brucei* of the insect vector and the stage parasitizing mammals is the way they generate energy, in particular the use of the mitochondrion, in the process. Remarkably, the overall metabolic changes observed in the FeS cluster-impaired cells resulted in a phenotype that mimics the interstagial transition of the organelle, most notably by decreased production of ATP and acetate. Based on these results we proposed that the function of FeS cluster assembly machinery is critical for the interstagial changes in the *T. brucei* life cycle.

FeS cluster assembly is so far the only known function of *G. intestinalis* mitosomes. To identify other metabolic pathways, we analysed protein content of these organelles. Interestingly, only proteins involved in FeS cluster biogenesis and mitosomal protein import were found by this approach. One of the identified proteins is the monothiol glutaredoxin. We demonstrated that, same as the homologue of *S. cerevisiae* that is involved in FeS cluster transfer to apoproteins, the *G. intestinalis* glutaredoxin binds an FeS cluster via glutathione. Even though we were not able to detect free glutathione in the mitosomal fraction of the parasite, the genes coding for enzymes of glutathione metabolism

found in *G. intestinalis* genome strongly indicate that the tripeptide is present in the parasite.

The components of the FeS cluster assembly machinery are encoded in the nucleus and translated in the cytosol. To investigate the mechanisms of their import into mitosomes and hydrogenosomes, we compared targeting and translocation of IscS, IscU, and 2Fe2S ferredoxin of *G. intestinalis* into mitosomes and hydrogenosomes. When the three components of FeS cluster assembly machinery were overexpressed in *G. intestinalis* or *T. vaginalis*, they were specifically delivered into the mitosomes or into the hydrogenosomes, respectively. The delivery of the proteins into G. intestinalis mitosomes was mediated by two different mechanisms requiring either N-terminal targeting sequences (ferredoxin, IscU) or internal targeting sequences (IscS). The N-terminal extensions predicted in IscU and ferredoxin were found to be both necessary and sufficient for targeting to mitosomes and resemble the targeting sequences found in mitochondrial and hydrogenosomal proteins in that they (*i*) are rich in serine residues, (*ii*) are predicted to form amphipathic helices, and (*iii*) possess cleavage site motifs recognized by mitochondrial-type processing peptidases.

We demonstrated that hydrogenosomal processing peptidase of *T. vaginalis*, HPP, is a heterodimeric metalloprotease composed of subunits homologous to α and β subunits of mitochondrial processing peptidase, MPP. So far uniquely among eukaryotes, mitosomal processing peptidase of *G. intestinalis*, GPP, functions as a βGPP monomer. Our phylogenetic and functional analyses show that GPP is a striking example of reductive evolution from a heterodimeric to a monomeric enzyme. The structure and negative surface charge distribution of βGPP appear to have co-evolved with the properties of mitosomal targeting sequences, which, unlike classic mitochondrial targeting signals, are short and devoid of positively-charged residues except for the arginine of the cleavage motif. The majority of hydrogenosomal presequences resemble those of mitosomes, but longer positively charged mitochondrial-type presequences were also identified, consistent with the retention of the *T. vaginalis* αHPP.

In my thesis I attempted to add to the knowledge of the essential processes of FeS cluster assembly and mitochondrial protein import in *T. brucei* and *G. intestinalis*. I believe that the presented results contribute to the notion that the eukaryotic diversity can only hardly be embraced by a generalized model system, the „deviated“ organisms like parasitic

protists adding interesting twists to the story, often with unexpected evolutionary implications.